EXPERIMENTAL INVESTIGATION ON SEISMIC PERFORMANCE OF REINFORCED CONCRETE BEAM-COLUMN JOINTS WITH AND WITHOUT ADEQUATE TIES AT JOINT REGION

A Thesis

By

SHAHRIAR SHARIF KHAN

MASTER OF SCIENCE IN CIVIL ENGNEERING (STRUCTURAL)

DEPARTMENT OF CIVIL ENGINEERING

BANGLADESH UNIVERSITY OF ENGINEERING AND TECHNOLOGY

November, 2014

EXPERIMENTAL INVESTIGATION ON SEISMIC PERFORMANCE OF REINFORCED CONCRETE BEAM-COLUMN JOINTS WITH AND WITHOUT ADEQUATE TIES AT JOINT REGION

A Thesis

By

SHAHRIAR SHARIF KHAN

Submitted to the Department of Civil Engineering, Bangladesh University of Engineering and Technology (BUET), Dhaka in partial fulfillment of the requirements for the degree of

MASTER OF SCIENCE IN CIVIL ENGNEERING (STRUCTURAL)

DEPARTMENT OF CIVIL ENGINEERING

BANGLADESH UNIVERSITY OF ENGINEERING AND TECHNOLOGY

November, 2014

This thesis titled **"EXPERIMENTAL INVESTIGATION ON SEISMIC PERFORMANCE OF REINFORCED CONCRETE BEAM-COLUMN JOINTS WITH AND WITHOUT ADEQUATE TIES AT JOINT REGION"**, submitted by SHAHRIAR SHARIF KHAN, Roll No. 0411042302P, Session: April 2011, has been accepted as satisfactory in partial fulfillment of the requirement for the degree of **Master of Science in Civil Engineering (Structural)** on 1st November, 2014.

BOARD OF EXAMINERS

_____

Dr. Raquib Ahsan — **Chairman**
Professor
(Supervisor)
Department of Civil Engineering, BUET

_____

Dr. A.M.M. Taufiqul Anwar — **Member**
Professor and Head — (Ex-officio)
Department of Civil Engineering, BUET

_____

Dr. Syed Ishtiaq Ahmad — **Member**
Professor
Department of Civil Engineering, BUET

_____

Dr. Ali Ahmed — **Member**
Associate Professor — (External)
Department of Civil Engineering,
Stamford University Bangladesh.

CANDIDATE'S DECLARATION

It is hereby declared that this project or any of it has not been submitted elsewhere for the award of any degree or diploma.

_____

(Shahriar Sharif Khan)

DEDICATION

This Thesis is Dedicated to My Mother Jahanara Begum.

ACKNOWLEDGEMENTS

The author expresses his deep gratitude to Almighty Allah who is very kind to allow completing the thesis work with good health and mind.

The author is very thankful to his thesis supervisor Dr. Raquib Ahsan, Professor, Department of Civil Engineering, Bangladesh University of Engineering and Technology (BUET) for his enormous supports, constant guidance, supervision, keen interest as well as resource management. He encouraged playful and independent thinking and gave the freedom to try out new ways. With his very positive approach he assisted in boiling the essential out of results and helped to make the work converge to a thesis.

The author would like to thank the members of thesis defence committee Prof. Dr. A.M.M. Taufiqul Anwar, Prof. Dr. Syed Ishtiaq Ahmad and Assost. Prof. Dr. Ali Ahmed for their advices and helps in reviewing the thesis.

The author expresses his deep appreciation and gratitude to BSRM and Holcim Cement (Bangladesh) Limited for their material and technical supports. The author also gives thanks to Bhuiyan Mohammad Golam Kibria, Major, Bangladesh Army, for his co-operation and technical advice. The author would also like to express his appreciation to the technical expertise of the laboratory personnel for their advice and technical support throughout his experimental program. The author would also like to express his thanks to Yaseen for his industrious works.

The author is very thankful to Iftekhar Kabir, Additional Chief Engineer, Roads and Highways Department, Md. Ahsan Habib, Executive Engineer, Roads and Highways Department, for helping author to continue M.Sc. Engineering Degree in one of the most prestigious universities of the country.

Author is undoubtedly grateful to his mother (Jahanara Begum) and family members for their unconditional love, encouragement, blessings and co-operation.

ABSTRACT

Beam-column joints are identified as potential critical components of reinforced concrete moment resisting frames subjected to seismic lateral loading. Severe damage within a joint panel may trigger deterioration of the performance of reinforced concrete beam-column connections.

A comprehensive study has been carried out to investigate the seismic behavior of beam-column joints with and without adequate ties at joint region. Seven half-scale specimens of reinforced concrete beam-column joints were constructed considering three types of categories. These test categories were a) joint region with and without seismic ties, b) application of conventional and seismic stirrups in the joint region and c) different column to beam cross-section ratios which were considered to observe their effects on the performance of beam to column joint.

The specimens were subjected to cyclic incremental moment with sustained gravity load. Different crack patterns were observed for different categories of specimens. Specimens without ties at joint region showed diagonal cracking at joint; on the other hand, control specimens with ties experienced vertical cracking at the faces of the joint where the beams framed into the joint. The experimental data obtained in four deflection controlled cycles were used to study overall performance of the beam to column joint. Load-displacement as well as moment-rotation characteristics of the joints were obtained. At the same time, maximum loads, load at first crack formation, maximum as well as residual deflections and stiffness were measured or observed. Finally, the test results of beam-column joints with and without seismic ties at joint region were compared.

The specimen with non-seismic stirrup detailing and without ties at joint region performed poorly. The reinforced concrete beam-column joints with seismic ties at joint region showed improved performance with respect to absorbed energy, relative resisting moment and secant stiffness.

TABLE OF CONTENTS

LIST OF FIGURES

Page No.

Page No.

Page No.

Page No.

Page No.

LIST OF TABLES

Page No.

NOTATIONS AND SYMBOLS

Ach = Cross sectional area of the member measured out to out of the transverse reinforcement

Ag = Gross area of section

Aj = Effective area of the joint

As = Area of non pre-stressed steel reinforcement

Ash = Total cross sectional area of the transverse reinforcement (including cross ties) within spacing s and perpendicular to dimension hc

Ast = Total area of longitudinal reinforcement

b = Width of rectangular cross section

bc = Effective width of the column

bj = Effective width of the beam column joint

B´s = Bond force contribution from top reinforcement

bw = Web width or diameter of circular section

Cb = Compressive force acting on beam reinforcement

C´s = Compression force developed in the top bars

Cf = Diagonal compressive force

Cult = Ultimate compressive force

d = Distance from extreme compression fiber to the neutral axis

Ec = Modulus of elasticity of concrete

Es = Modulus of elasticity of steel

fc = Compressive stress in concrete

f´c = Specified compressive strength of concrete, psi (MPa)

√f´c = Square root of specified compressive strength of concrete

fy = Specified yield strength of non pre-stressed steel reinforcement

h = Overall thickness of a member,

hc = Depth of column

hj = Depth of the beam column joint

k = Ratio of the depth of the neutral axis to the reinforcement depth measured on the same side of neutral axis

lc = Height of the story

Mp = Plastics moment capacity

Ms = Sagging Moment

Mh = Hogging moment

S = Spacing of the transverse reinforcement

Tb = Tensile force acting on the beam reinforcement

Tult = Ultimate Tensile force

Vb = Vertical beam shear

Vcol = Column shear force

Vch = Shear force contribution from the concrete strut

VSh = Shear force contribution from the concrete truss

Vn = Nominal shear strength

Vs = Nominal shear strength provided by steel stirrups

Vjh = Horizontal shear force within joint core

α = Angle of inclination of stirrups or spirals, degrees

β = Ratio of the bottom reinforcement to top reinforcement

Δy = Yield deflection

Δu = Ultimate deflection

θy = Yield rotation

θu = Ultimate rotation

γ = Factor used to express the stress level in the reinforcing bars

ρg = Gross reinforcement ratio

ρs = Ratio of non pre-stressed reinforcement

CHAPTER 1

INTRODUCTION

1.6 General

A beam-column joint is defined as the portion of a column within the depth of beams that frame into it (Nelson 1997, MacGregor 1988). Beam-column joints are recognized as the critical and vulnerable zone of a Reinforced Concrete (RC) moment resisting structure subjected to seismic loads. In reinforced concrete structures, during severe earthquake attacks, brittle shear failure can occur in the joints, as well as cracking and frictional sliding under reverse cyclic loading. The ultimate resistance capacity depends directly on their different material behavior (concrete damage, steel plasticity) but it must deal with crack opening and degradation of bonding between concrete and steel.

1.2 Background of the Research

During an earthquake, global response of a structure is mainly governed by the behavior of its joints. The joints of a non-seismically detailed structure are more vulnerable to earthquakes compared to the joints of a seismically detailed structure. It has been identified that the deficiencies of joints are mainly caused by inadequate transverse reinforcement and insufficient anchorage capacity in the joint. The transverse reinforcement of a joint reduces stress. Additional ties are placed in the joint region in order to provide adequate joint shear strength. Since past three decades, extensive research has been carried out on studying the behavior of joints under seismic conditions through experimental and analytical studies. Various international codes of practices have been undergoing periodic revisions to incorporate the research findings into practice. However, in the past, most of the beam-column joints in Bangladesh were without ties. It is necessary to investigate the behavior of beam-column joints with and without ties, in order to assess performance of the existing buildings in Bangladesh. The present study is concerned about investigating the behavior of beam-column joints with and without adequate ties in the joint region.

1.3 Objectives of the Research

The objectives of the investigation are as follows:

1. To experimentally observe the failure mode of beam-column joints.

2. To inspect the load at first crack formation of beam-column joints.

3. To observe the moment-rotation behavior of beam to column joints subjected to cyclic loading without inertia force.

4. To investigate the differences in behavior of beam-column joints with and without ties at joints considering different beam to column joint parameters.

1.4 Scope of the Research and Limitations

Reinforced concrete beam-column joints of normal strength concrete were considered in this study. Three different column to beam cross-section ratios were considered with and without ties at joint region. Tie spacing was also varied in equal beam-column joints. Half scale models were considered in this research work.

Scope of this work was limited to interior beam-column joints made of stone chips. Exterior or corner beam-column joints and brick chips were not considered in this study. Load was not given simultaneously at two beams. Cyclic load was applied by turn to the beam ends by movable hydraulic jack. Furthermore, cyclic load was not introduced dynamically rather it was applied statically. At the same time main focus was given on dial gauge reading of beam. There were also limitations on taking dial gauge reading as it was taken manually.

1.5 Organization of the Thesis

The outcomes of the research carried out have been divided into different topics and presented in five chapters.

In the first chapter, the overall perspective of the research is discussed. Furthermore, this chapter points out the objectives and scope of the research.

In the second chapter, the literature review corresponding to this research is covered. All the relevant literatures about beam-column joints are discussed here.

The third chapter is covered with properties and test results of materials used for construction, preparation of scaffolding and reinforcement, casting, curing and finally white coloring of beam-column joints.

In the fourth chapter, an outline of the experimental work is described in details. Analysis of results also illustrated in this chapter. The analysis from the experimental data is carried out through graphs and tables. A discussion on the analysis is also done.

In the fifth and last chapter, an elaborate conclusion is drawn based on the outcomes of the research. This chapter also includes possible way forward to explore future research possibilities.

CHAPTER 2

LITERATURE REVIEW

2.1 Introduction

Beam column joint is an important component of a reinforced concrete moment resisting frame and should be designed and detailed properly, especially when the frame is subjected to earthquake loading. Beam-column joints are recognized as the critical and vulnerable zone of a Reinforced Concrete (RC) moment resisting structure subjected to seismic loads. Failure of beam column joints during earthquake is governed by bond and shear failure mechanism which are brittle in nature. During an earthquake, the global response of the structure is mainly governed by the behavior of the joints. If the joints behave in a ductile manner, the global behavior generally will be ductile, whereas if the joints behave in a brittle fashion then the structure will display a brittle behavior. The joints of old and non-seismically detailed structures are more vulnerable and behave poorly under the earthquakes.

The behavior of reinforced concrete moment resisting frame structures in recent earthquakes all over the world has highlighted the consequences of poor performance of beam-column joints. Beam-column joints in a reinforced concrete moment resisting frame are crucial zones for transfer of loads effectively between the connecting elements (i.e. beams and columns) in the structure. In the analysis of reinforced concrete moment resisting frames, the joints are generally assumed as rigid. In general practice, the joint is usually neglected for specific design with attention being restricted to provision of sufficient anchorage for beam longitudinal reinforcement. This may be acceptable when the frame is not subjected to earthquake loads. There have been many catastrophic failures reported in the past earthquakes, which have been attributed to beam-column joints. The poor design practice of beam column joints is compounded by the high demand imposed by the adjoining flexural members (beams and columns) in the event of mobilizing their inelastic capacities to dissipate seismic energy. Unsafe design and detailing within the joint region jeopardize the entire structure, even if other structural members conform to the design requirements.

In RC buildings, portions of columns that are common to beams at their intersections are called beam-column joints. Since their constituent materials have limited strengths, the joints have limited force carrying capacity. When forces larger than those are applied during earthquakes, joints are severely damaged. Repairing damaged joints is difficult, and so damage must be avoided. Thus, beam-column joints must be designed to retain earthquake effects.

Under earthquake shaking, the beams adjoining a joint are subjected to moments in the same (clockwise or counterclockwise) direction. Under these moments, the top bars in the beam-column joint are pulled in one direction and the bottom ones in the opposite direction. These forces are balanced by bond stress developed between concrete and steel in the joint region. If the column is not wide enough or if the strength of concrete in the joint is low, there is insufficient grip of concrete on the steel bars. In such circumstances, the bar slips inside the joint region, and beams lose their capacity to carry load. Further, under the action of the above pull-push forces at top and bottom ends, joints undergo geometric distortion; one diagonal length of the joint elongates and the other compresses. If the column cross-sectional size is insufficient, the concrete in the joint develops diagonal cracks.

2.2 Overview

Under the action of seismic forces, beam-column connections are subjected to large shear stresses in the joint region. These shear stresses are a result of moments and shear forces of opposite signs on the member ends on either side of the joint core. Typically, high bond stresses are also imposed on reinforcement bars entering into the joint. The axial compression in the column and joint shear stresses result in principal tension and compression stresses that lead to diagonal cracking and/or crushing of concrete in the joint core. These problems have been highlighted in recent past by the damage observed in devastating earthquakes in different countries. A typical example of a beam-column joint failure during the 1999 Turkey earthquake is shown in Figure 2.1 (Ghobarah and Said, 2002). The two major failure modes for the failure at joints are (a) joint shear failure and (b) end anchorage failure (Figure 2.2). The stresses in the joint core are

resisted by the so-called strut and tie mechanism (Paulay and Priestley, 1992). To assure an increase of the shear strength after the cracking of the joint core by diagonal tension and sufficient rotational capacity, joint shear reinforcement is needed, which is therefore prescribed by the newer design codes (ACI 318, 2008; NZS 3101, 1995; IS 13920, 2002). Moreover, these codes prescribe a large anchorage length of the bars terminating in case of exterior joints, so that a bond failure may be avoided.

Figure 2.1: Typical Beam-Column Joint Failures in Turkey Earthquake, 1999 (Ghobarah and Said, 2002)

a) Joint Shear Failure.

b) Inadequate Reinforcement Anchorage.

c) Inadequate Ties at Interior Joint

d) Inadequate Ties at Corner Joint

Figure 2.2: Major Failure Modes for RC Beam-Column Joint (Ghobarah and Said, 2002)

However, a vast majority of RC buildings worldwide consist of structures designed prior to the advent introduction of modern seismic design codes. It has been identified that the deficiencies of joints are mainly caused by inadequate transverse reinforcement and insufficient anchorage capacity in the joint (Liu, 2006). Figure 2.3(a) shows a few typical deficiencies found in the beam-column joints of old structures and Figure 2.3(b) shows the corresponding new seismic detailing recommended by current codes.

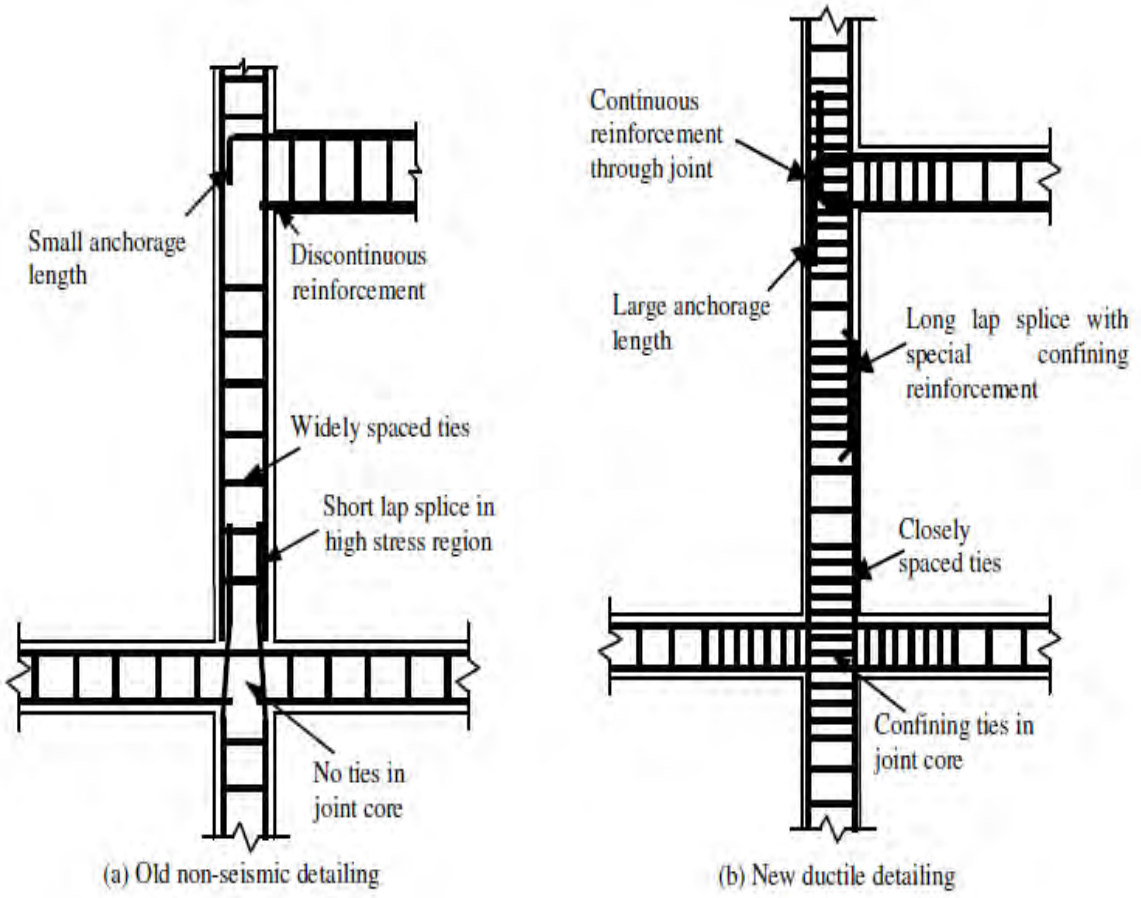

Figure 2.3: Typical Non-Ductile and New Ductile Detailing Prescribed by Codes of Practice (Liu, 2006)

2.3 Beam Column Joints

A beam-column joint is defined as the portion of a column within the depth of beams that frame into it (Nelson, 1997 and MacGregor, 1988). The functional requirement of a joint is to enable the adjoining members to develop and sustain their ultimate capacity. Earlier, the design of monolithic joints was limited to providing adequate anchorage (Nelson, 1997). But now the design of the joints has got importance due to the consideration of large forces induced by the seismic events. The joints should have adequate strength and stiffness to resist the internal forces induced by the framing members.

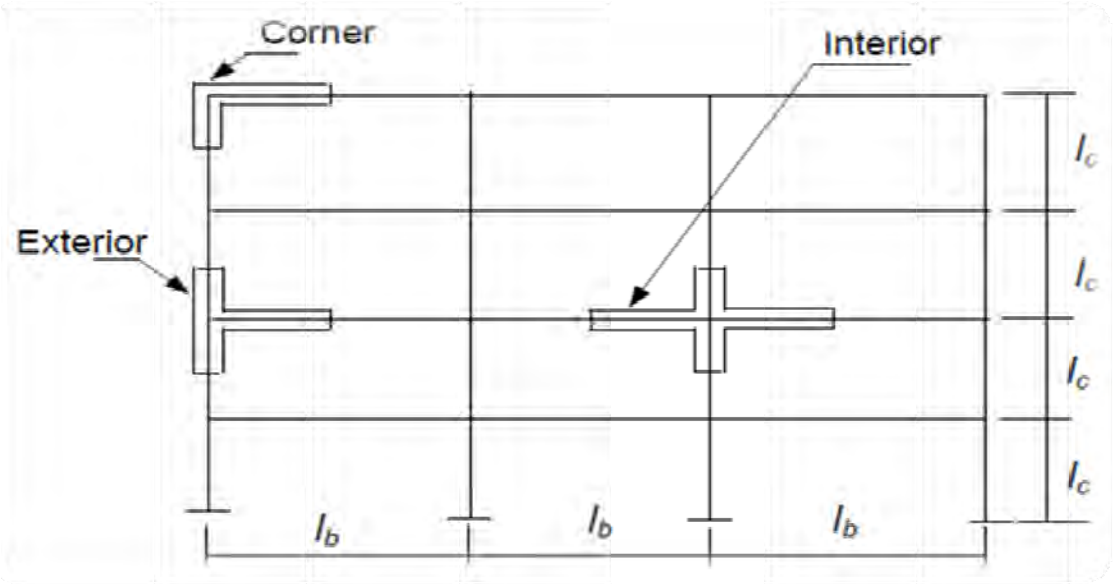

Figure 2.4: Types of Joints in a Structure (Nelson, 1997 and MacGregor, 1988)

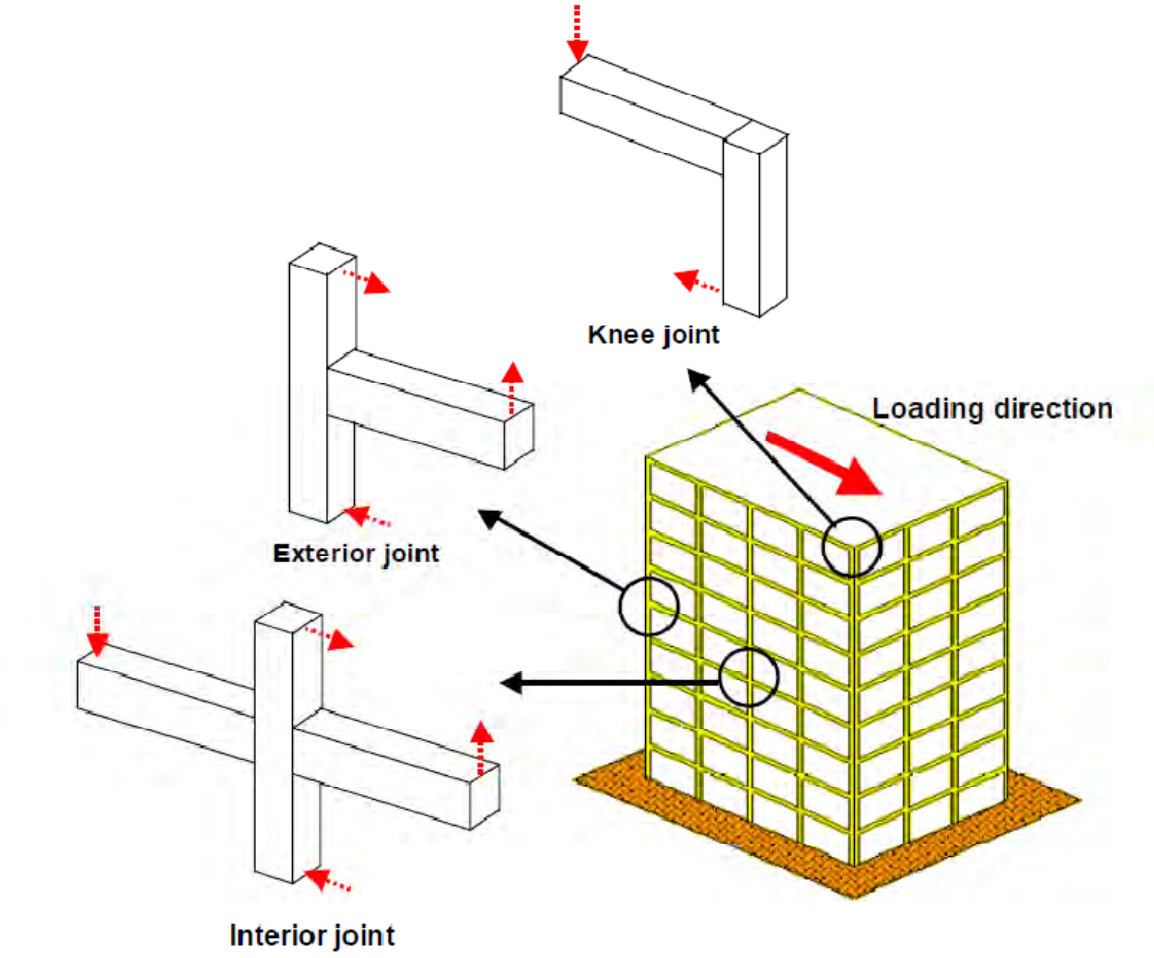

Figure 2.5: Forces acting on beam-column joints in a building structure (James M. Lafave, 2009)

2.3.1 Classification of Joints

The joints of a moment resisting RC frame can be classified as interior, exterior and corner joints as they are shown in Figure 2.6. The joints must be able to resist the forces induced by the earthquake or cyclic loading. As this research deals with the behavior of internal joints so the behavior of internal joints under cyclic loading are discussed.

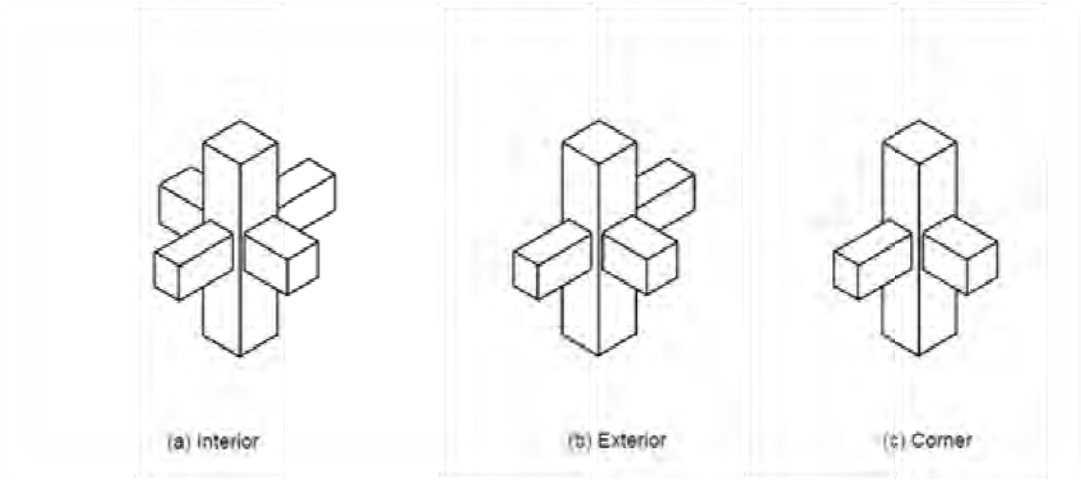

Figure 2.6: Types of Joints (Nelson, 1997 and MacGregor, 1988)

2.4 Interior Beam-Column Joint

Most failure of reinforced concrete structures occurs because of insufficient attention given to the detailing of the joint. Other failures may also result in inadequacies of structural members. The principal mechanisms of failure of interior beam-column joints are:

- shear within the joint
- anchorage failure of bars, if anchored within the joint and
- bond failure of beam or column bars passing through the joint.

The joint is designed based on the fundamental concept that failure should not occur within the joint; that is, it is strong enough to withstand the yielding of connecting beams (usually) or columns. The functional requirement of a joint, which is the zone of intersection of beams and columns, is to enable the adjourning members to develop and

sustain their ultimate capacity (Nelson et al., 2004).The requirement for joint design has been always serious particularly under seismic loading. The joints should have adequate strength and stiffness to resist the internal forces induced by the framing members. Joint is of great importance, as all forces that occur at the ends of the members must be transmitted through the joint to the supporting members. These forces develop complex stresses at the junction of beam and column joints.

The behavior of forces developed at the joint vicinity corresponds to detailing and geometry configuration of the joint itself as well as various forces transferred to the joint. The forces experienced in all three types of joints differ from one to another. The resultant forces due to seismic loading at these joints are elaborated in latter in terms of stresses and crack propagation associated thereof (MayField et al., 1971).

The high internal forces developed at plastic hinges cause critical bond conditions in the longitudinal reinforcing bars passing through the joint and also impose high shear demand in the joint core. In a recent experimental research, it was noted that the joint loading behavior showed an extremely complex interaction between shear and bond (ACI Committee 408, 1970). The bond requirements of the longitudinal reinforcement bars in reinforced concrete beam-column joint have greater impacts on the shear resisting mechanism behavior to a certain limit.

In an interior joint, the stresses prolonging simultaneously throughout the joint alter from compression to tension. This generates a push-pull effect that emphasizes greater demand on bond strength and provides sufficient development length within the joint core. The development length has to satisfy compression and tension force requirements in the same longitudinal reinforcement bar. Insufficient development length and the spread of splitting cracks in the joint core may result in slippage of bars. Leon (1990), observed that when the development length was higher than 28 diameters, obtained lower or no bond degradation with respect to various shear stress levels in the joint.

The diagonal concrete strut action mechanism (MacGregor, 1988; Nelson et al., 2004 and Park & Pauley, 1975) is formed by the major diagonal concrete compression force in the joint. This force is produced by the vertical and horizontal compression stresses as well as critical section of shear stresses on concrete of the beam and column. The truss mechanism (MacGregor, 1988: Nelson et al., 2004 and Park & Pauley, 1975) is formed

by a combination of the bond stress transfer along the beam and column longitudinal reinforcement, the tensile resistance of lateral reinforcement and compression resistance of uniform diagonal concrete struts in the joint panel. The strength of the strut mechanism depends on the comprehensive strength of concrete and that of the truss mechanism on the tensile yield strength of the lateral reinforcement crossing the failure plane.

In resisting the joint shear, the diagonal strut mechanism can exist without any bond stress transfer along the beam and column reinforcement within the joint, while the truss mechanism can develop only when a good bond transfer is maintained along the beam and column reinforcement.

In recent years, researchers developed different methods in order to predict the shear strength in various types of RC joints more accurately. Some researchers proposed mathematical models to predict joint shear strength (Hwang and Lee, 1999 and 2000 and Attaalla, 2004), while some introduced methodologies to construct joint shear strength models for RC joints (Kim et al., 2007).

2.5 Forces Acting on Interior Joints

Beam-column joints have important roles to maintain the strength hierarchy of the moment resisting RC structure. The failure must not be at the column region which leads to a catastrophic failure. The joints should have sufficient strength to allow the flexural members to develop their maximum capacity. The failure should occur at the plastic hinges. The high internal forces developed at the plastic hinges cause critical bond conditions in the longitudinal reinforcing bars passing through the joint and also impose high shear demand in the joint core (Paulay et al., 1992 and Hakuto et al., 2000). The joint behavior exhibits a complex interaction between bond and shear. The bond performance of the bars anchored in a joint affects the shear resisting mechanism to a significant extent.

The forces on an interior joint subjected to gravity loading can be depicted as shown in Figure 2.7 (a). The tension and compression from the beam ends and axial loads from the columns are transmitted directly through the joint. In the case of lateral (or seismic) loading, the equilibrating forces from beams and columns, as shown in Figure 2.7 (b)

develop diagonal tensile and compressive stresses within the joint. Cracks develop perpendicular to the tension diagonal *A-B* in the joint and at the faces of the joint where the beams frame into the joint. The compression struts are shown by dashed lines and tension ties are shown by solid lines. Concrete being weak in tension, transverse reinforcements are provided in such a way that they cross the plane of failure to resist the diagonal tensile forces.

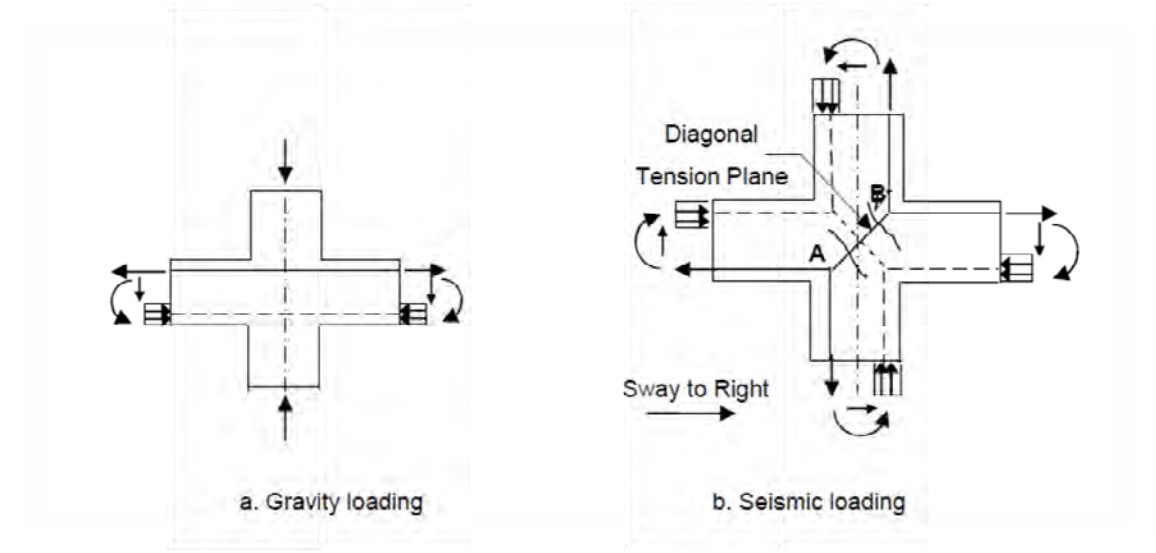

Figure 2.7: Interior Forces Resisting (a) Gravity Loading (b) Seismic Loading (MacGregor, 1988; Nelson et al., 2004 and Park & Pauley, 1975)

The bond requirement has a direct implication on the sizes of the beams and columns framing into the joint. The flexural forces from the beams and columns cause tension or compression forces in the longitudinal reinforcements passing through the joint. During plastic hinge formation, relatively large tensile forces are transferred through bond. When the longitudinal bars at the joint face are stressed beyond yield splitting cracks are initiated along the bar at the joint face which is referred to as 'yield penetration'. Adequate development length for the longitudinal bar is to be ensured within the joint taking yield penetration into consideration.

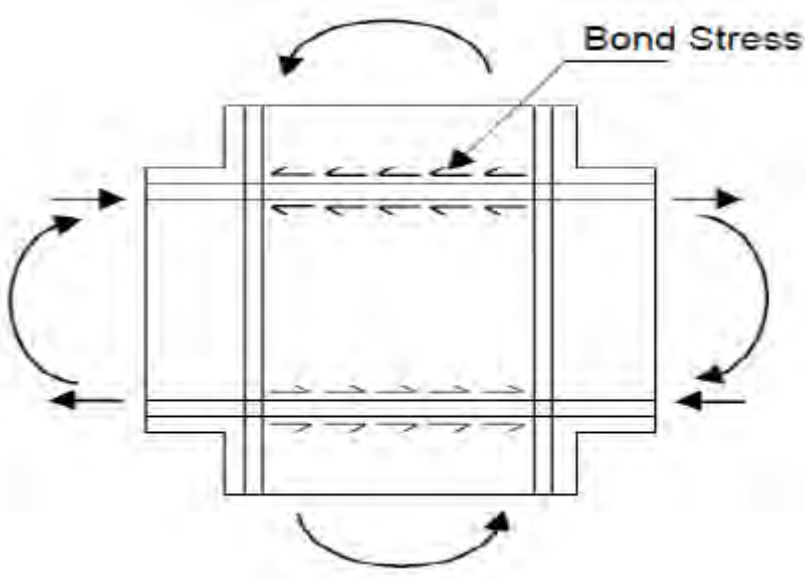

Figure 2.8: Bond Stresses in Interior Joint (Leon, 1990)

The adjoining beams of an interior joint are subjected to moments in the same direction under earthquake shaking. The top and bottom bars are pulled in the opposite direction by these moments and balanced by the bond stress developed between concrete and steel in the joint region as shown in Figure 2.8. The bond stress may be insufficient in case of poor strength, thin column or even both. Under these circumstances, the bars may slip inside the joint region and beams lose their carrying capacity. When the development length is greater than 28 bar diameters little or no bond degradation was observed with respect to shear stress levels in the joint (Leon, 1990). In other way, this dictates the minimum depth of the column with respect to the bar diameter i.e. depth should be 20 times of the bar diameter (ACI 21.5.1).

The bond performance of the reinforcing bars is influenced by confinement, clear distance between bars and nature of surface between bars. The confinement in the joint region is obtained by the column axial load and horizontal reinforcement arresting the splitting crack (Shear reinforcement) (Ichinose, 1991). Better bond performance is achieved when the clear distance between the longitudinal bars is less than 5 times the

diameter of the bar (Eligehausen et al., 1983). The deformed bar and concrete with high strength give better bond strength (Ichinose, 1991).

The external forces induced by the earthquake or seismic loading acts on the face of the joints and develop large shear stresses within the joint. The combined effect of the shear stresses causes diagonal cracking when the tensile stresses exceed the tensile strength of the concrete. Extensive cracking occur due to load reversals under seismic events. Joints strength and stiffness are affected by extensive cracking causing joints to become flexible enough to undergo large deformation.

The shear forces acting on an interior beam column joint can be determined by using equilibrium criteria. For an interior beam column joint, sub-assemblage between the points of contra flexure is considered. The centre to centre column distance and beam span is l_c and l_b respectively. The forces and moment acing on the sub-assemblage, shear force and moment distribution of the interior joints are shown in Figure 2.9 (a), (b) and (c) respectively. The nature of the moment changes within the joint region. A steep gradient of the moment causes large shear force within the joint compared to the adjacent columns. The horizontal shear force within the joint region can be computed by equilibrium criteria. The moments acting on the opposite sides of the joint are M_h and M_s and the vertical shear force from the beam is V_b. Assuming the beam is symmetrically reinforced, the tensile force T_b and C_b acting on the beam reinforcement are equal. The column shear V_{col} will be

$$V_{col} = \frac{2T_bZ_b+V_bh_c}{l_c} \quad \text{..... (2.1)}$$

Where l_c is the height of the storey and h_c is the depth of the column and Z_b is the lever arm of the tensile and compressive force. The horizontal shear within the joint core can be computed as

$$V_{jh} = V_{col}\left(\frac{l_c}{Z_b} - 1\right) - V_b\left(\frac{h_c}{Z_b}\right) \quad \text{……..…(2.2)}$$

The horizontal shear force V_{jh} can be reduced by increasing the column depth h_c or increasing the vertical shear from beam V_b. Equations (2.1) and (2.2) can be simplified by

considering the moment M_s and M_h and compressive and tensile strength of the reinforcing bars.

Column shear,

$V_{col} = (M_s + M_h) / l_c$ ……...…(2.3)

And horizontal shear force,

$V_{jh} = C + T - V_{col}$ ……...……...(2.4)

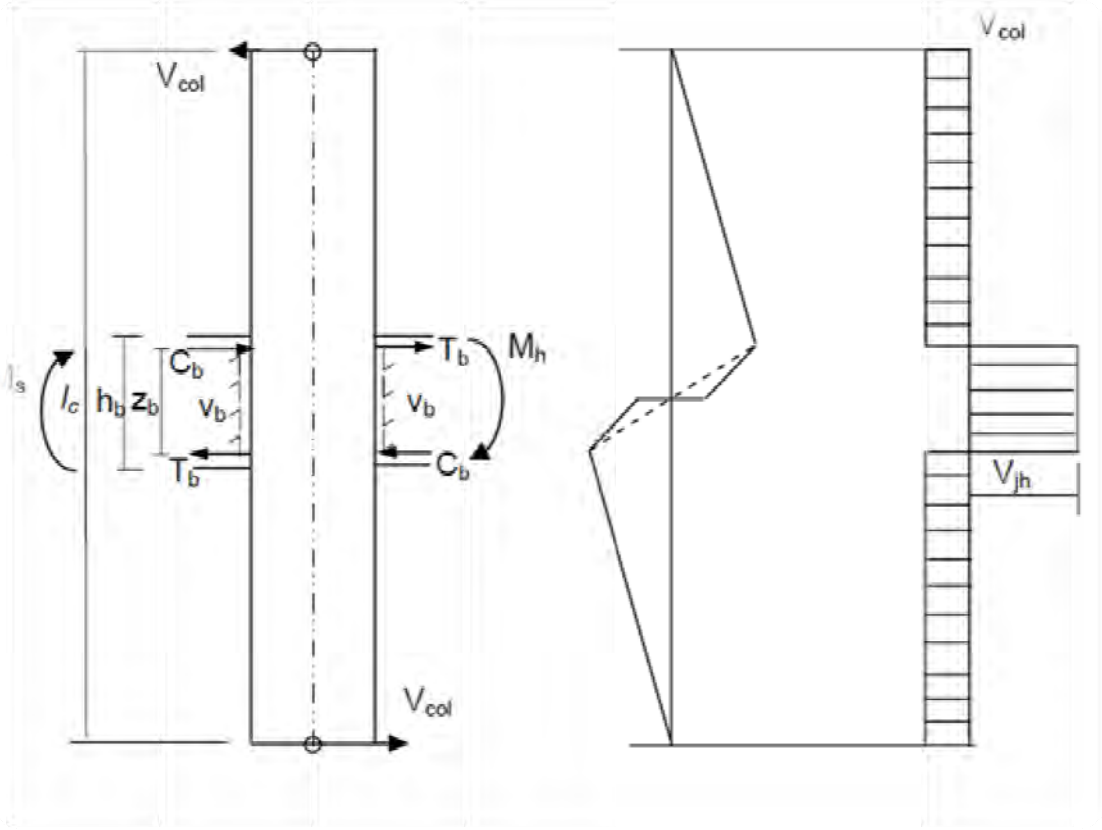

(a) Column Forces (b) Bending Moment (c) Shear Force

Figure 2.9: Forces Acting on an Interior Joint (Nelson, 1997 and Uma & Prasad, 2005)

The effective shear area is specified based on the dimension of the beam and column (Nelson, 1997 and Uma & Prasad, 2005). The effective shear area of the joint A_j is defined by the width of the joint b_j and depth of the joint h_j. The area may not be as large as the column cross section since the width of the beam and column b_w and b_c respectively may differ from each other. When the beam width is less than the column width, the effective joint width is the average of the beam width and column width but should not exceed the beam width b_b plus one half the column depth h_c on each side of the beam (ACI 352.2R, 2002).

$$b_j = \frac{b_b + b_c}{2} \quad \text{.....(2.5)}$$

and must $be \leq (b_b + h_c)$ .....(2.6)

The beam width b_b is the average width of the beam framing into the column from opposite direction and h_j is taken as the depth of the column h_c.

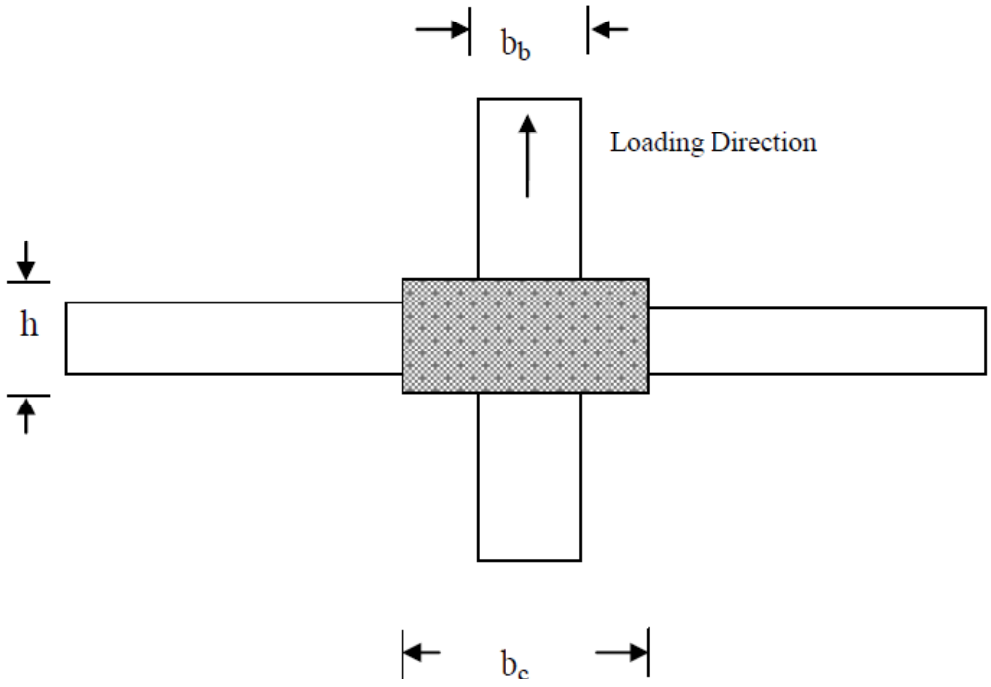

Figure 2.10: Determination of Effective Joint Width (Nelson, 1997)

The shear forces in the joint region develop diagonal compressive and tensile forces within the joint core. As a result, diagonal failure plane occurs within the joint region. The shear resisting mechanism is explained by strut and truss action (Figure 2.13).

Diagonal concrete strut mechanism is formed by major diagonal compression force in the joint. This force is produced by the vertical and horizontal compression stresses and shear stresses on concrete at the beam and column critical section. The truss mechanism is a combination of bond stress transfer along the beam and column longitudinal reinforcement, tensile resistance of lateral reinforcement and compressive resistance of uniform diagonal concrete struts in the panel region (Uma & Prasad, 2005 and Inchinose, 1991).

The strength of the strut and truss mechanism depends on compressive strength of the concrete and tensile yield strength of the lateral reinforcement crossing the failure plane respectively. The strut mechanism can exist without any bond stress transfer along the beam column reinforcement within the joint where as truss mechanism can develop only when a good transfer is maintained along the beam and column reinforcement. With the outset of bond deterioration under seismic loading condition, the truss mechanism starts to diminish and the diagonal strut mechanism must resist the most dominant part of the joint shear. The tensile force in the beam reinforcement not transmitted to the joint concrete by bond must be resisted by the concrete at the compression face of the joint thereby increasing the compression stress in the main strut. The strut is progressively weakened by the reversed cyclic loading. Concurrently, concrete compressive strength is reduced by the increasing tensile strain perpendicular to the direction of the main strut. The combination of these two phenomenon results in the failure of the concrete strut in shear compression. The principal role of the lateral reinforcement in this case is to confine the cracked core concrete (Uma and Prasad 2005). The shear force in the joint region is considered to be resisted by strut and truss mechanism.

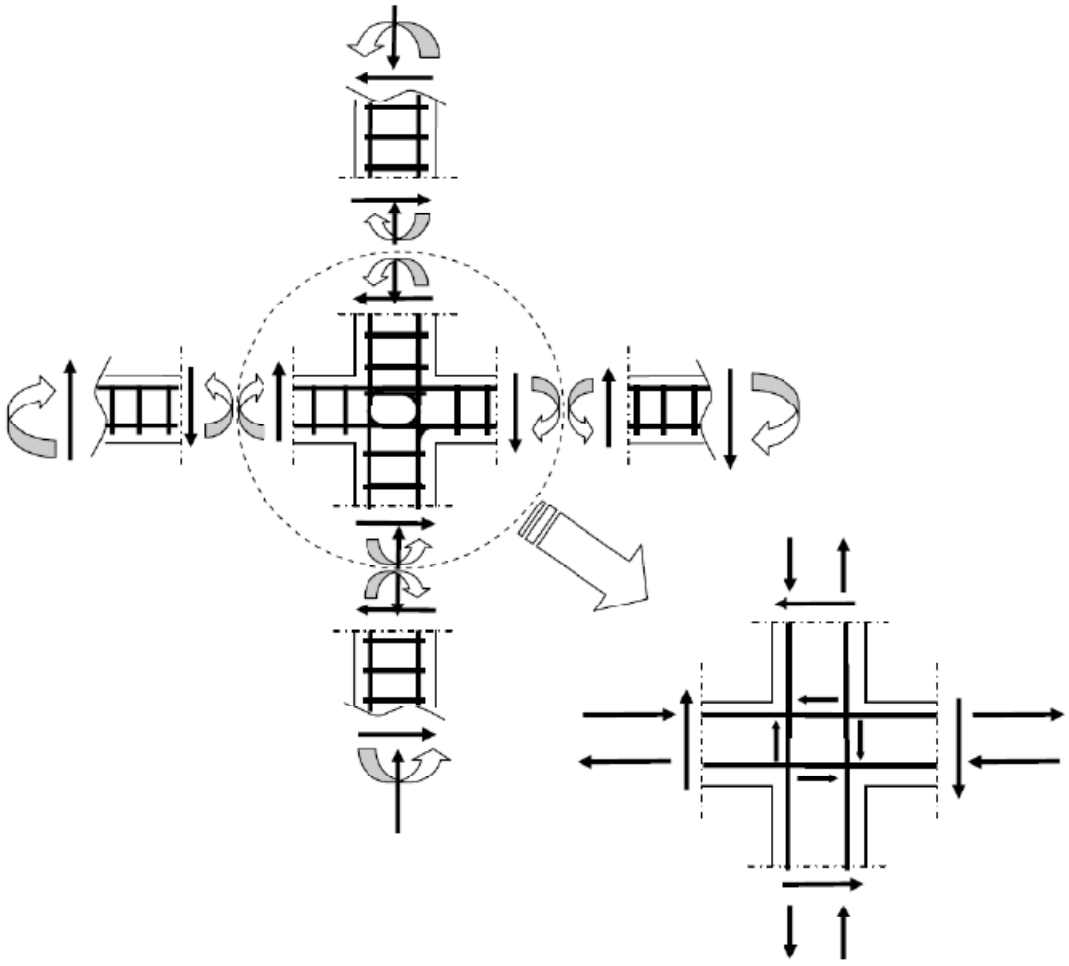

Figure 2.11: Behavior of Interior BC Joint under Seismic Loading (Uma & Prasad, 2005)

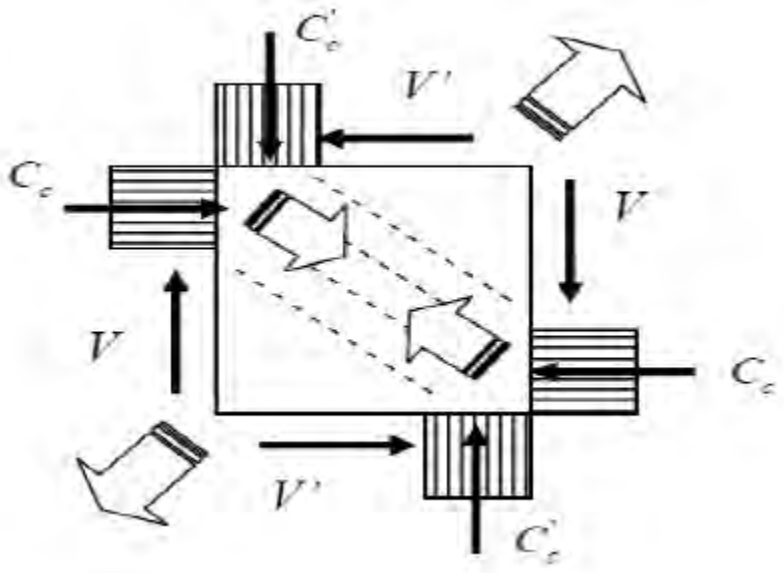

Figure 2.12: Concrete Shear under Seismic Loading (Uma & Prasad, 2005 and Inchinose, 1991)

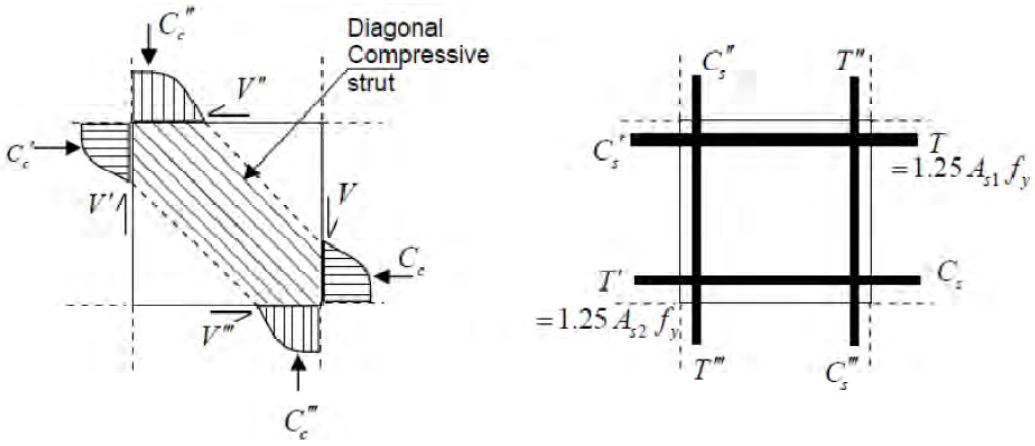

a) Compression Mechanism b) Force in the Reinforcement Only

Figure 2.13: Idealized Behavior of Interior Beam Column Joint (Uma, 2005)

$V_{jh} = V_{ch} + V_{sh}$ ……..(2.7)

$V_{jh} = (T - T_f) + C_f + C'_c + C'_s - V_{col}$ ……..(2.8)

The shear strength provided by the truss mechanism can be written as

$V_{sh} = V_{jh} - V_{ch}$ ……..(2.9)

$= T_b + C'_s - B'_s$ ……..(2.10)

B'_s is the combined effect of compression and tension forces from the top reinforcement anchored in the joint core.

$T_b = (T - T_f) = 1.25 f_y (A_{s1} - A_{sf}) = 1.25 f_y A_s$ ……..(2.11)

$C'_s = \gamma f_y A_s$ ……..(2.12)

is compression force developed in top beam bars. γ is the factor used to express the stress level in the bars in terms of yield stress.

After some bond deterioration, the compressive stress in the top beam reinforcement is not likely to exceed the stress level of $0.7f_y$ (Cheung et al., 1991 from Uma, 2004). At the same time, this stress cannot exceed $1.25\beta f_y$, here β is the ratio of bottom reinforcement to top reinforcement in the rectangular beam and is expressed as A_{s2}/A_s with $1.25\beta \geq \gamma \leq 0.70$. The value of γ may be less than 0.70 when the bottom reinforcement is about 50% of the top reinforcement or when the bottom beam reinforcement cannot yield at column face. Then C'_s can be obtained from the actual stress, f_{s2} in the bottom reinforcement.

Shear reinforcement design is governed by minimum reinforcement area needed to support the truss mechanism and the maximum permissible area based on the limit stress corresponding to diagonal compression failure. Horizontal hoop reinforcement has to be designed for 40% of the total horizontal shear force as a minimum requirement (NZS 3101:1995). ACI353R-02 recommends horizontal reinforcement basing on the confinement of the core concrete required to maintain the axial load carrying capacity of the columns.

2.6 Characteristic Behavior of Interior Beam-Column Joint under Lateral Loading

The behavior characteristics of joints due to factored lateral loadings (seismic loading) are quite unique and serious in seismic regions unlike joints designed only for vertical loadings (gravity loading). Most international codes (GB 50010-2002, ACI 318-05, NZS 3101 1995, EC8 2003) specify standards, design factors and design formulae particularly for moment resisting frames under seismic loading. Though various codes attempt to explain the design of joint, little attention was given to the design of reinforced concrete structures. It appears that after the evaluation of working stresses in adjacent members, most designers normally assume that conditions within the joint, which often have somewhat larger dimensions than the members it joined, were not critical. The gradual adoption of the philosophy of limit stage design has exposed the weakness of this assumption. The truth is, joints are often the weakest link in a structural system due to seismic loadings.

The structural demand on joints is greatly affected by the type of loading system and loading path in any type of joint (interior, exterior or corner). Therefore, it is of certain importance to use design procedures in which the severity of each type of loading is properly recognized. For instance, strength under monotonic loading without stress reversals will be the design criterion for continuous reinforced concrete structures subjected to gravity loading only. In other cases, both strength and ductility of the adjoining members under reversed loading will govern the design of joints, like a rigid jointed multistory frame under seismic loading. A large amount of joint reinforcement can be expected for the second case because strength degradation of the concrete under repeated reversal loading will occur.

2.7 Seismic Shear Resistance in Beam-Column Joints

Horizontal shear force of resistance within the joint can be calculated by,

$V_h = (A_{s1} + A_{s2})\, f_{sy}^{*} + C' - V_{col}$ ……..……..(2.13)

where,

A_{s1} = area of tension steel in beam 1

A_{s2} = area of compression steel in beam 2

C' = compressive force in concrete = k f_{ck} b x

f_{sy}* = factored yield strength which allows for over strength (the value of f_{sy}* may be taken to be 1.25 times f_{sy}, the characteristic strength of steel)

b = breadth of the beam

k, x = stress block parameters

f_{ck} = characteristic strength of concrete

V_{col} = net column shear force

This shear V_h is resisted by compressive strut action in the concrete and the horizontal stirrups as shown in Figure 2.14. Conservatively, the area of horizontal stirrups can be calculated for steel of design strength f_y (= f_{sy}/g ; being the partial safety factor of steel) as

$= V_h/f_y$ ……..……(2.14)

ACI 318 . 1999 recommends that the cross-sectional area of horizontal stirrups should not be less than either

$A_{sh} = 0.3 (sh_c f'_c / f_{yh}) [(A_g / A_c) - 1]$ ……(2.15)

or

$A_{sh} = 0.09 sh_c f'_c / f_{yh}$ ……...……..(2.15a)

In the case of circular columns,

$A_{sh} \geq 0.12 sh_c f_c / f_{yh}$ ……..(2.15b)

where,

A_{sh} = area of stirrups and cross-ties,

s = stirrup spacing,

h_c = dimension of the concrete core perpendicular to transverse reinforcement under consideration (centre-to-centre of perimeter reinforcement),

A_g = gross area of the concrete section,

A_c = area of the concrete core (to the outside of the stirrups),

f'_c = concrete cylinder compressive strength,

f_{yh} = yield strength of the stirrups.

The American code also stipulates that the spacing of these transverse reinforcement should not exceed the least of one quarter of the minimum column dimension, six times the diameter of the longitudinal bars to be restrained or Sx given by

$S_x = 100+[(350-h_x)/3]$ ……..……(2.16)

where,

h_x = maximum horizontal spacing of cross ties or hoops.

Recently Saaticioglu and Razvi modified this equation to take into account the allowable storey drift ratio of 2.5 percent

as

$$\rho_c = \frac{0.35f'c}{fyh}\left(\frac{Ag}{Ac} - 1\right)\frac{Pu}{\sqrt{(k2\phi Po)}} \quad \text{……..……(2.17)}$$

where,

r_c = [A_{sh} / (h_c s)], the area ratio of transverse confinement reinforcement

f = Capacity reduction factor (= 0.90)

P_o = Nominal concentric compressive capacity of column

P_u = Maximum axial load on column during earthquake

k_2 = Confinement efficiency parameter [= 0.15 $\sqrt{(b_c b_c)/(ss_1)}$]

b_c = Core dimension, centre to centre of perimeter ties

s = spacing of transverse reinforcement along the column height

s_l = spacing of longitudinal reinforcement, laterally supported by corner of hoop or hook of cross tie.

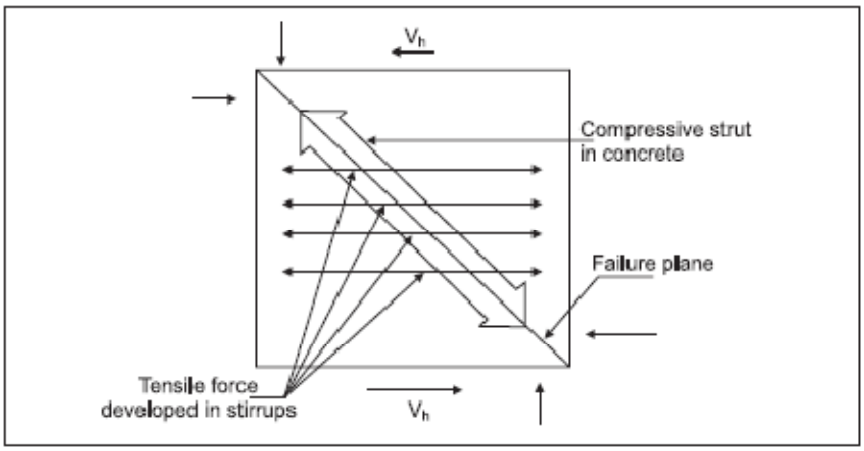

Figure 2.14: Horizontal Shear Resistance in Beam-Column Joint (Uma & Prasad, 2005)

The amount of transverse steel required by equations (2.15) and (2.16) is linearly related to the compressive strength of concrete, f_{ck}. This may result in very large amount of transverse steel when high strength concrete is used.

Stirrups must cross the failure plane shown in Figure 2.14, and be anchored at a distance that is not less than one-third of the appropriate column dimension on each side of it. The maximum spacing of stirrups should not exceed that appropriate to the adjacent column.

2.8 ACI Design Guidelines – General Issues

The ACI 352R-02 design guidelines seek to induce the most desirable governing failure mode at RC beam-column connections (i.e. for their maximum overall response to be controlled by the flexural capacity of longitudinal beam(s) while the joint essentially remains in the cracked elastic region of behavior). This is accomplished by suggesting four types of recommendations, related to the column-to-beam moment strength ratio, the cross-sectional area and spacing of joint transverse reinforcement, the column depth for development of longitudinal beam reinforcement, and the joint shear strength vs. demand.

The recommended minimum column-to-beam moment strength ratio is intended to favor Strong column – weak beam behavior, and it is defined in the form of equation (2.18); that is:

$$\frac{\sum M_c}{\sum M_b} \geq 1.20 \quad \text{.....(2.18)}$$

In equation (2.18), ΣM_c is the summation of column moment strength at a given column axial force and ΣM_b is the summation of beam moment strength without considering the stress multiplier (1.25) for longitudinal reinforcement.

The minimum cross-sectional area and maximum spacing of joint transverse reinforcement are recommended to maintain proper confinement within a joint panel (and to ensure joint shear strength). Maximum spacing of joint transverse reinforcement is the smallest value of one-fourth of the minimum column dimension, six times the diameter of longitudinal column reinforcement, and 150 mm. ACI 352R-02 considers that additional

use of joint transverse reinforcement (above the minimum recommended amount) does not provide any significant improvement in joint shear strength. Thus, the ACI 352R-02 joint shear strength definition is not a function of the amount and spacing of joint transverse reinforcement (assuming that the minimum amount and maximum spacing recommendations will have been met).

The minimum column depth (or available development length for longitudinal beam reinforcement) is recommended to prevent severe bond deterioration within a joint panel. For interior connections, beam reinforcement passes through a joint panel. ACI 352R-02 recommends a minimum column depth; that is:

$$\frac{h_c}{d_b} \geq 20 \frac{f_{by}}{420} \geq 20 \quad \text{……..……..(2.19)}$$

In equation (2.19), hc is the column depth, db is the diameter of beam reinforcement, and f_{by} is the yield stress of beam reinforcement (MPa).

For exterior and knee connections, beam and/or column reinforcement are anchored within a joint panel by using 90-degree standard hooks. ACI 352R-02 also recommends a required development length for hooked beam and/or column reinforcement; that is:

$$l_{dh} = \frac{1.25 f_y d_b}{6.2 f_c^{'}} \quad \text{……...(2.20)}$$

2.9 Minimum Confinement within a Joint Panel

A concrete strut and/or a truss are generally considered to comprise the joint shear resistance mechanism in RC beam-column connections subjected to cyclic lateral loading. When joint shear input demand exceeds the resistance capacity of the concrete strut and truss mechanisms, then joint shear failure is initiated, and it causes excessive volumetric expansion within the joint panel. Thus, possible inadequate confinement provided by horizontal transverse reinforcement could trigger a reduction in joint shear capacity.

Joint transverse reinforcement typically consists of rectangular (closed) hoops and crossties. An “Ash ratio” (provided amount of joint transverse reinforcement divided by the recommended amount, in the direction of loading, following ACI 352R-02) can be used to assess the minimum cross-sectional area of horizontal joint transverse

reinforcement needed for proper confinement within a joint panel. In ACI 352R-02, the recommended cross-sectional area of joint transverse reinforcement is computed using equation (2.21); that is:

A_{sh} = larger $(0.3 \frac{S_h b_c'' f_c'}{f_{yh}} (\frac{A_c}{A_g} - 1)$ and $0.09 \frac{S_h b_c'' f_c'}{f_{yh}})$ ……..(2.21)

In equation (2.21), S_h is the spacing of joint transverse reinforcement; b_c'' is the core dimension of a tied column (outside to outside edge of transverse reinforcement bar); f_{yh} is the yield stress of joint transverse reinforcement; A_g is the gross area of column section; and A_c is the area of column core measured from outside edge to outside edge of hoop reinforcement. If the joint panel is effectively confined on all sides by longitudinal and transverse beams, the required amount of joint transverse reinforcement is $0.5A_{sh}$.

2.9.1 Requirement of Transverse Reinforcement for Joint

According to BNBC 1993, hoop reinforcement will be provided within the joint unless it is confined by the structural member. The requirement of transverse reinforcement of the column is determined by the following equations:

a. The volumetric ratio of spiral or circular hoop reinforcement, ρ_s shall be indicated by the following equation:

   $\rho_s = \frac{0.12 f_c'}{f_{yh}}$ ……..…(2.22)

   and shall not be less

   $\rho_s = 0.45(\frac{A_g}{A_c} - 1)\frac{f_c'}{f_y}$ ……...…(2.23)

b. The total cross-sectional area of rectangular hoop reinforcement shall not be less than that given by the following equations :

   $A_{sh} = 0.3(sh_c f_c'/f_{yh})[(A_g/A_{ch}) - 1]$ ……...(2.24)

   $A_{sh} = \frac{0.09 sh_c f_c'}{f_{yh}}$ ……..……..(2.25)

c. Transverse reinforcement shall be provided by either single or overlapping hoops or cross ties of the same bar size and spacing. Each end of the cross ties shall

engage a peripheral longitudinal reinforcing bar. Consecutive cross ties shall be alternated end for end along the longitudinal reinforcement.

d. If the design strength of member core satisfies the requirements of the specified loading combinations including earthquake effect, equation 2.22 to 2.25 need not be satisfied.

Within the depth of the shallowest framing member, transverse reinforcement equal to at least one-half the amount mentioned above shall be provided where members frame into all four sides of the joint and where each member width is at least three-fourths the column width. At these locations, the spacing of the transverse reinforcement may be increased to 150 mm. Transverse reinforcement shall be provided through the joint to provide confinement for longitudinal beam reinforcement outside the column core if such confinement is not provided by a beam framing into the joint.

The nominal shear strength for the joint shall be taken not greater than the forces:

$1.66\sqrt{f_c'}\ A_j$ for joints confined on all four faces

$1.24\sqrt{f_c'}\ A_j$ for joints confined on three faces or on two opposite faces

$1.0\sqrt{f_c'}\ A_j$ for others.

A member that frames into a face is considered to provide confinement to the joint if at least three-quarters of the face of the joint is covered by the framing member. A joint is considered to be confined if such confining members frame into all faces of the joint.

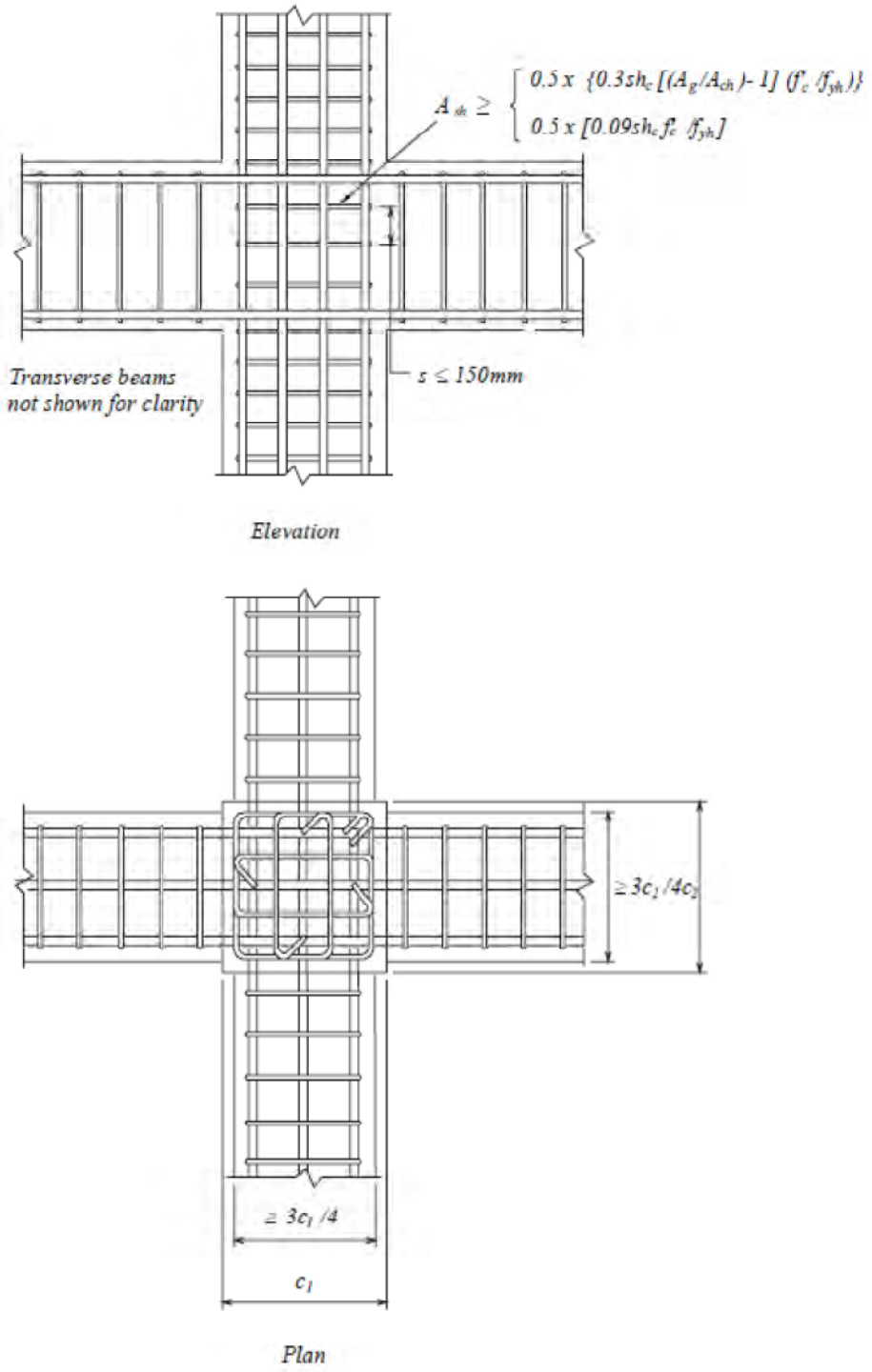

Figure 2.15: Transverse Reinforcement Required for Joint Confined by Structural Member (Source: BNBC(1993))

2.10 Ductility Requirements for Building

2.10.1 Ductility

Ductility can be defined as the “ability of material to undergo large deformations without rupture before failure”. Member or structural ductility is also defined as the ratio of absolute maximum deformation to the corresponding yield. This can be defined with respect to strains, rotations, curvature or deflections. Strain based ductility definition depends almost on the material, while rotation or curvature based ductility definition also includes the effect of shape and size of the cross-sections.

Each design code recognizes the importance of ductility in design because if a structure is ductile it ability to absorb energy without critical failure increases. Ductility behavior allows a structure to undergo large plastic deformations with little decrease in strength.

In general the ductility is increased by,

- An increase in compression steel content.
- An increase in concrete compressive strength.
- An increase in ultimate concrete strain.

And is decreased by,

- An increase in tension steel content.
- An increase in steel yield strength.
- An increase in axial load.

2.10.2 Comparison with Brittle Material

Brittleness is a property of material that will fail suddenly without undergoing noticeable deformations. Brittle structures do not give notice before failure and may collapse and the occupants may not have time to take measures to prevent collapse.

Concrete is an example of brittle material. To avoid failure of structure the structural engineer must take all provisions to increase the ductility of structure. The structural engineer should design a structure functioning as a ductile one. By suitably anchoring the reinforcement, the ductility of a structure can be increased to a greater extent with little increase in cost.

Reinforced concrete structures, unlike steel structures, tend to fracture or fail in a relatively brittle fashion as the ductility or deformation capacity of conventional concrete is limited. In such structures the brittle failure as result of inelastic deformation can be avoided only if the concrete is made to behave in a ductile manner so that the member can absorb and dissipate large amount of energy.

Hence in the case of reinforced concrete members subjected to inelastic deformation, not only strength but also ductility plays vital role in the design. A ductile material is the one that can undergo large strains while resisting loads. Graph shown below also show comparison between brittle and ductile material regarding to deformation.

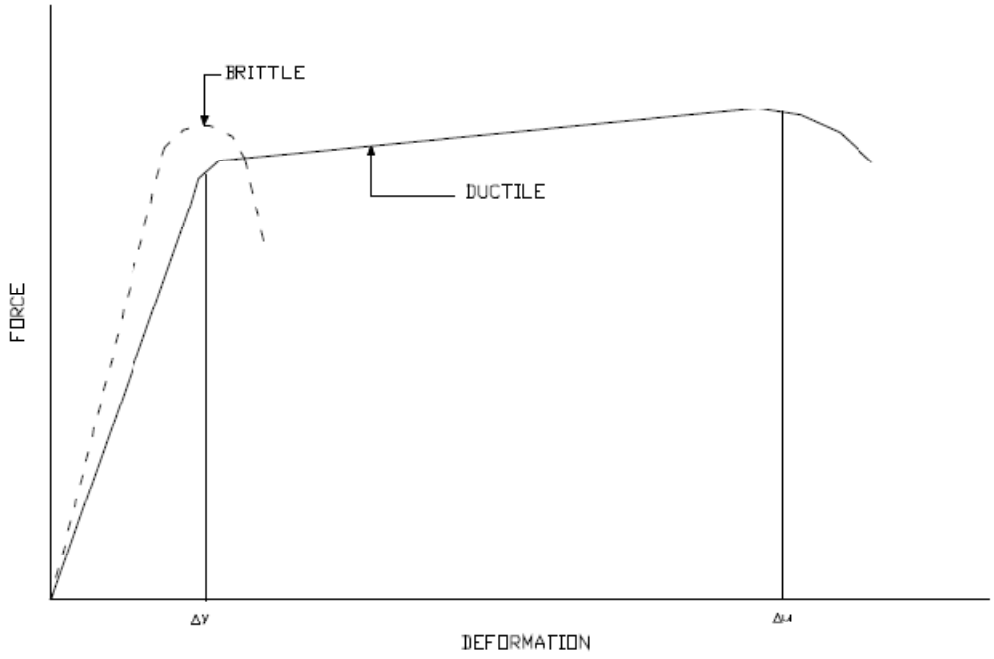

Figure 2.16: Brittle and Ductile Force-Deformation Behavior (IS 1893 – 2002)

2.10.3 Necessity of Ductile Detailing

Ductile detailing is provided in structures so as to give them adequate toughness and ductility to resist severe earthquake shocks without collapse. Ductile detailing is provided for the following structures (ACI):

- The structures is located in seismic zone IV and V.

- The structure is located in seismic zone III and has the important factor (I) greater than 1.
- The structure is located in seismic zone III and is an industrial structure.
- The structure is located in seismic zone III and is more than 5 storeys high.

2.10.4 Variables Affecting Ductility

- Tension steel ratio p_t

The ductility of a beam cross-section increases as the steel ratio p or (p-p0) decreases. If excessive reinforcement is provided the concrete will crush before the steel yields, leading to brittle failure corresponding to $\mu 0=1.0$. In other words, a beam should be designed as under reinforced.

The ductility is directly affected by the values ρa, σck, and δy. the ultimate strain εu is a function of a number of variables such as the characteristic strength of concrete, rate of loading and strengthening effect of stirrups. The code recommends a value of 0.0035 for εu. Ductility increases with the increase in characteristic strength of concrete and decrease with the characteristic strength of steel. In fact, ductility is inversely proportional to square of δy. It suggests that Fe 250 grade mild steel is more desirable from the ductility point of view as compared with the Fe 415 grade or Fe 500 grade high strength steels.

- Compression steel ratio p_c

Compression steel ratio is an important parameter defining the ductility ratio. The ductility increases with the decrease in (p-p0) value, that is, ductility increases with increase in compression steel.

- Shape of cross-section

The presence of an enlarged compression flange in a T-beam reduces the depth of the compression zone at collapse and thus increases the ductility.

- Lateral reinforcement

Lateral reinforcement tends to improve ductility by preventing premature shear failures and by confining the compression zone, thus increasing deformation capability of a reinforced concrete beam.

2.10.5 Ductility Increasing Criteria

Ductility can be increased by -

- Decrease in the% tension steel (p_t).
- Increase in the % compression steel (p_c).
- Decrease in the tensile strength of steel.
- Increase in the compressive strength of concrete (But very high grades of concrete are undesirable).
- Increase in the compression flanges area in flanged beams.
- Increase in the transverse (shear) reinforcement.

2.10.6 Design for Ductility

Following certain simple design details such as can ensure sufficient amount of ductility:

- The structural layout should be simple and regular avoiding offsets of beams to columns, or offsets of columns from floor to floor. Changes in stiffness should be gradual from floor to floor.
- The amount of tensile reinforcement in beam should be restricted and more compression reinforcement should be provided. The latter should be enclosed by stirrups to prevent it from buckling.
- Beams and columns in a reinforced concrete frame should be designed in such a manner that inelasticity is confined to beams only and the columns should be remain elastic. To ensure this, sum of the moment capacities of the columns for the design axial loads at a beam-column joint should be greater than the moment capacities of the beams along each principal plane.

- The shear reinforcement should be adequate to ensure that the strength in shear exceeds the strength in flexure and thus, prevent a non-ductile shear failure before the fully reversible flexure strength of a member has been developed.
- Closed stirrups or spirals should be used to confine the concrete at sections of maximum moment to increase the ductility of members. Such sections include upper and lower ends of columns and within beam-column joints, which do not have beams on all sides. If axial load exceed 0.4 times the balanced axial load, spiral column is preferred.
- Splices and bar anchorages must be adequate to prevent bond failures.
- The reversal of stresses in beams and columns due to reversal of direction of earthquake force must be taken into account in the design by appropriate reinforcement.
- Beam-column connections should be made monolithic.

2.10.7 Ductile Detailing for Flexure Member

- The factored axial stress on the member under earthquake loading shall not exceed $0.1f_{ck.}$
- The member shall have preferably had a width-to-depth ratio of more than 0.3.
- The width of the member shall not be less than 200 mm.
- The depth of the member shall preferably be not less than ¼ of the clear span.

2.10.8 Longitudinal Reinforcement

- The top as well as bottom reinforcement shall consist of at least two bars throughout the member length
- The tension steel ratio on any face, at any section, shall not be less than

$\rho_{min} = 0.24(f_{ck}/f_y)^{1/2}$.

- The maximum steel ratio on any face at any section, shall not exceed $\rho_{max} = 0.025$.
- The positive steel at a joint face must be at least equal to half the negative steel at that face.

2.10.9 Anchorage of Beam Bars in an External Joint

- In an external joint, both the top and the bottom bars of the beam shall be provided with anchorage length, beyond the inner face of the column, equal to the development length in tension plus 10 times the bar diameter minus the allowance for 90 degree bend.
- In an internal joint, both face bars of the beam shall be taken continuously through the column.

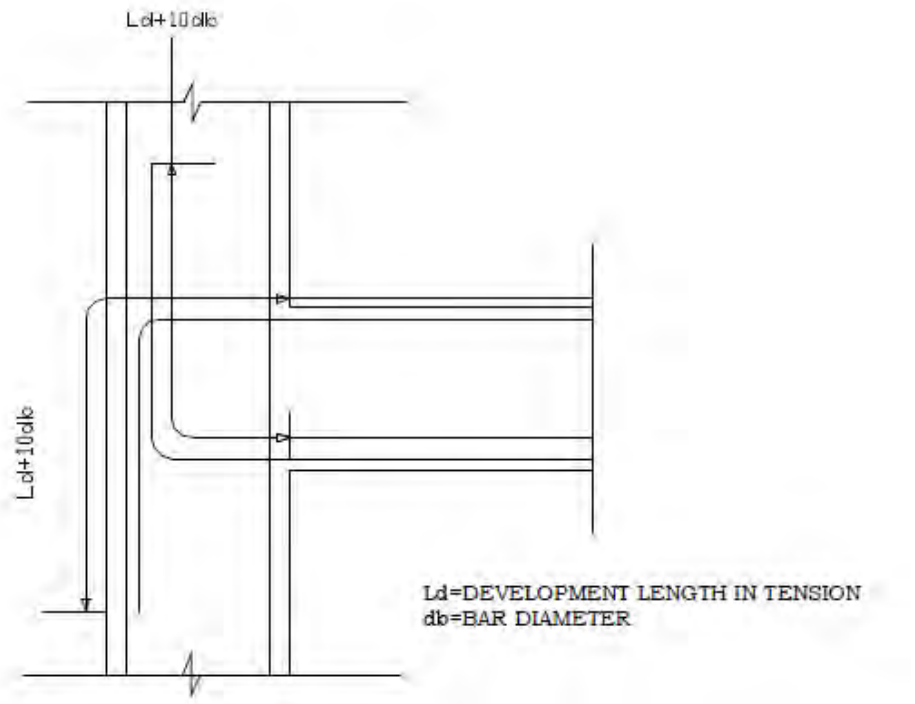

Figure 2.17: Anchorage of Beam Bars in External Joints (IS 1893 – 2002)

Purpose:

Flexure members of lateral force resisting ductile frames are assumed to yield at the design earthquake load. To ensure proper development of reversible plastic hinges near continuous supports (beam column connections) where they are usually develop in such members.

2.10.10 Lap, Splice in Beam

- The longitudinal bars shall be spliced, only if hoops are provided over the entire splice length, at spacing not exceeding 150 mm.

Purpose

For confining the concrete and to support longitudinal bars.

- The lap length shall not be less than the bar development length in tension.
- Lap splices shall not be provided

  Within a joint

  Within a distance of 2d from joint face

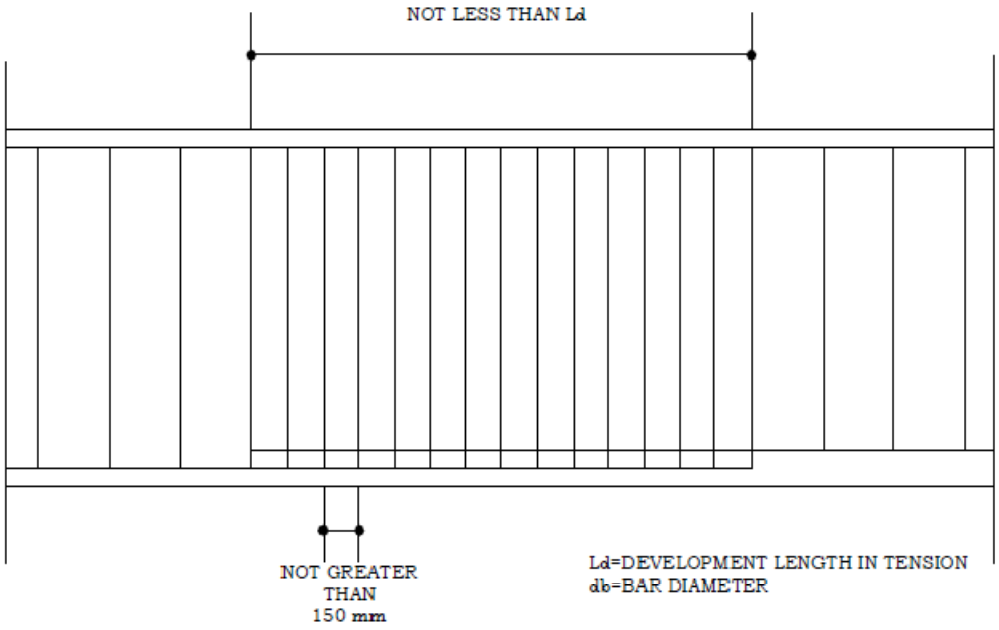

Figure 2.18: Lap, Splice in Beam (IS 1893 – 2002)

Within a quarter length of the member where flexural yielding may generally occur under the effect of earthquake forces.

- Not more than 50% of the bars shall be spliced at one section.

Purpose:

To avoid the possibility of spalling of concrete cover under large reversed strains.

2.10.11 Beam Reinforcement

- The spacing of hoops over a length of 2d at either end of a beam shall not exceed
  d/4
  8 times the diameter of the smallest longitudinal bar (it must not less than 100 mm).
- The first hoop shall be at a distance not exceeding 50 mm from the joint face.
- Vertical hoops at the same spacing shall also be provided over a length equal to 2d on either side of a section where flexural yielding may occur under the effect of earthquake forces.
- Elsewhere, the beam shall have vertical hoops at a spacing not exceeding d/2.

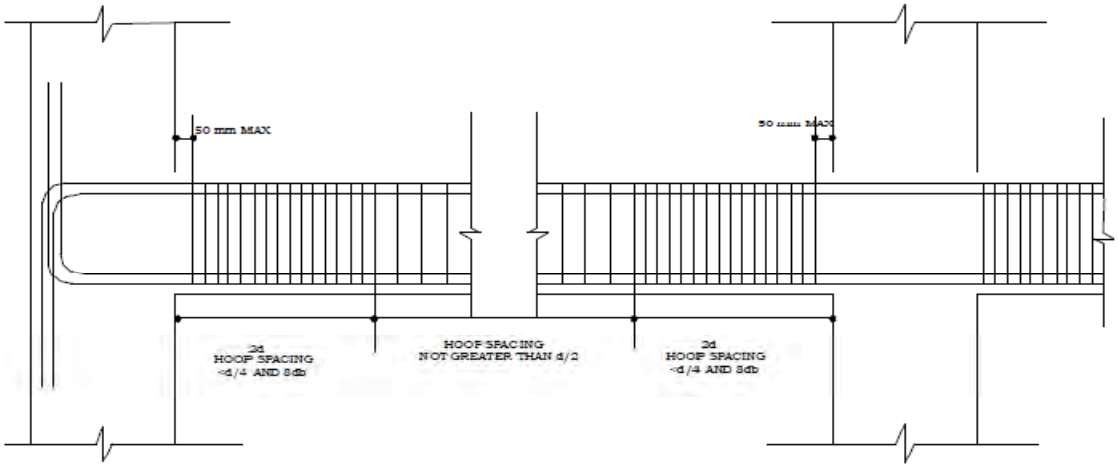

Figure 2.19: Beam Reinforcement (IS 13920 – 1993)

2.10.12 Provision of Special Confining Reinforcement in Footing

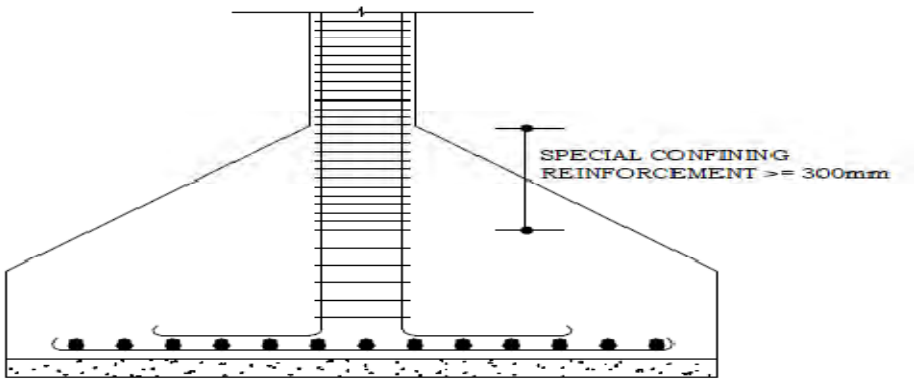

Figure 2.20: Provision of Special Confining Reinforcement in Footing (IS 13920 – 1993)

- When a column terminates into a footing or mat, special confining reinforcement shall extend at least 300 mm into the footing or mat.

2.10.13 Column and Joint Detailing

- Lap splice shall be provided only in the central half of the member length. It should be proportioned as a tension splice. Hoops shall be provided over the entire splice length at spacing not exceeding 150mm center to center. Not more than 50% of the bars shall be spliced at one section.
- The spacing of the hoops shall not exceed half the least lateral dimension of the column, except where special confining reinforcement is provided.
- Special confining reinforcement shall be provided over a length l0 from each joint face, towards mid-span, and on either side of any section, where flexural yielding may occur under the effect of earthquake forces.
- The length l0 shall not be less than
  Larger lateral dimension of the member at the section where yielding may occurs
  1/6 of the clear span of the member
  450mm.
- The special confining reinforcement as required at the end of column shall be provided through the joint.
- A joint, which has beams framing into all vertical faces of it and where each beam width is at least ¾ of the column width, may be provided with half the special confining reinforcement required at the end of the column. The spacing of the hoops shall not exceed 150 mm.

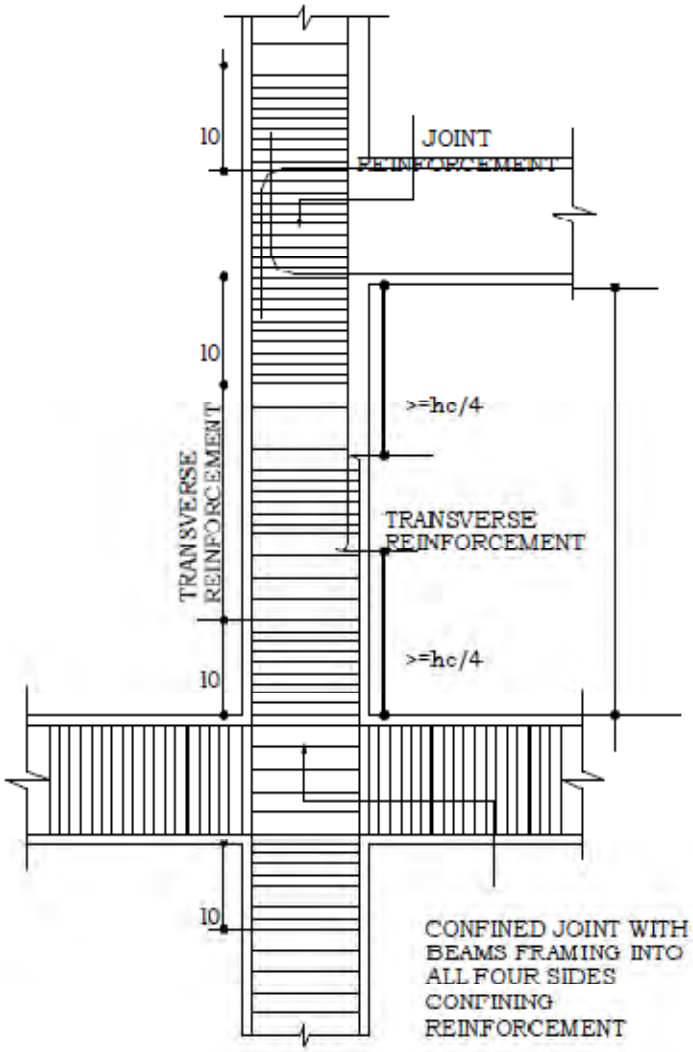

Figure 2.21: Column and Beam-Column Joint Detailing (IS 13920 – 1993)

2.11 Ductility of the Structure

It is essential that an earthquake resistant structure should be capable of deforming in a ductile manner when subjected to lateral loads in several cycles in the inelastic range. The structures subjected to cyclic loading need to dissipate the energy stored in it. Dissipation of energy can be explained by a simple phenomenon exhibited by an oscillator with a single degree of freedom as shown in Figure 2.22.

In the elastic response, the oscillator has the maximum response at *a*. The area *oab* represents the potential energy stored when maximum deflection occurs. The energy is converted into kinetic energy when the mass returns to zero position. Figure 2.22 (b) shows the oscillator forming a plastic hinge at a much lower response *c* when the deflection response continues along *cd, d* being the maximum response. The potential energy at the maximum response is now represented by the area *ocde*. When the mass returns to zero position, the part of the potential energy converted to kinetic energy is represented by *fde*, while the other energy under the area *ocdf* is dissipated by the plastic hinge by being transferred into heat and other forms of irrecoverable energy. From this, it can be concluded that the response in elastic state of a structure differs significantly from the response of the same structure in elasto-plastic state where potential energy converts to kinetic and other forms of irrecoverable energy.

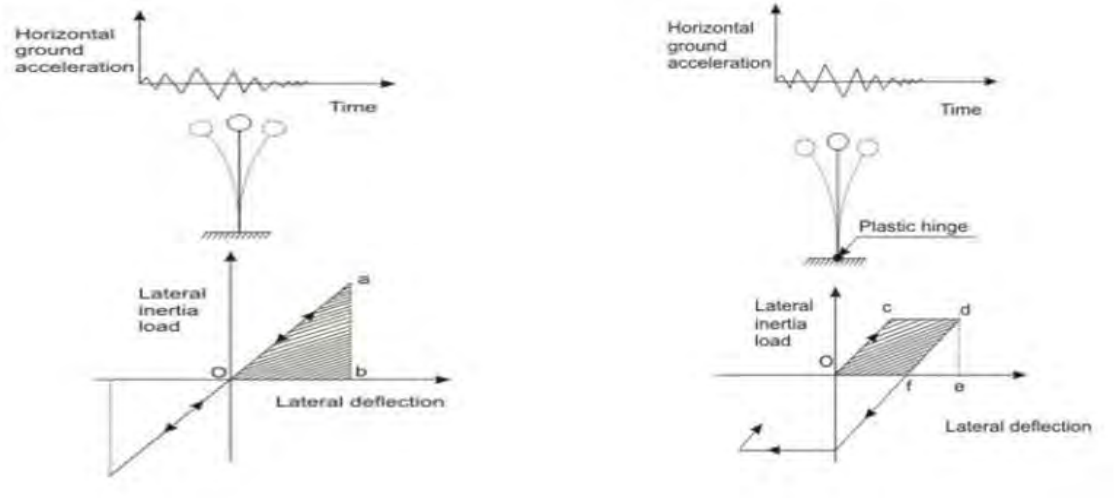

a) Elastic Response b) Elasto-Plastic Response

Figure 2.22: Response of a Structure with Single Degree of Freedom

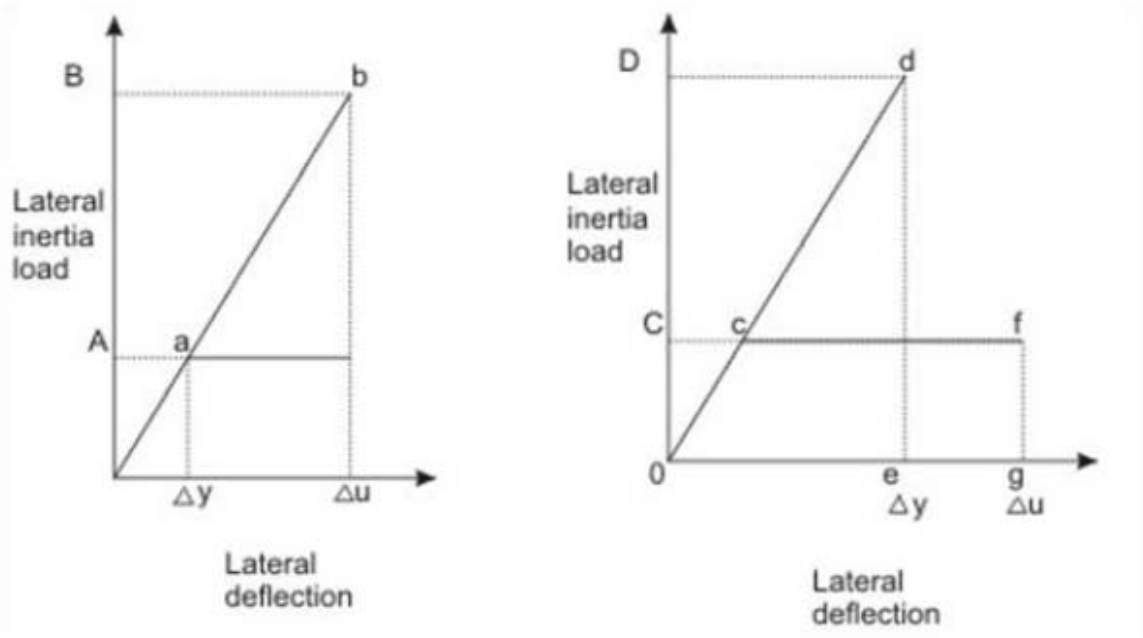

Figure 2.23: Ductility of the Structure (Ray W. Clough, 1993)

The displacement ductility factor μ, a measure of ductility of a structure, is defined as the ratio of Δ_u, and Δ_y, where Δ_u and Δ_y are the respective lateral deflections at the end of post elastic range and when the yield is first reached. Thus, we have

μ (with respect to displacement) = Δ_u / Δ_y

The values of displacement ductility factor should range from 3 to 5. In a similar manner, the rotational ductility factor μ is defined as the ratio of θ_u and θ_y, where θ_u and θ_y are the respective rotations of at the end of post-elastic range and at the first yield point of tension steel. Thus, we have μ (with respect to rotation) = θ_u / θ_y.

2.11.1 Displacement Ductility Factor

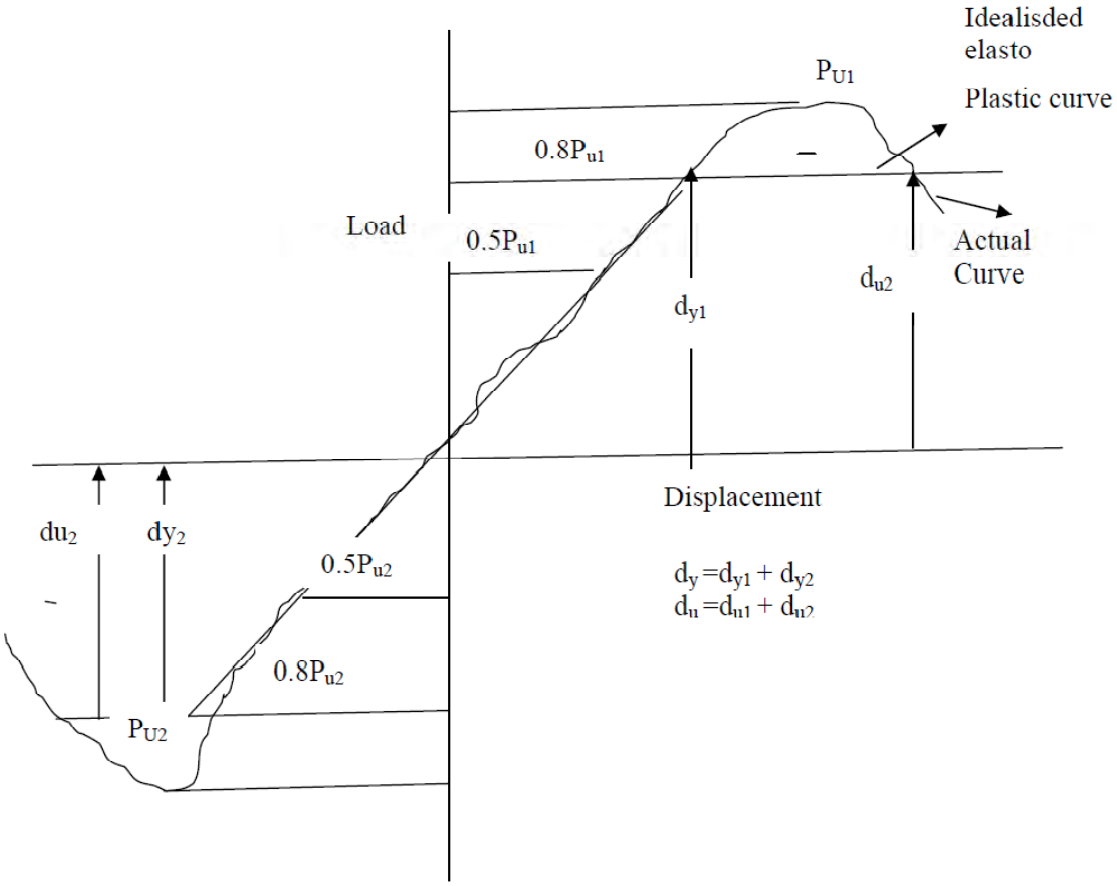

Figure 2.24: Method Used to Define the Yield and Ultimate Displacements (Source: Uma and Prasad, 2005)

2.12 Stiffness Behavior

Stiffness is defined as the load required to causing unit deflection of the beam-column joint. Stiffness is termed as the ratio of load to the corresponding displacement. In the case of reinforced concrete beam-column joints, stiffness of the joint gets reduced when the joint is subjected to cyclic/repeated/dynamic loading. This reduction in stiffness is due to the following reasons.

During cyclic loading, the materials, viz. concrete and steel, are subjected to loading, unloading, and reloading processes. This will cause initiation of micro-cracks inside the joint and will sometimes lead to the fatigue limit of the materials. This, in turn, increases the deformations inside the joints, thus resulting in reduction in the stiffness. Hence, it is necessary to evaluate degradation of stiffness in the beam-column joints subjected to cyclic or repeated loading.

2.12.1 Stiffness Recommendations

When analyzing a special moment frame, it is important to appropriately model the cracked stiffness of the beams, columns, and joints, as this stiffness determines the resulting building periods, base shear, story drifts, and internal force distributions. Table 2.1 shows the range of values for the effective, cracked stiffness for each element based on the requirements of ACI 318 - 8.8.2. For beams cast monolithically with slabs, it is acceptable to include the effective flange width of ACI 318 - 8.12.

Table 2.1**:** Cracked Stiffness Modifiers

Element	I_e/I_g
Beam	0.35-0.50
Column	0.50-0.70

More detailed analysis may be used to calculate the reduced stiffness based on the applied loading conditions. For example, ASCE 41 recommends that the following (Table 2.2) *Ie*/*Ig* ratios be used with linear interpolation for intermediate axial loads.

Table 2.2**:** ASCE 41 Supplement No. 1

Effective Stiffness Modifiers for Columns

Compression Due to Design Gravity Loads	I_e/I_g
$\geq 0.5 A_g f_c^{'}$	0.7
$\leq 0.1 A_g f_c^{'}$	0.3

Note that for beams this produces *Ie*/*Ig* = 0.30. When considering serviceability under wind loading, it is common to assume gross section properties for the beams, columns, and joints.

ACI 318 does not contain guidance on modeling the stiffness of the beam-column joint. In a special moment frame the beam-column joint is stiffer than the adjoining beams and columns, but it is not perfectly rigid. As described in ASCE 41 (including Supplement No. 1) the joint stiffness can be adequately modeled by extending the beam flexibility to the column centerline and defining the column as rigid within the joint.

2.13 M - ϕ Characteristics

Modern technology in concrete construction is to use high strength or high performance concrete which ultimately reduces the member sizes and proportions. Such reduction in the cross section of structural components, specially in a framed structure, results in more flexible structural system for which the sway characteristics are becoming more and more important from the serviceability point of view. Correct and rational prediction of such sway characteristics of reinforced concrete (RC) framed structures eventually necessitates the knowledge of the semi-rigid characteristics of joints. In a RC framed structure, beam to column joints are perhaps among the most complicated yet one of the least understood components of a building system. Proper understanding of the joint characteristic is one of the most challenging fields among researchers.

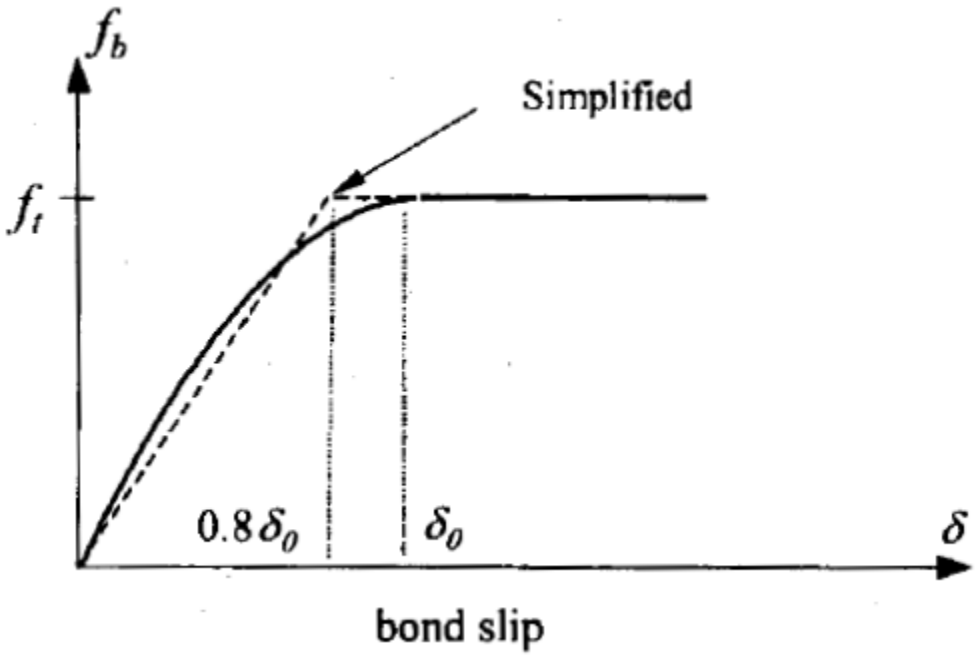

Figure 2.25: Bond Stress Vs Slip Relationship (Dorr, 1980)

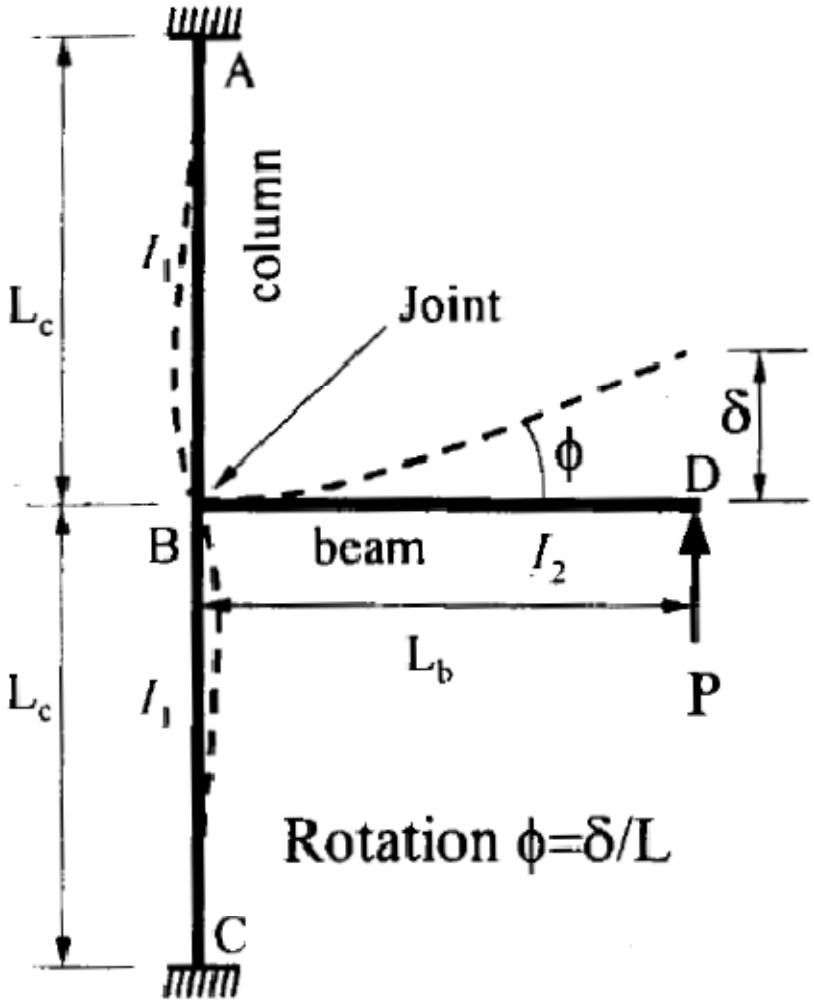

Figure 2.26: The Beam-Column Joint Moment-Rotation Criteria (Chen and Liu, 1983)

It has been recognized that the key to appreciating the effects of joint performance on the behavior of frames is the knowledge of the connection's moment-rotation (M-ϕ) characteristics. The primary distortion of a connection is the rotational deformation ϕ, caused my moment M. Methods have been proposed for calculating the M-ϕ relationship for semi-rigid connections, but most M-ϕ curves must be determined experimentally. The American Concrete Institute report ACI 352R-91, suggests that the designer should consider the possible effect of joint rotations on cracking and deflection. Figure 2.26 shows beam-column joint Moment-rotation calculating criteria.

2.14 Literature Review on Earlier Research

2.14.1 Xilin Lu et al. (2011)

Xilin Lu et al. (2011) carried out the experiment on ten full-scale interior beam-column specimens constructed with various additional reinforcement details and configurations. The results of the experiment showed that adding additional bars is a promising approach in reinforced concrete structures where earthquakes are eminent. In terms of overall cracking observation during the test, the specimens with additional bars (diagonal and straight) compared with the ones without them showed fewer cracks in the column. Furthermore, concrete confinement is certainly an important design measure as recommended by most international codes.

2.14.2 Shiohara et al. (2010)

Shiohara et al. 2010 carried out the experiment on twenty interior beam column joints on a one third scale. They investigated the effects of design parameters of joints on lateral capacity and post yielding behavior. Three major parameters of the test program were (1) amount of longitudinal reinforcement, (2) column-to-beam flexural strength ratio, and (3) column-to-beam depth ratio. The test results indicate that maximum story shear of some specimens fall 5% to 30% short of the story shear calculated from the flexural strength of the beam or the column, although the joints have some margin of the nominal joint shear strength by 0% to 50% compared to the calculated values by a current seismic provision. The extent of insufficiency in the story shear was larger if the flexural strength of the column is equal or nearer to the flexural strength of the beam, and if the depth of the column is larger than that of the beam. This kind of design parameters are common to the existing reinforced concrete buildings and not addressed in many seismic design codes.

2.14.3 Shiohara (2008)

Shiohara 2008 reexamined twenty reinforced concrete interior beam-to-column joint failed in joint shear. The data indicated that joint shear stress had increased in the most specimens, even after apparent joint shear failure starts, while beam moment decreases due to decrease of flexural resistance which is caused by reduction of distance between stress resultants in beam at column face. The cause of the deterioration of story shear is identified to be a degrading of moment resistance of joint, originated from a finite upper limit of anchorage capacity of beam reinforcements through the joint core. To reflect the fact, Hitoshi introduced a new mathematical model and proposed a new approach for the design of beam-to-column joint in seismic zone based on the prediction of the model.

2.14.4 Pampanin et al. (2002)

Pampanin et al. 2002 carried out an experiment on six different types of exterior and interior joints designed for gravity loads only. Plane reinforcement was used in the test models. Structural inadequacies, as typical of the Italian construction practice before the introduction of seismic code provisions in the mid- 70's were reproduced. The combined use of smooth reinforcing bars with end-hook anchorage as well as lack of any capacity design considerations showed to be a critical source of significantly brittle damage mechanisms as in the case of exterior joints, where additional sources of shear transfer mechanisms cannot develop after first diagonal cracking in the joint. An apparent satisfactory level of deformability as well as ductility, due to the combined effects of slippage phenomena and low column reinforcement ratio, were observed in knee and interior cruciform subassemblies, where no joint degradation occurred and column flexural damage dominated the behavior. Moreover, the comparison of different anchorage solutions for beam-bars in interior specimens showed a higher deformability due to slippage phenomena, without resulting in flexural strength reduction. When considering the overall seismic behavior of a frame structure, the implications of the aforementioned flexural damage on the overall seismic behavior might be significant, with soft storey mechanisms being likely to occur at early stages.

2.14.5 Joh et al. (2000)

Osamu et al 2000 conducted test on RC interior beam-column sub-assemblages using plane and three-dimensional frame specimens. The influence of joint shear input and bond condition of beam bars on frame behavior after beam yielding was examined, in particular about joint concrete deterioration in large displacement. Following results were derived from two experimental studies. 1) Bond condition of beam bars within joint did not make large influence on energy dissipation of frame, if joint shear deterioration occurred after beam yielding. 2) Joint shear strength was increased by the existence of transverse beams, because they behaved confinement of joint core concrete. 3) The damage of joint core concrete occurred during one way loading up to large displacement made weak in frame performance at following perpendicular loading. 4) If the excess of joint shear strength to beam flexural is enough large, the damage in joint concrete would not make unfavorable effect on frame ductility.

CHAPTER 3

EXPERIMENTAL PROGRAM

3.1 Introduction

This chapter presents the experimental program of this research consisting of sample preparation of half scale models of concrete frames. The chapter describes the method of the research work, design specification, casting, curing and coloring. The major properties of the material used for construction and the techniques for construction are also illustrated. To study the effect of tie at joint region, seven reinforced concrete beam-column joints with different column to beam cross-section ratios have been tested.

3.2 Test Procedure

A comprehensive study was carried out to investigate the cyclic loading behavior of beam-column joints with and without adequate ties at joint region. Seven half-scale specimens of reinforced concrete beam-column joints were prepared. There were three categories of specimens depending on numbers of stirrups and ties in joint members and column to beam section ratio. Those are a) specimens of joint region with and without seismic ties in column b) specimens implementing conventional and seismic stirrups in beam and ties in column c) specimens with varying column to beam cross-section ratios. Each joint consisted 1.5m length of column and 2m length of beam.

A total of seven specimens of beam-column joints were prepared under the three categories of beam-column joints:

1. Two specimens of beam-column joint were prepared considering equally wide column and beam with and without seismic stirrups in beam and ties in column. In each specimen, beam and column cross sections were taken 150 mm x 150 mm and 150 mm x 150 mm respectively; thus, the ration of column to beam cross-sectional areas turned out to be 1. Seismic spacing of stirrups and ties were considered. (Figure 3.3 and 3.4)
2. Two specimens of beam-column joint were prepared considering wider column than beam width with and without seismic stirrups in beam and ties in column. In

each specimen, the beam and column cross sections were taken 125 mm x 125 mm and 150 mm x 150 mm respectively; thus, the ratio of column to beam cross-sectional areas turned out to be 1.44. Seismic spacing of stirrups and ties were considered. (Figure 3.3 and 3.4)

3. Two specimens of beam-column joint were prepared considering wider beam than column width with and without seismic stirrups in beam and ties in column. In each specimen, the beam and column cross sections were taken 175 mm x 175 mm and 150 mm x 150 mm respectively; thus, the ratio of column to beam cross-sectional areas turned out to be 0.73. Seismic spacing of stirrups and ties were considered. (Figure 3.3 and 3.4)
4. One specimen of beam-column joint was prepared considering equally wide column and beam without seismic stirrups in beam and ties in column. In the specimen, beam and column cross sections were taken 150 mm x 150 mm and 150 mm x 150 mm respectively; thus, the ration of column to beam cross-sectional areas turned out to be 1. Conventional spacing of stirrups and ties were considered. (Figure 3.5)

The specimens were subjected to cyclic incremental vertical loading on the beam ends with sustained gravity load on the center of the column. The vertical cyclic loads were applied about 762 mm from the column vertical axis. Different crack patterns were observed for different categories of specimens. The experimental data obtained in four deflection controlled cycles were used to study overall performance. Load-displacement as well as moment-rotation characteristics were obtained. At the same time maximum loads, loads at first crack formation, maximum as well as residual deflections and secant stiffness were calculated.

3.3 Selection and Preparation of Test Specimen

The test specimen models were selected considering a full scale six storied RC Frame Structured Building as shown in Figure 3.1. The building was analyzed following BNBC (1993) codes and specifications. An interior joint at the mid height of the structure was selected for the experimental program as shown in Figure 3.2. Considering the existing laboratory set up an half scale model was finally selected.

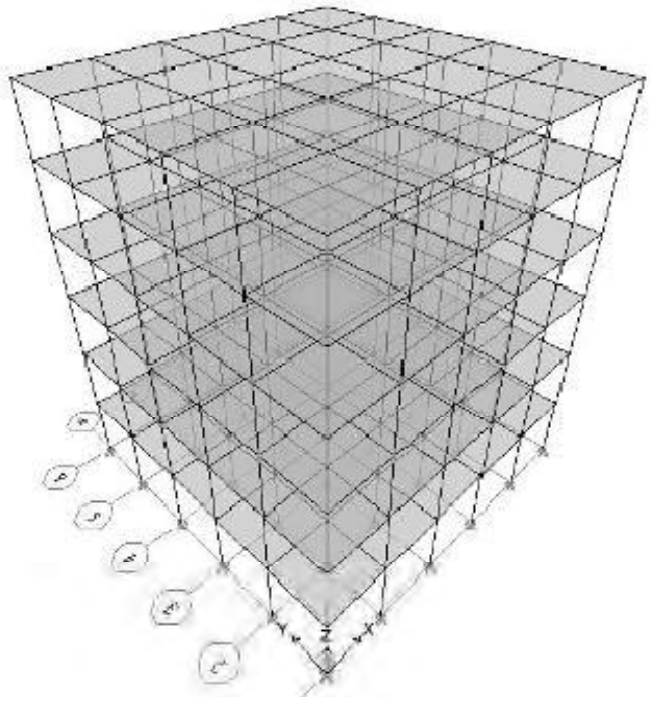

a) 3D view of building model using ETABS

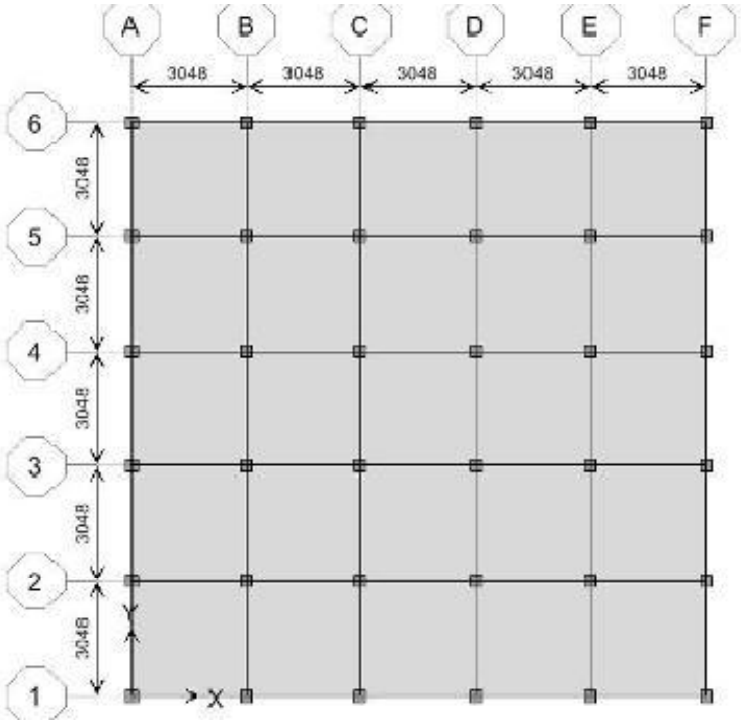

b) Plan view of the building model

Figure 3.1: 3D and Plan View of the Structure

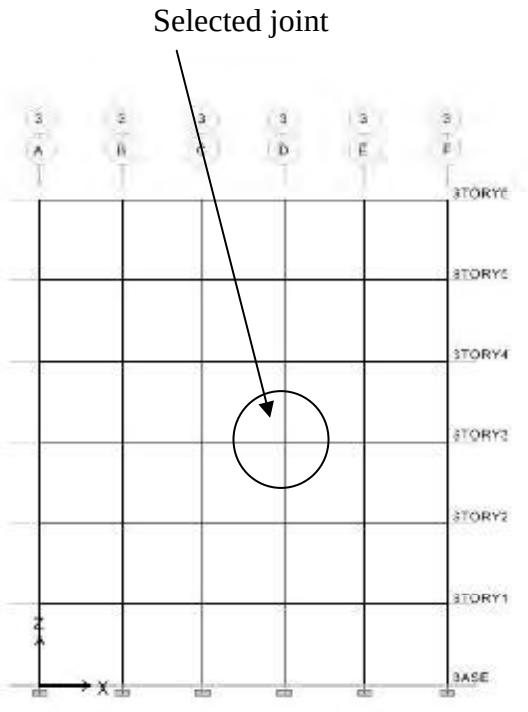

Figure 3.2: Selection of the Test Model

3.4 Typical Test Specimen Model

All specimens are divided in three categories. Category A represent joints with seismic ties, category B interprets joints without seismic ties and category C stands for joint with conventional spacing of stirrups.

Type 1: There were two models of similar specimens.

Column size: 150 mm x 150 mm

Main Bars: 6-∅10 mm deformed bars; Shear Reinforcement: ∅ 8 mm for ties @ 75 mm c/c for middle $\frac{2}{3}$ length and rest $\frac{1}{3}$ length @ 150 mm c/c with 90 degree hook

Beam size: 125 mm x 125 mm

Main Bars: 2-∅10 mm top bars and 2-∅10 mm bottom bars; Shear Reinforcement: ∅ 8 mm for stirrup @ 75 mm c/c for middle $\frac{2}{3}$ length and rest $\frac{1}{3}$ length @ 150 mm c/c with 90 degree hook

The ratio of column to beam cross-sectional areas: 1.44

Beam Column Connection: One shear reinforcement of ∅8 mm for category A and no shear reinforcement for category B.

Type 2: There were three models of similar specimens.

Column size: 150 mm x 150 mm

Main Bars: 6-∅ 10 mm deformed bars; Shear Reinforcement: ∅ 8 mm for ties @ 75 mm c/c for middle $\frac{2}{3}$ length and rest $\frac{1}{3}$ length @ 150 mm c/c with 90 degree hook. For category C ∅ 8 mm @150 with 90 degree hook

Beam size: 150 mm x 150 mm

Main Bars: 3-∅ 10 mm top bars and 2-∅ 10 mm bottom bars; Shear Reinforcement: ∅ 8 mm for stirrup @ 75 mm c/c for middle $\frac{2}{3}$ length and rest $\frac{1}{3}$ length @ 150 mm c/c with 90 degree hook. For category C ∅ 8 mm @150 c/c with 90 degree hook

The ratio of column to beam cross-sectional areas: 1.00

Beam Column Connection: Two shear reinforcements of ∅ 8 mm for category A and no shear reinforcement for category B and category C.

Type 3: There were two models of similar specimens.

Column size: 150 mm x 150 mm

Main Bars: 6-∅ 10 mm deformed bars; Shear Reinforcement: ∅ 8 mm for ties @ 75 mm c/c for middle $\frac{2}{3}$ length and rest $\frac{1}{3}$ length @ 150 mm c/c with 90 degree hook

Beam size: 175 mm x 175 mm

Main Bars: 3-∅ 10 mm top bars and 3-∅ 10 mm bottom bars; Shear Reinforcement: ∅ 8 mm for stirrup @ 75 mm c/c for middle $\frac{2}{3}$ length and rest $\frac{1}{3}$ length @ 150 mm c/c with 90 degree hook

The ratio of column to beam cross-sectional areas: 0.73

Beam Column Connection: Three shear reinforcements of ∅ 8 mm for category A and no shear reinforcement for category B.

Length of column = 1500 mm, length of beam = 2000 mm. f_{ck} = 32 N/mm^2 = 32 MPa, f_y = 550 N/mm^2 = 550 MPa. Column factor load is 100 kN (10 tons). Half scale dimensions were considered.

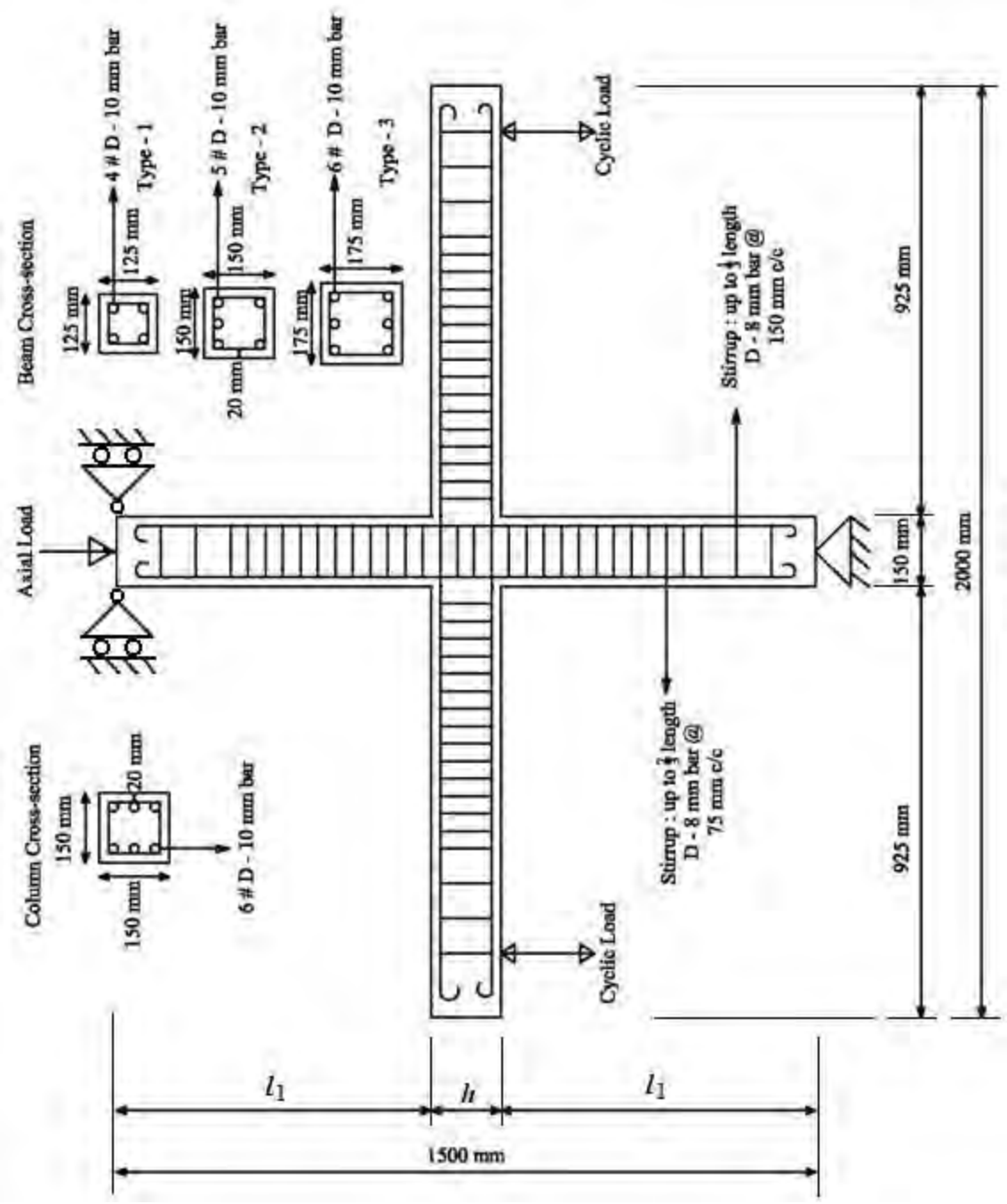

where, l_1 = (1500 – h)/2 and h = depth of the beam

Figure 3.3: Beam-column Joints with Ties at Joints (Type – 1A, 2A, 3A)

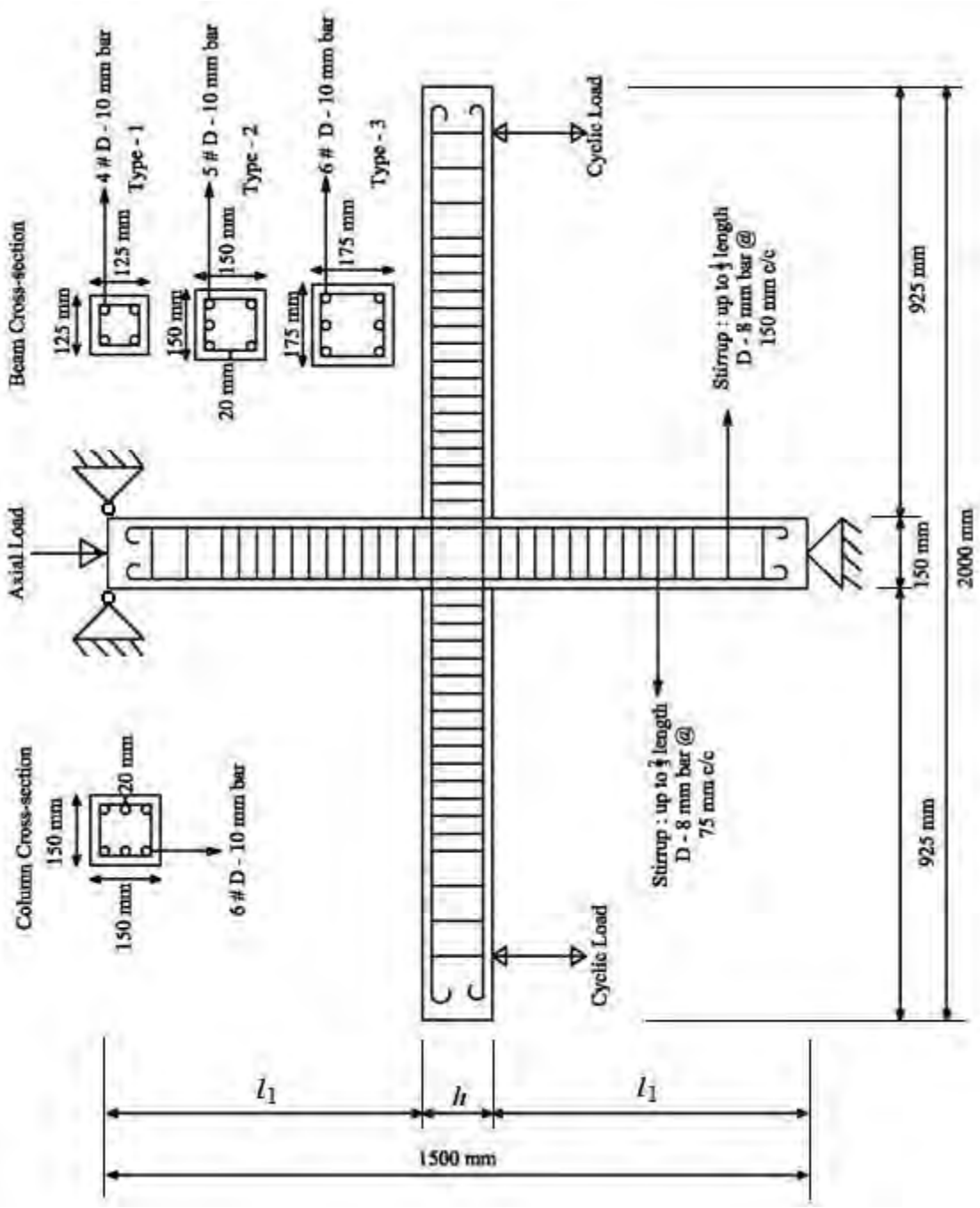

where, l_1 = (1500 – h)/2 and h = depth of the beam

Figure 3.4: Beam-column Joints without Ties at Joints (Type – 1B, 2B, 3B)

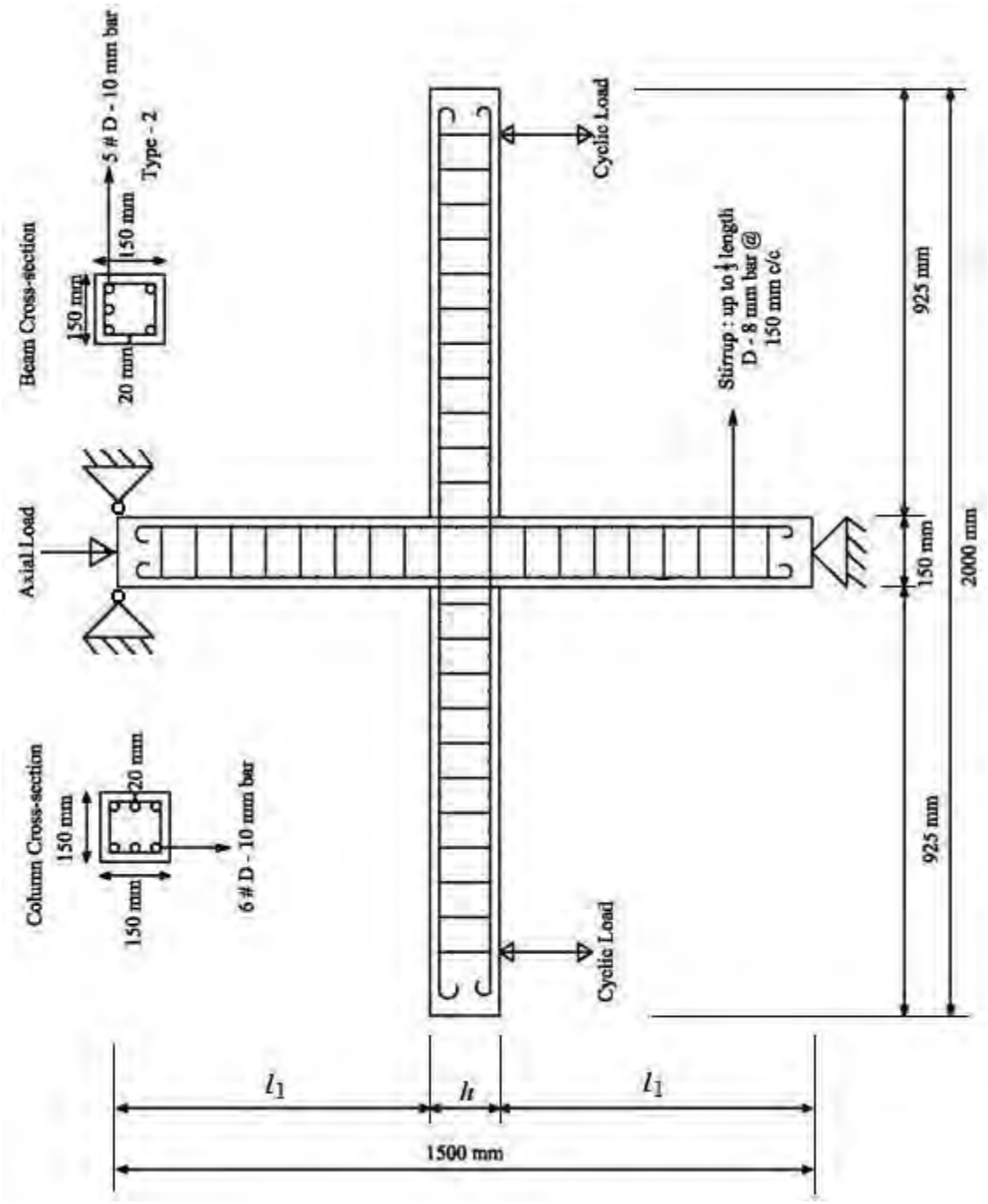

Where, l_1 = (1500 – h)/2 and h = depth of the beam

Figure 3.5: Conventional Beam-column Joint of without Ties at Joint (Type – 2C)

3.5 Material Properties

The constituent materials used for the beam-column joints were cement, coarse aggregates, fine aggregates, reinforcement and water. Normal tap water of potable quality was used in preparing concrete mixture for all the test beam-column joints. The strength, durability and elastic properties of concrete are greatly influenced by the quality of cement. It is essential to know about the strength of cement and the physical properties of aggregates, which constitute the body of concrete. Two types of aggregates were used – fine aggregate and coarse aggregate.

3.5.1 Sand

Sand is treated as fine aggregate to use in the cement concrete to fill the voids of coarse aggregates and Neville (1995) used 35% to 45% by mass of total aggregates. Physical and chemical properties of the sand influence the strength and durability of concrete. Coarse Sylhet sand and fine river sand had been used for all specimens. Sylhet sand is a natural sand produced by erosion of natural rocks. Important qualities of sand those influence the quality of fresh and hardened concrete are specific gravity, absorption capacity, moisture content, grading and chemical properties. If the dry sand absorbs large amount of water then w/c ratio of the fresh concrete will be changed and if the sand contains free water then the free water participates in the hydration process affecting the design strength of concrete. Gradation of fine aggregates has direct impact on workability of fresh concrete and strength of hardened concrete. Higher percentage of fines will add to workability of fresh concrete (Neville,1995).

The Fineness Modulus (FM) of sands can range from 1.75 to 2.93 within the gradation limit of ASTM C 144 (BNBC 1993). Sylhet Sand and local river sand had been mixed in 1:1 proportion. FM of mixed sands had been found 2.71.

3.5.2 Coarse Aggregate

Strength and durability of concrete depend on the type, quality and size of the aggregates. In Bangladesh, stone particles and brick chips are mostly used as coarse aggregate. According to BNBC (1993) maximum size of the aggregates should not exceed $1/5^{th}$ of

the narrowest dimension between two sides, 1/3rd depth of the slab and 3/4th of the clear spacing between the reinforcing bars and the form works (BNBC 1993).

Coarse aggregates (stone chips) had been made from crushing good quality stone and 10 mm down grade stone chips had been collected for the model preparation. Absorption capacity and moisture content of the coarse aggregate influence the property of the fresh concrete by altering the w/c cement ratio. Absorption capacity of the stone aggregates should not exceed 15-20% of its weight.

3.5.3 Cement

Cement is the binding material used for providing strength to the concrete. The properties of the cement depend on chemical constituents of the cement. The most important properties of the cement are hydration, setting, fineness and strength. For Portland cement, the specification should conform to ASTM C150 (BNBC1993). For controlled and strengthened specimens Portland Cement CEM-I had been used.

3.5.4 Reinforcement

Reinforcing bars are used to take high tension, compression and shear forces induced in the concrete member. Transfer of forces between concrete and the reinforcement depends on the bond strength between them. At present, all commercial reinforcing bars are deformed bars and have better bond performance with concrete than the plain reinforcing bars.

Two types of reinforcing bars were used in the construction of seven specimens specified as Φ 8 mm and Φ 10 mm bar. 500W steel bars were used as reinforcement with a characteristic yield stress of 550 MPa verified by Universal Testing Machine. The frames in all groups were characterized by steel reinforcement ratio = A_s/bd. Specimen at the Universal Testing Machine are given in the Figure 3.6 and 3.7. Material properties of reinforcement tested in the laboratory are in the Table 3.1.

Figure 3.6: UTM Test Set-up of 8 mm Reinforcement Bar

Figure 3.7: UTM Test Set-up of 10 mm Reinforcement Bar

Table 3.1: Material Properties of Reinforcement

SL No.	Dia (mm)	Weight (gm)	Length (cm)	Cross-section Area, A_s (mm^2)	Yield Load, YL (N)	Ultimate Load (N)	Yield Strength $f_y = \frac{YL}{As}$ (MPa)	Average Yield Strength, f_y (MPa)	Elog-ation (%)
1.	08	233	60.70	50.27	27926.3	33669.45	555.53	564.31	11
2.	08	232	60.60	50.27	28368.1	33227.67	564.31		14
3.	08	233	60.70	50.27	28809.9	33669.45	573.10		12
1.	10	430	60.20	78.54	44400.0	52392.00	565.32	570.97	14
2.	10	433	60.40	78.54	44844.0	52836.00	570.97		13
3.	10	435	60.50	78.54	45288.0	53280.00	576.62		15

Provide yield strength of steel, f_y = 550 N/mm^2 = 550 MPa.

3.5.5 Concrete

Concrete became very popular in 19th century; however, its limited tension resistance prevented its wide use in construction. To overcome this weakness, steel bars are embedded in concrete to form a composite material called reinforced concrete.

The concrete used for the preparation of beam-column joints was made from Portland cement, stone chips as the coarse aggregate, Sylhet sand and normal sand (1:1) as the fine aggregate. The maximum size of coarse aggregate was 12.5 mm. The aggregates used for concreter work are shown in the Figure 3.8 and 3.9.

Figure 3.8: Fine Aggregate Used for Concrete

Figure 3.9: Coarse Aggregate Used for Concrete

The proportion of ingredients in concrete was Cement: Fine Aggregate: Coarse Aggregate = 1 : 1.65 : 3.45 (in Wt) = 1 : 1.5 : 3 (in Volume). Water cement ratio (W/C) was 0.45. The concrete was mixed by mixer machine as shown in Figure 3.10. Workability measurement was carried out on the fresh concrete as slump value, was approximately 40 mm, as shown in Figure 3.11. The shrinkage factor 1.5 was used.

Figure 3.10: Production of Fresh Concrete

Figure 3.11: Slump Test of Fresh Concrete

3.5.6 Strength of Concrete

A measurement on hardened concrete was conducted as compressive strength according to standard EN 12390-3:200. Seven cylinders were prepared for testing compressive strength of concrete. After 28 days curing cylinders were placed under machine for testing. Compressive strength of concrete after 28 days are in Table 3.2. Figure 3.12 to Figure 3.14 express the various stage of crushing of cylinders.

Figure 3.12: Cylinders for Testing

Figure 3.13: Cylinder at Machine before Crushing

Figure 3.14: Cylinder at Machine after Crushing

Table 3.2: Compressive Strength of Concrete.

SL No.	Diameter (mm)	Cross-section Area,A (mm^2)	Load,L (N)	Stress, $f_c' = \frac{L}{A}$ (MPa)	Average Stress, f_c' (MPa)
1.	101.50	8091.37	275100	34.00	32.97
2.	101.50	8091.37	273300	33.78	
3.	101.75	8131.28	252000	31.00	
4.	101.25	8051.56	280700	34.86	
5.	105.00	8659.01	303600	35.06	
6.	101.75	8131.28	256700	31.57	
7.	105.00	8659.01	264500	30.54	

Provide stress of concrete, f_c'= 32 N/mm^2 = 32 MPa.

3.6 Specimen Preparation

Seven specimens of different cross-section were prepared for research purposes.

3.6.1 Scaffolding Preparation

Formwork is used to support and control the shape of fresh concrete. The formwork must be capable of handling all of the loads imposed on it through the weight and pressure of the concrete as well as any other loads imposed by personnel, materials, equipment, or environmental loads. It must also support the concrete structure until the concrete has gained enough strength to support itself and all imposed loads. Good formwork should satisfy the following requirements:

1. It should be strong enough to withstand all types of dead and live loads.
2. It should be rigidly constructed and efficiently propped and braced both horizontally and vertically, so as to retain its shape.
3. The joints in the formwork should be water-tight against leakage of cement grout.

4. Erection of formwork should permit removal of various parts in desired sequences without damage to the concrete.
5. The material of the formwork should be cheap, easily available and should be suitable for reuse.
6. The formwork should be set accurately to the desired line and levels. It should have plane surface.
7. It should be as light as possible.
8. The material of the formwork should not warp or get distorted when exposed to the elements.
9. It should rest on firm base.

Seven wood formworks were prepared for construction of beam-column joint. Three formworks were prepared for type 2, two formworks were prepared for type 1 and two formworks were prepared for type 3. One category formwork differed in cross-section from others. Close and distant view of formworks after preparation are given in Figure 3.15.

Figure 3.15: Wood Formworks for Construction of Specimens

3.6.2 Reinforcement Preparation

Reinforcement is the most vital factor in this research purposes, so great importance and carefulness was given for preparation of reinforcement. For type 1A one tie, for type 2A two ties and for type 3A three ties were placed at the joint region. For type 1B, 2B, 2C,

and 3B no tie was placed at joint region. For category A and B 2/3rd distance from center ties were placed @ 75 mm c/c and the rest 1/3rd distance ties were placed @ 150 mm c/c. For category C ties were placed uniformly @ 150 mm c/c for the whole distance. Separate as well as combined picture of specimens are given from Figure 3.16 to 3.22.

Figure 3.16: Joint Reinforcement Arrangement of Type 1A (With One Tie at Joint)

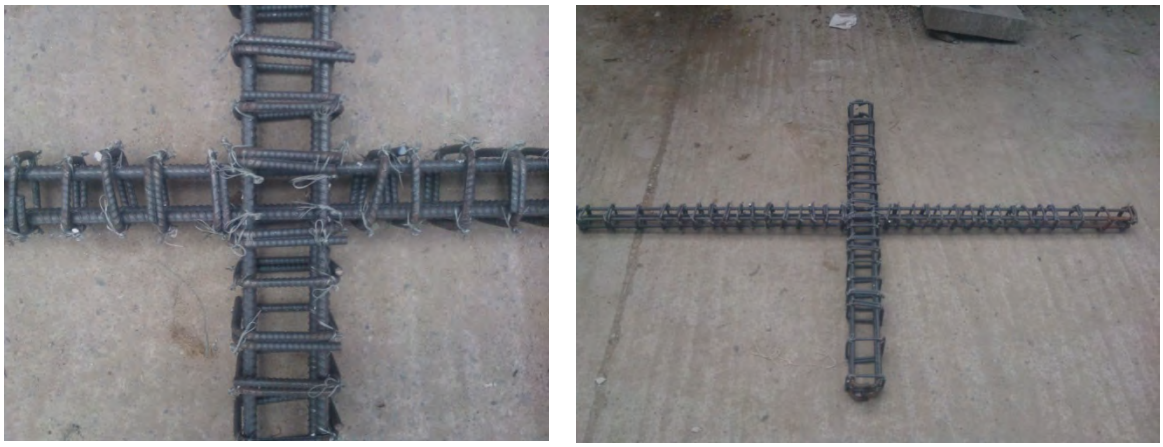

Figure 3.17: Joint Reinforcement Arrangement of Type 1B (Without Tie at Joint)

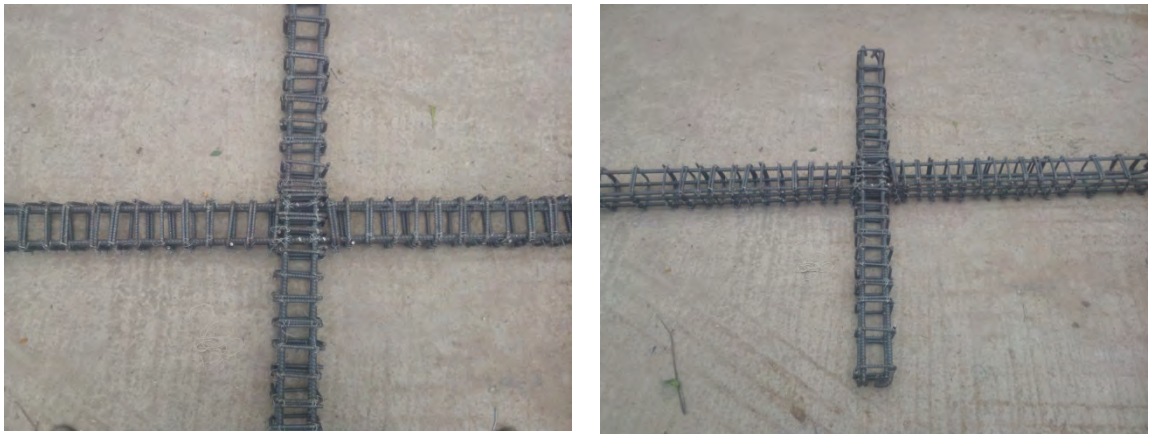

Figure 3.18: Joint Reinforcement Arrangement of Type 2A (With Two Ties at Joint)

Figure 3.19: Joint Reinforcement Arrangement of Type 2B (Without Tie at Joint)

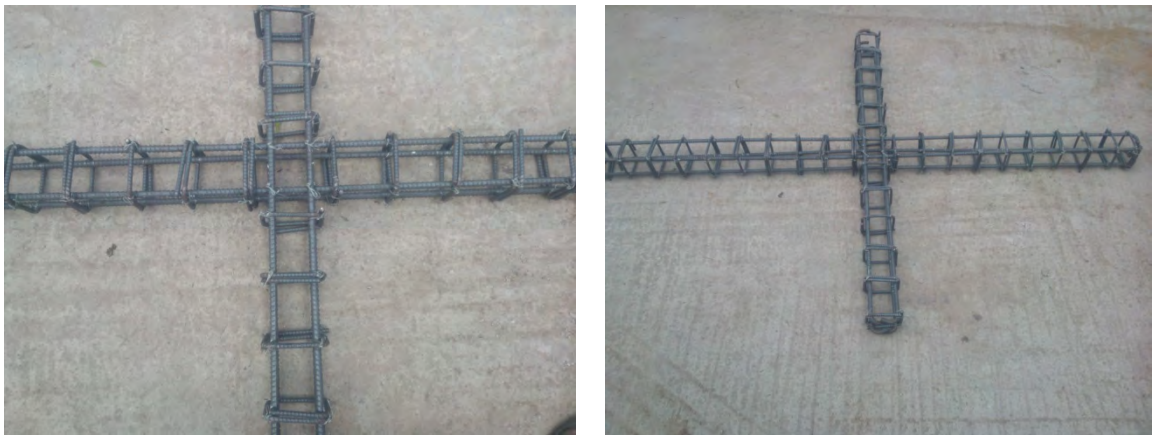

Figure 3.20: Joint Reinforcement Arrangement of Type 2C (Conventional, Without Tie at Joint)

Figure 3.21: Joint Reinforcement Arrangement of Type 3A (With Three Ties at Joint)

Figure 3.22: Joint Reinforcement Arrangement of Type 3B (Without Tie at Joint)

3.6.3 Casting

After proper placement of reinforcement over the formwork fresh concrete was poured over it. A limited quantity of fresh concrete placed over the formwork and a vibrator machine was used to vibrate so that no air void existed at the concrete. Compacted form of hardened concrete was gained for this effort. Figure 3.23 and 3.24 represent proper vibration of concrete and fresh concrete at formwork respectively.

Figure 3.23: Compaction of Fresh Concrete into Formwork using Vibrator

Figure 3.24: Casted Specimens with Formwork

3.6.4 Curing

Curing supplies required hydration and has significant influence to complete the reaction of cement. Thus, water curing method was applied after final setting of cement. Formwork attachment remained for 28 days curing period as it prevents the evaporation of the existing moisture of concrete. Thick jute cloths and rice straw were used to absorb the water applied externally for curing.

Figure 3.25: Curing of Specimens

3.6.5 White Coloring

After 28 days formworks were removed and the specimens were white washed. For better visibility of cracks, fractures and their exact locations white coloring of the specimen was done after curing period. Figures 3.26 and 3.27 represent specimens after removing formwork and white coloring respectively.

Figure 3.26: Formwork Free Specimens

Figure 3.27: White Washed Specimens

Figure 3.28: Seven Beam-Column Joints Ready for Testing at Laboratory

3.7 Experimental Set Up

The experiments were carried out in Concrete Laboratory of BUET. The models were placed on a steel base plate which had the arrangement of column seat. The base plate was intended to allow column rotation. The base plate was fixed on a steel beam which was fixed with the concrete floor as shown in Figure 3.29. A hydraulic jack was set to provide axial load on the top of the column. Two sets of steel frame had been designed for this experiment. They were fixed at both side of the column to arrest any horizontal movement of the column. Two manually operated hydraulic jacks were used to provide cyclic loading at the tip of the beams. Experimental set up is shown in Figure 3.29. Total two dial gauges were used to measure the deflection of the beam and column. One dial gauge was set at below the top of column and at about 200 mm distance from the center of beam-column joint. Another dial gauge was set at the top of beam and at about 500 mm distance from the center of beam-column joint.

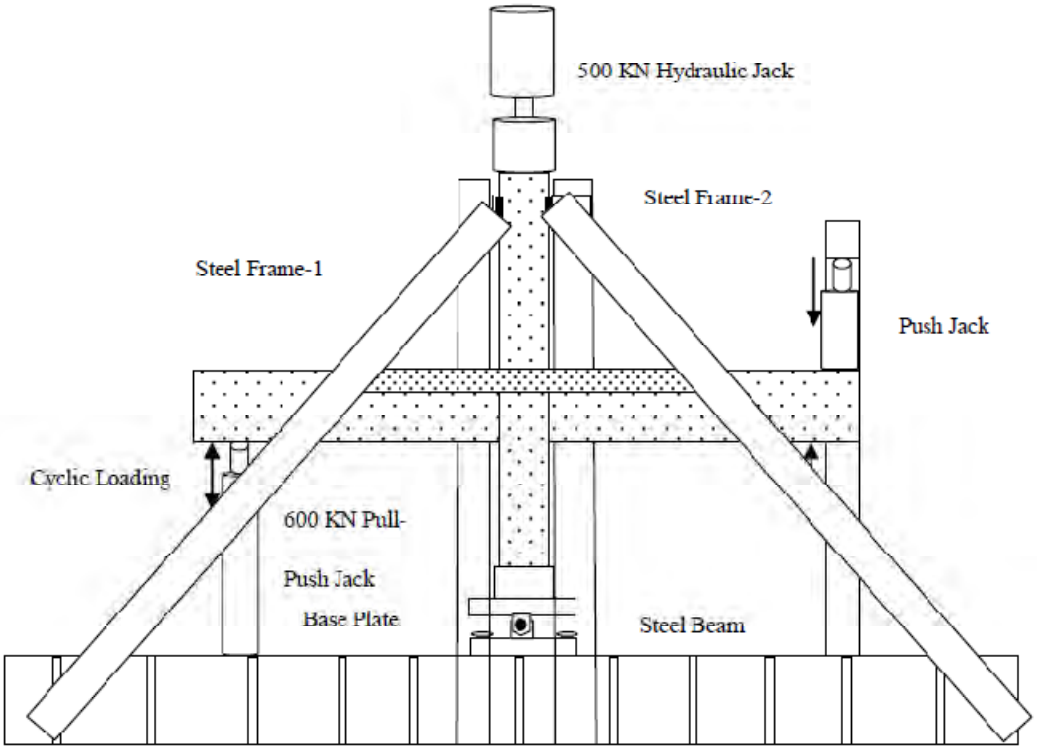

Figure 3.29: Experimental Set Up

3.8 Instrumentation and Data Acquisition

The beam-column joints were tested under vertical incremental cyclic loading at the ends of the beam along with constant axial load on the column. Vertical loading was applied at the end of beam using displacement control. The specimens were tested under cyclic loading conditions displacing them vertically from the axis along the beam. Loading and unloading was applied in 5 mm increments in the positive and negative direction for 1st cycle. Whereas 10 mm, 20 mm and 40 mm displacement increments were maintained for 2nd, 3rd and 4th cycle respectively in both upward and downward directions. A constant loading rate per cycle was maintained until the specimens experienced significant loss of capacity. The loading history applied to the specimens is shown in Figure 3.30.

The test set-up began with picking up the beam-column joints by the crane and then placed under the testing machine. The vertical static repeated load was applied manually by hydraulic jack at an increasing rate of displacement. During the test the load was recorded and displacement was also measured by two deflection gages to identify the deflection behavior.

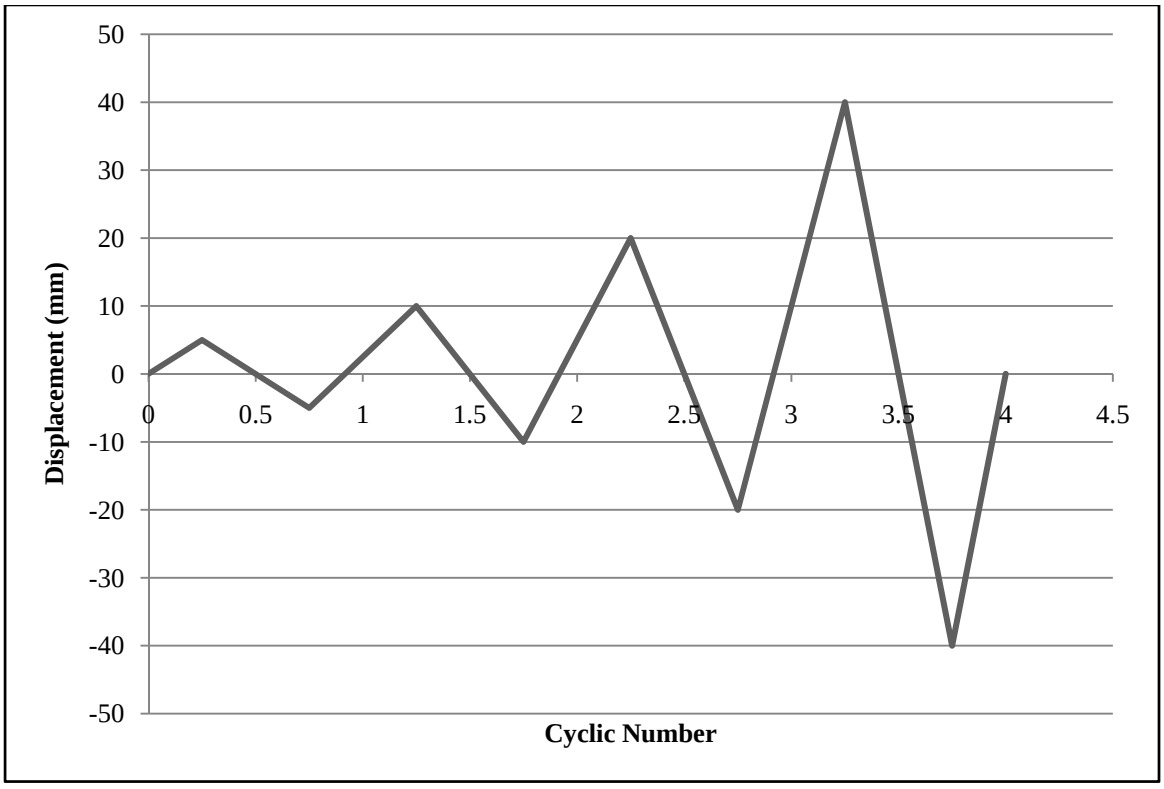

Figure 3.30: Applied Displacement Type of Loading History

CHAPTER 4

RESULT ANALYSIS AND DISCUSSION

4.1 Introduction

This Chapter summarizes the qualitative and quantitative experimental results of beam-column joints from test specimens Sample -1 to Sample -7. The qualitative results include photographs of each specimen through the course of testing and displaying the crack patterns. Load corresponding to displacements and different crack history were recorded for producing the quantitative results.

4.2 Test Procedure

Prior to commencing each test, the loading hydraulic jack was anchored into position. The vertical hydraulic jack was set in its position at the top of the column. The manually movable vertical hydraulic jack was placed at the bottom face of beam end and then also at the top face of beam end. Before applying the axial load, two dial gauges were set and readings were taken as reference points to determine the deflection throughout the loading regime. The vertical hydraulic jack was first loaded to a force of 10 ton (about 100 KN), on column top. Dial gauge readings were also recorded after imposing the vertical load to determine the amount of compressive shortening. The manually movable hydraulic jack was responsible for imposing the cyclic displacements to the specimen through complete cycles of 5, 10, 20 and 40 mm displacements. All cycle consisted of first loading and unloading the specimens toward the positive direction hereafter referred to as the negative direction. The displacements were monitored by two dial gauges located one at the column side and the other at the beam side. One dial gauge was placed at a distance of about 200 mm from center of column joint and another dial gauge was placed at a distance of about 500 mm from center of beam joint. Characteristics and Parameters of Seven Specimens are given in Table 4.1.

Table 4.1: Characteristics and Parameters of Seven Specimens.

Type	Tie at joint region	Cross-sectional area of beam	Cross-sectional area of column	Column to Beam cross-sectional ratio	No. of ties at joint region	Spacing of Stirrups
1B	Without ties	125mm x 125mm	150mm x 150mm	1.44	Nil	For middle $\frac{2}{3}$ length @ 75 mm c/c and rest $\frac{1}{3}$ length @ 150 mm c/c
1A	With ties	125mm x 125mm	150mm x 150mm	1.44	1	For middle $\frac{2}{3}$ length @ 75 mm c/c and rest $\frac{1}{3}$ length @ 150 mm c/c
2C	Without ties	150mm x 150mm	150mm x 150mm	1.00	Nil	For whole length @150 c/c
2B	Without ties	150mm x 150mm	150mm x 150mm	1.00	Nil	For middle $\frac{2}{3}$ length @ 75 mm c/c and rest $\frac{1}{3}$ length @ 150 mm c/c
2A	With ties	150mm x 150mm	150mm x 150mm	1.00	2	For middle $\frac{2}{3}$ length @ 75 mm c/c and rest $\frac{1}{3}$ length @ 150 mm c/c
3B	Without ties	175mm x 175mm	150mm x 150mm	0.73	Nil	For middle $\frac{2}{3}$ length @ 75 mm c/c and rest $\frac{1}{3}$ length @ 150 mm c/c
3A	With ties	175mmx 175mm	150mm x 150mm	0.73	3	For middle $\frac{2}{3}$ length @ 75 mm c/c and rest $\frac{1}{3}$ length @ 150 mm c/c

4.3 Cracking Characteristics

All seven specimens did not exhibit similar cracking patterns throughout the course of testing. From category A specimens category B and C specimens cracking patterns were totally different. Where category B and C specimens exhibited diagonal cracking at the joint region; category A exhibited vertical cracking at the faces of the joint where the beams frame into the joint. However, joint type 1B, 2B, 2C and 3B exposed similar cracking where type 2C exposed severe cracks. On the other hand, type 1A, 2A and 3A exposed similar cracks.

The first signs of damage occurred at the beam-column interface consisted of small flexural cracks whose width did not significantly increase during the test. Then, several shear cracks start to develop in the joint region. When the cracks along the four diagonal of the panel became dominant these affected the member strength. In absence of joint confinement, the failure of the specimen was carried out in the same way. The control specimens of joint with ties at beam-column connection highlighted a significant vulnerability of the joint panel region. The joint strengthening was able to significantly improve the cyclic behavior of the joint panel by moving the rupture of the specimen to the beam. In this case, the strength of the specimen was controlled by the maximum flexural capacity of the beam. The damage of the control specimens were followed by the development of relevant vertical cracks which, starting from the beam-column interface, propagated along the beam.

In case of Type 1B and Type 1A specimens cracking in columns did not occurred rather it happened at beam, which is very preferable. Furthermore, in case of samples Type 2C, Type 2B and Type 2A a limited number of cracking occurred in columns where maximum cracking occurred in beams, which is not preferable. Lastly, in case of Type 3B and Type 3A specimens a huge number of cracking occurred in columns where severe cracking also occurred in beams, which is highly avoidable.

4.3.1 Cracking Characteristics and Test Results of Type 1B (Specimen 1)

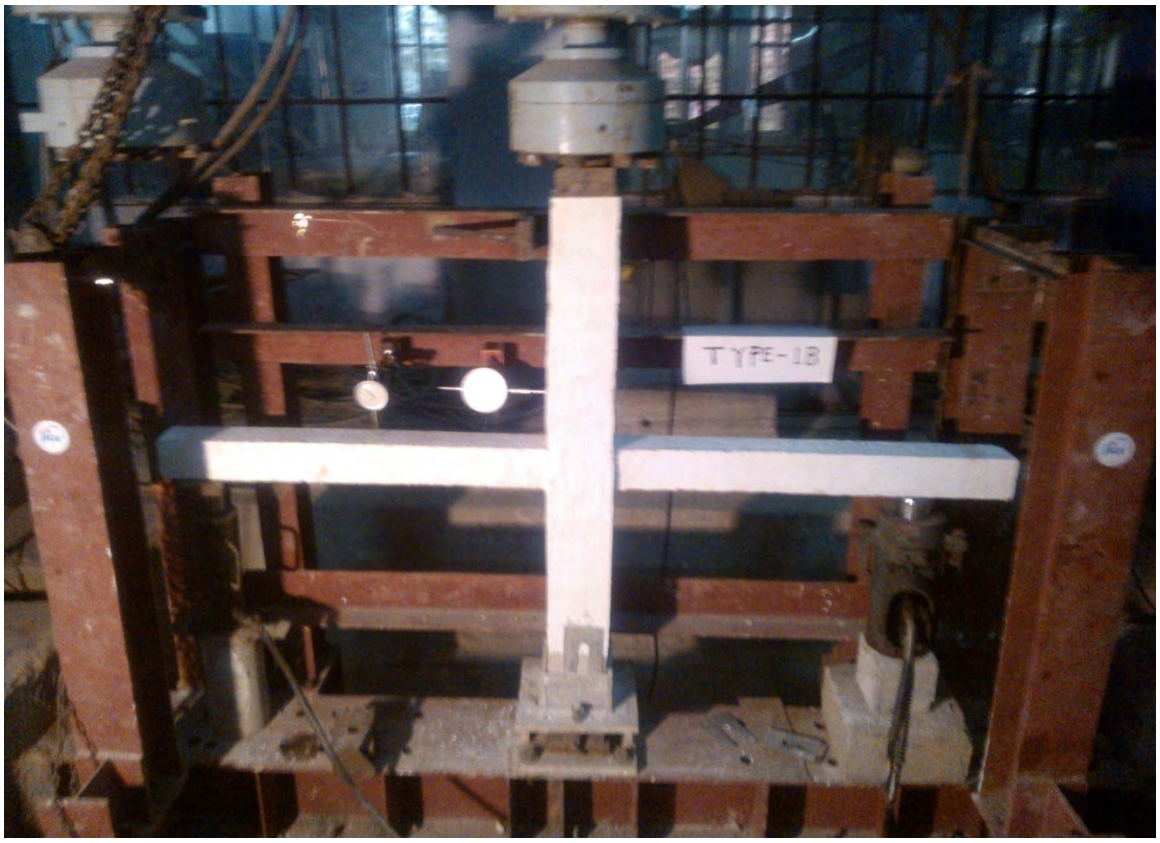

Figure 4.1: Type 1B Specimen at the Machine for Testing

The specimen Type 1B was prepared without tie at joint region. In reality after testing this specimen exhibited diagonal cracking at beam-column joint region. The shear cracking seemed to be more widespread. The evidence of these statements can be achieved from Figure 4.2 and 4.3. First crack occurred at left side beam for forward loading when load was 16 KN with displacement of 16 mm at 2nd cycle. Flexural cracks, on the beam, also initiated in the same cycle. Numbers of flexural cracks appeared during 3rd cycle on both of the beams. With increase of cyclic loading the number and extent of diagonal cracking increased gradually. Maximum load for this specimen was 17 KN. After last unloading about 18 mm of displacement remained in the specimen. This type of specimen was prepared for much wide column and less wide beam properties. Hence, it was practically observed that most of the cracking occurred at the beam where no mentionable cracking occurred at column. Figure 4.4 represents these deformation properties.

Figure 4.2: Diagonal Cracking at Joint (1B)

Figure 4.3: Cracking at Joint Corner (1B)

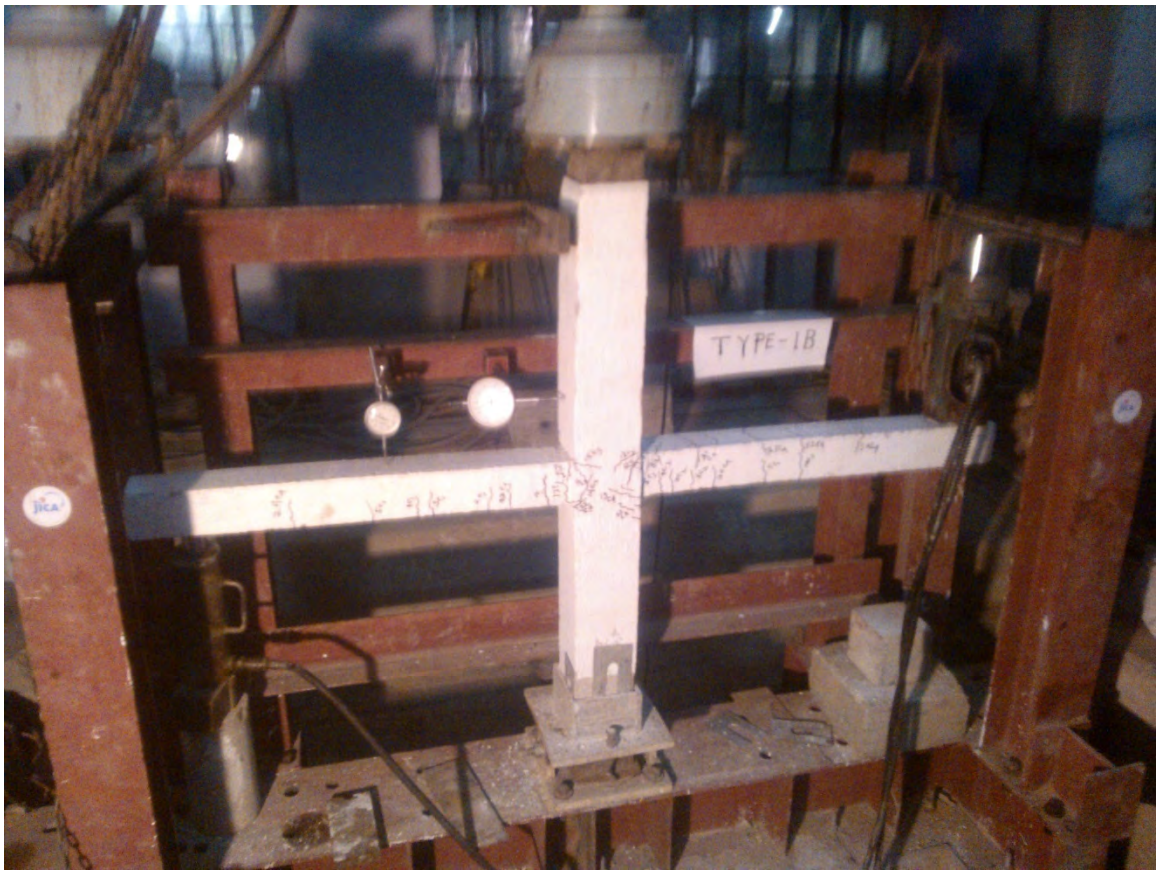

Figure 4.4: Final Crack Pattern of Type 1B Specimen

4.3.2 Cracking Characteristics and Test Results of Type 1A (Specimen 2)

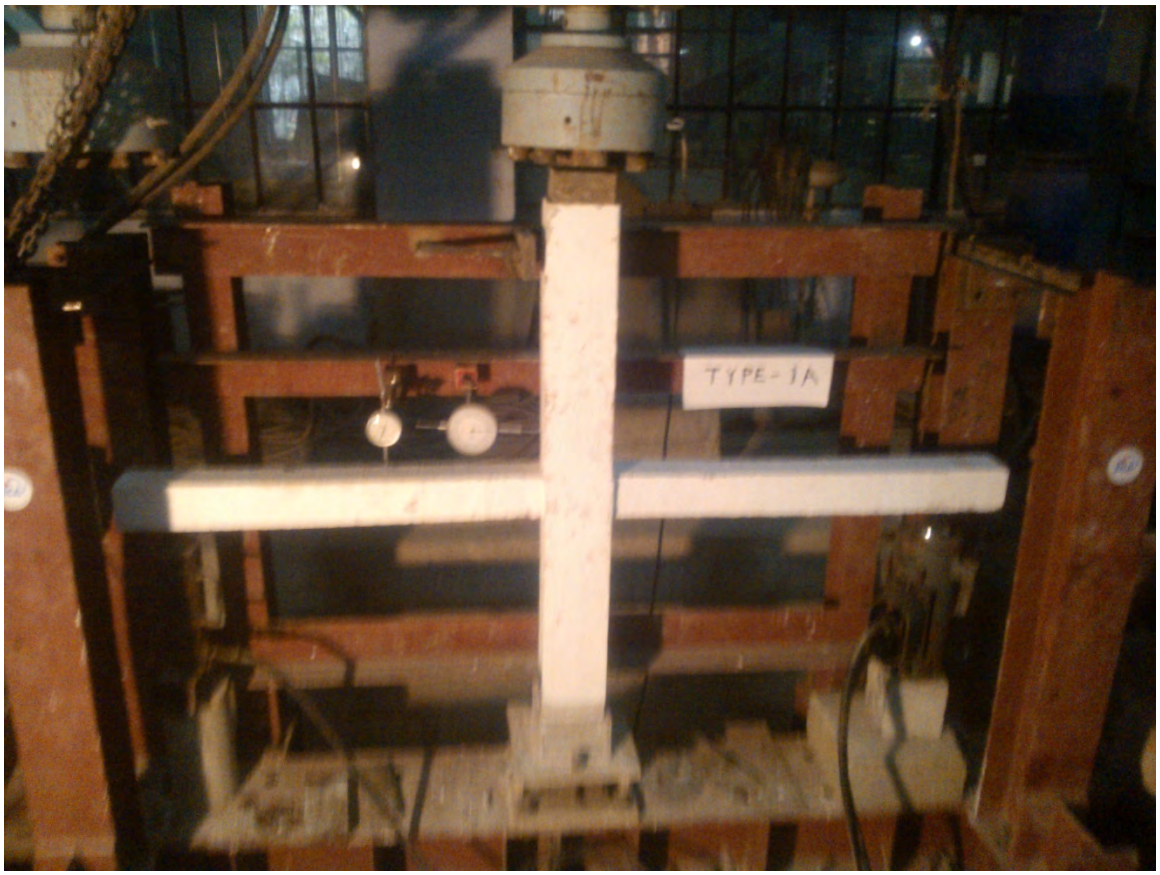

Figure 4.5: Type 1A Specimen at the Machine for Testing

The specimen Type 1A was prepared with tie at joint region. In reality after testing this specimen exhibited vertical cracking at the faces of the joint where the beams frame into the joint. The shear cracking seemed to be less widespread. The evidence of these statements can be achieved from Figure 4.6. Cyclic load application at beam by hydraulic jack was shown in Figure 4.7. First crack occurred at left side beam for forward loading when load was 20 KN with displacement of 15 mm at 2nd cycle. Flexural cracks, on the beam, also initiated in the same cycle. Numbers of flexural cracks appeared during 3rd cycle on both of the beams. With increase of cyclic loading the number and extent of vertical cracking at the face of the joint increased gradually. Maximum load for this specimen was 20 KN. After last unloading about 15 mm of displacement remained in the specimen. This type of specimen was prepared for much wide column and less wide beam properties. Hence, it was practically observed that most of the cracking occurred at

the beam where no mentionable cracking occurred at column. Figure 4.8 represents the deformation and cracking pattern of the test specimen.

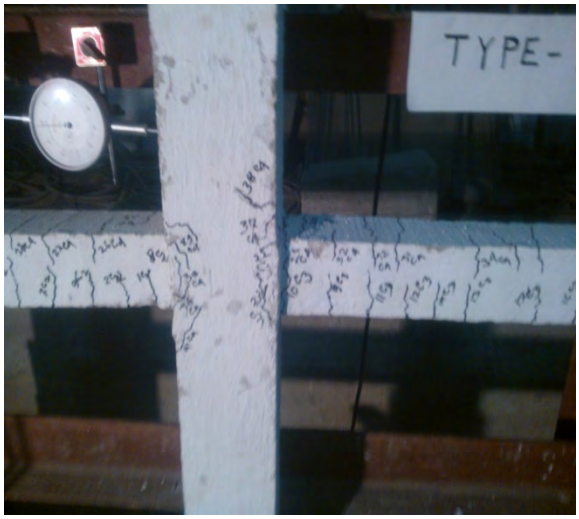

Figure 4.6: Cracking at Joint (1A)

Figure 4.7: Cyclic Load at Beam by Jack

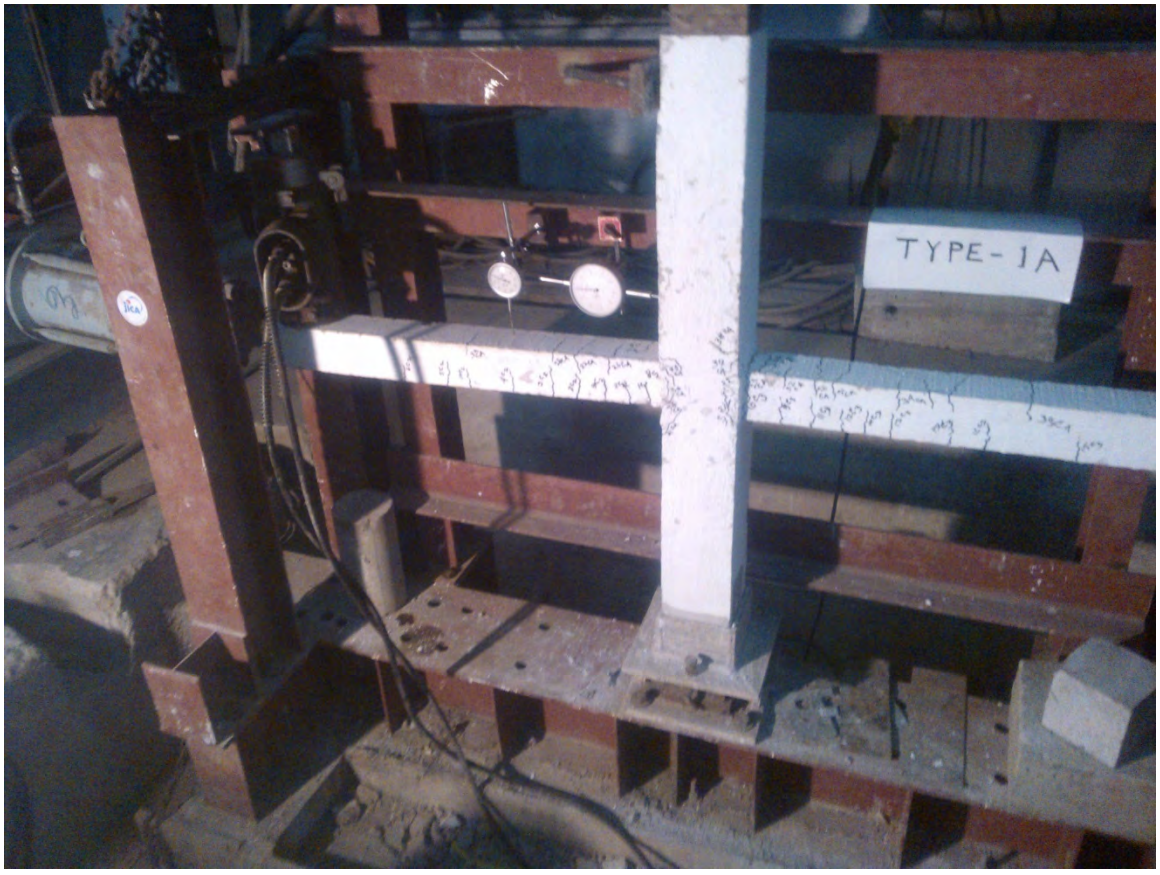

Figure 4.8: Final Crack Pattern of Type 1A Specimen

4.3.3 Cracking Characteristics and Test Results of Type 2C (Specimen 3)

Figure 4.9: Type 2C Specimen at the Machine for Testing

The specimen Type 2C was prepared without tie at joint region and wide equal spacing of ties at rest portion. In reality after testing this specimen exhibited diagonal cracking at beam-column joint region and the cracks were also comparatively more in number. The shear cracking seemed to be most widespread. The evidence of these statements can be achieved from Figure 4.10. First crack occurred at left side beam for forward loading when load was 22 KN with displacement of 14 mm at 2^{nd} cycle. Flexural cracks, on the beam, also initiated in the same cycle. Numbers of flexural cracks appeared during 3^{rd} cycle on both of the beams. With increase of cyclic loading the number and extent of diagonal cracking increased gradually. Maximum load for this specimen was 24 KN. Some small flexural cracks were marked on the Column at this stage. After last unloading about 13 mm of displacement remained in the specimen. Type 2C sample gave huge number of cracking as the stirrup spacing was conventionally more. This type of

specimen was prepared for equal wide column and beam properties. Hence, it was practically observed that most of the cracking occurred at the beam where very few cracking occurred at column. Figure 4.11 represents these deformation properties after replacement of sample from machine.

Figure 4.10: Diagonal Cracking at Joint (2C)

Figure 4.11: Final Crack Pattern of Type 2C Specimen

4.3.4 Cracking Characteristics and Test Results of Type 2B (Specimen 4)

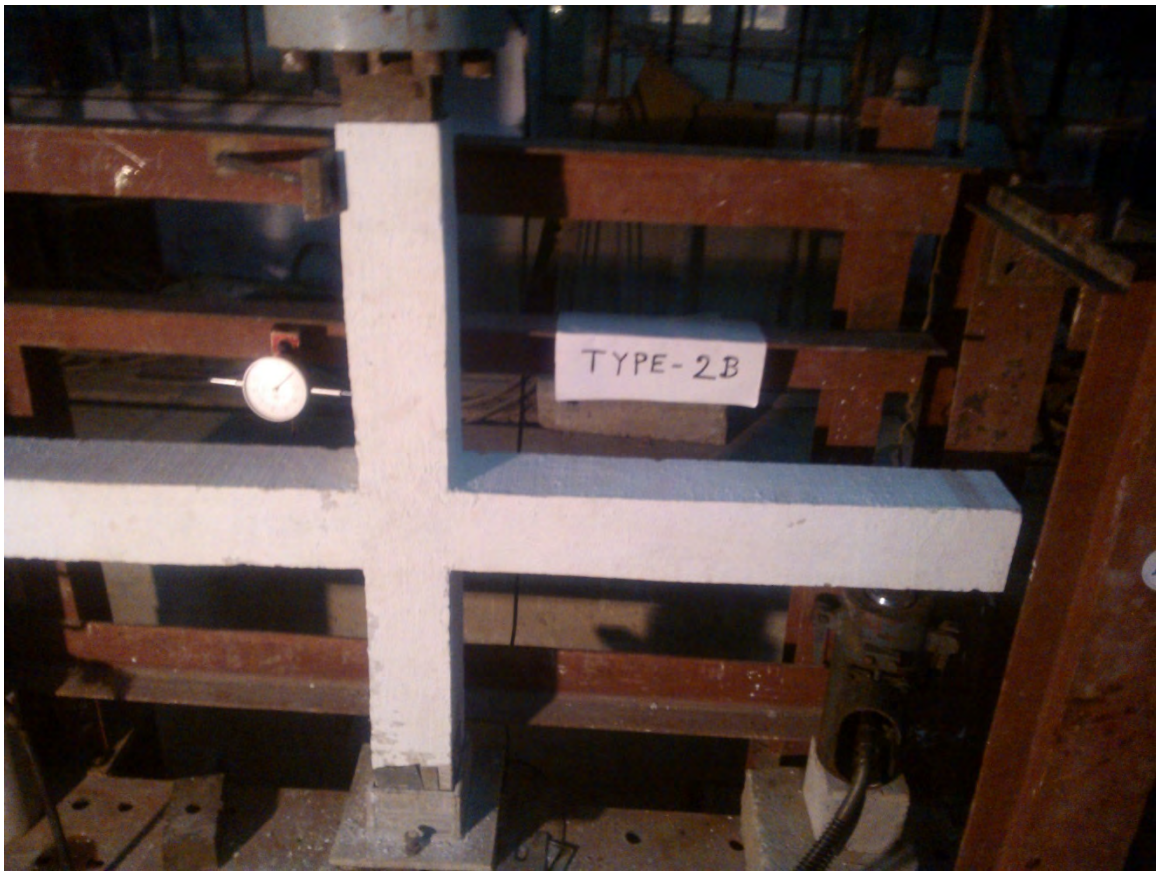

Figure 4.12: Type 2B Specimen at the Machine for Testing

The specimen Type 2B was prepared without tie at joint region. In reality after testing this specimen exhibited diagonal cracking at beam-column joint region. The shear cracking seemed to be more widespread. The evidence of these statements can be achieved from Figure 4.13. First crack occurred at left side beam for forward loading when load was 27 KN with displacement of 13 mm at 2nd cycle. Flexural cracks, on the beam, also initiated in the same cycle. Numbers of flexural cracks appeared during 3rd cycle on both of the beams. With increase of cyclic loading the number and extent of diagonal cracking increased gradually. With increase of cyclic loading the number and extent of diagonal cracking increased gradually. Maximum load for this specimen was 28 KN. Some small flexural cracks were marked on the Column at this stage. After last unloading about 10 mm of displacement remained in the specimen. This type of specimen was prepared for equal wide column and beam properties. Hence, it was practically

observed that most of the cracking occurred at the beam where very few cracking occurred at column. Figure 4.14 represents these deformation properties.

Figure 4.13: Diagonal Cracking at Joint (2B)

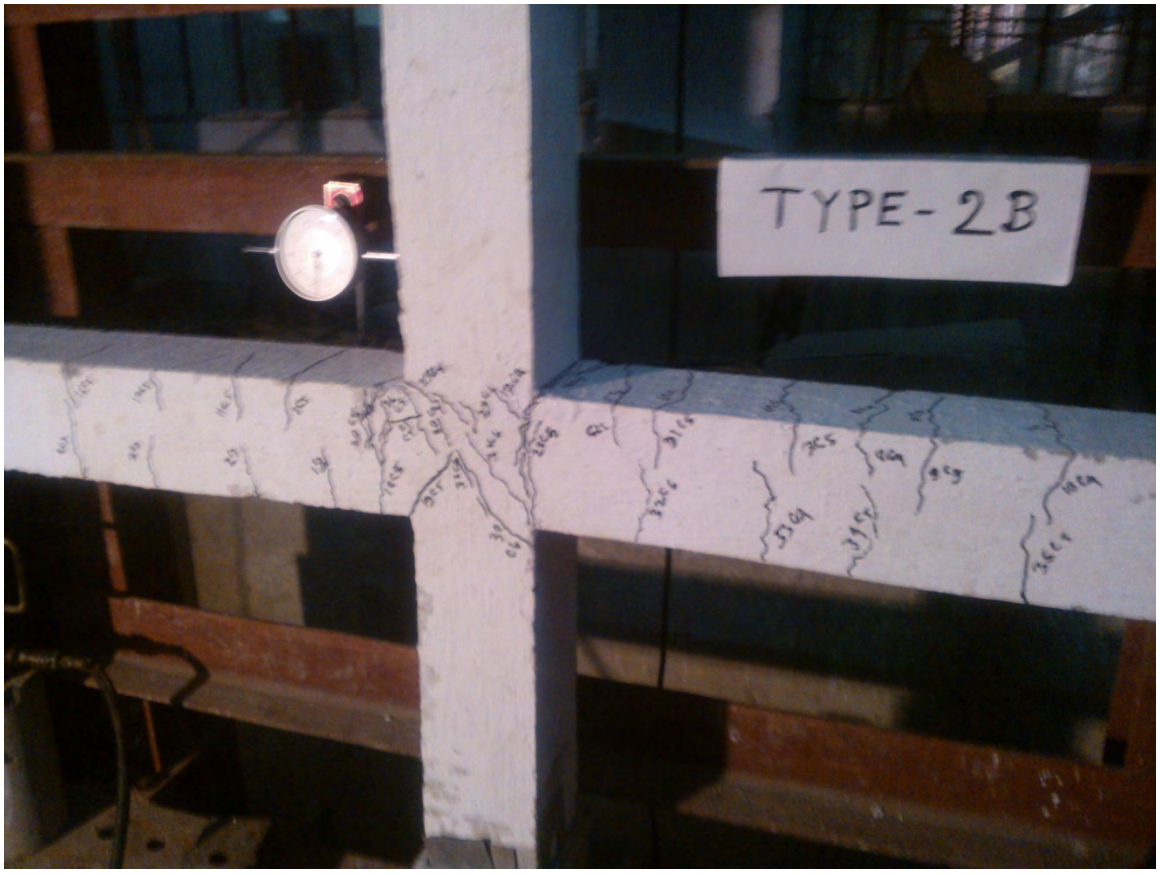

Figure 4.14: Final Crack Pattern of Type 2B Specimen

4.3.5 Cracking Characteristics and Test Results of Type 2A (Specimen 5)

Figure 4.15: Type 2A Specimen during Testing at the Machine

The specimen Type 2A was prepared with tie at joint region. In reality after testing this specimen exhibited vertical cracking at the faces of the joint where the beams frame into the joint. The shear cracking seemed to be less widespread. The evidence of these statements can be achieved from Figure 4.16. Taking record of necessary reading was shown in Figure 4.15. First crack occurred at right side beam for forward loading when load was 31 KN with displacement of 24 mm at 3rd cycle. Flexural cracks, on the beam, also initiated in the same cycle. Numbers of flexural cracks appeared during 4th cycle on both of the beams. With increase of cyclic loading the number and extent of vertical cracking at the face of the joint increased gradually. Maximum load for this specimen was 33 KN. Some small flexural cracks were marked on the Column at this stage. After last unloading about 8 mm of displacement remained in the specimen. This type of specimen was prepared for equal wide column and beam properties. Hence, it was

practically observed that most of the cracking occurred at the beam where very few cracking occurred at column. Figure 4.17 represents these deformation properties.

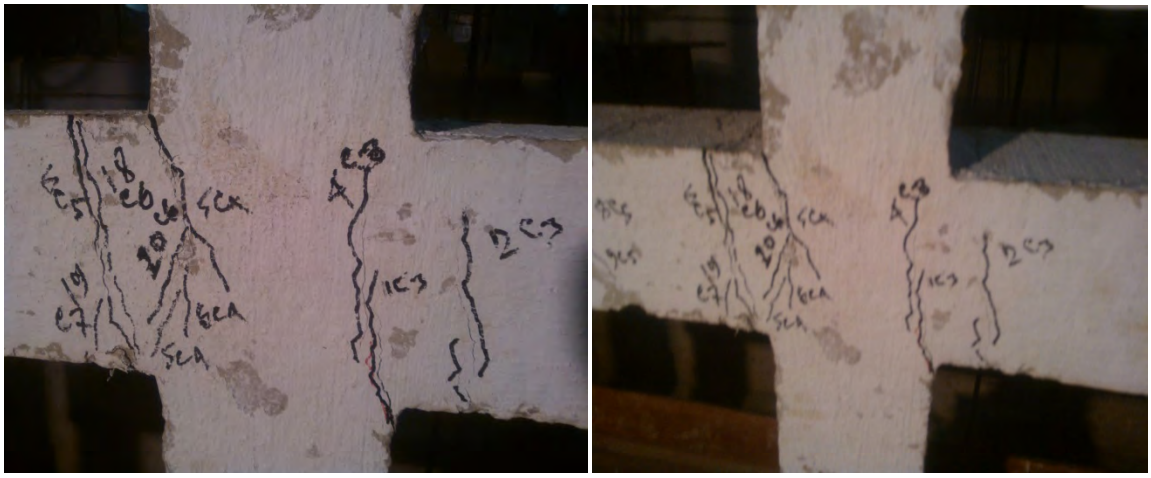

Figure 4.16: Pattern of Cracking at Joint (2A)

Figure 4.17: Final Crack Pattern of Type 2A Specimen

4.3.6 Cracking Characteristics and Test Results of Type 3B (Specimen 6)

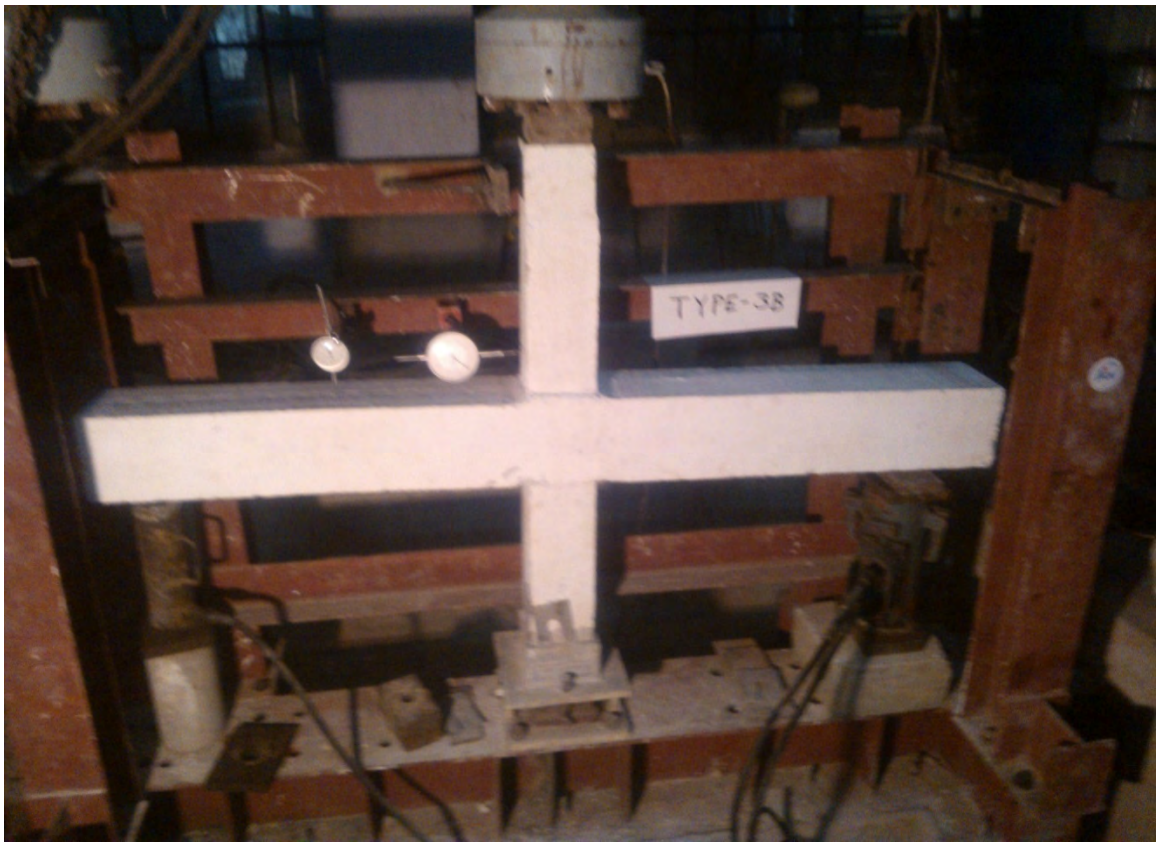

Figure 4.18: Type 3B Specimen at the Machine for Testing

The specimen Type 3B was prepared without tie at joint region. In reality after testing this specimen exhibited diagonal cracking at beam-column joint region. The shear cracking seemed to be more widespread. The evidence of these statements can be achieved from Figure 4.19. First crack occurred at left side beam for forward loading when load was 37 KN with displacement of 9 mm at 2^{nd} cycle. With increase of cyclic loading the number and extent of diagonal cracking increased gradually. Flexural cracks, on the column, also initiated in the same cycle. Numbers of flexural cracks appeared during 4^{th} cycle on both of the beams. At the same time a mentionable number of flexural cracks were marked on the column near the joint. With increase of cyclic loading the number and extent of vertical cracking at the face of the joint increased gradually. Maximum load for this specimen was 39 KN. After last unloading about 7 mm of displacement remained in the specimen. This type of specimen was prepared for less

wide column and much wide beam properties. Hence, it was practically observed that most of the cracking occurred at the beam where a mentionable cracking occurred at column at the same time. Figure 4.20 represents these deformation properties.

Figure 4.19: Diagonal Cracking at Joint (3B)

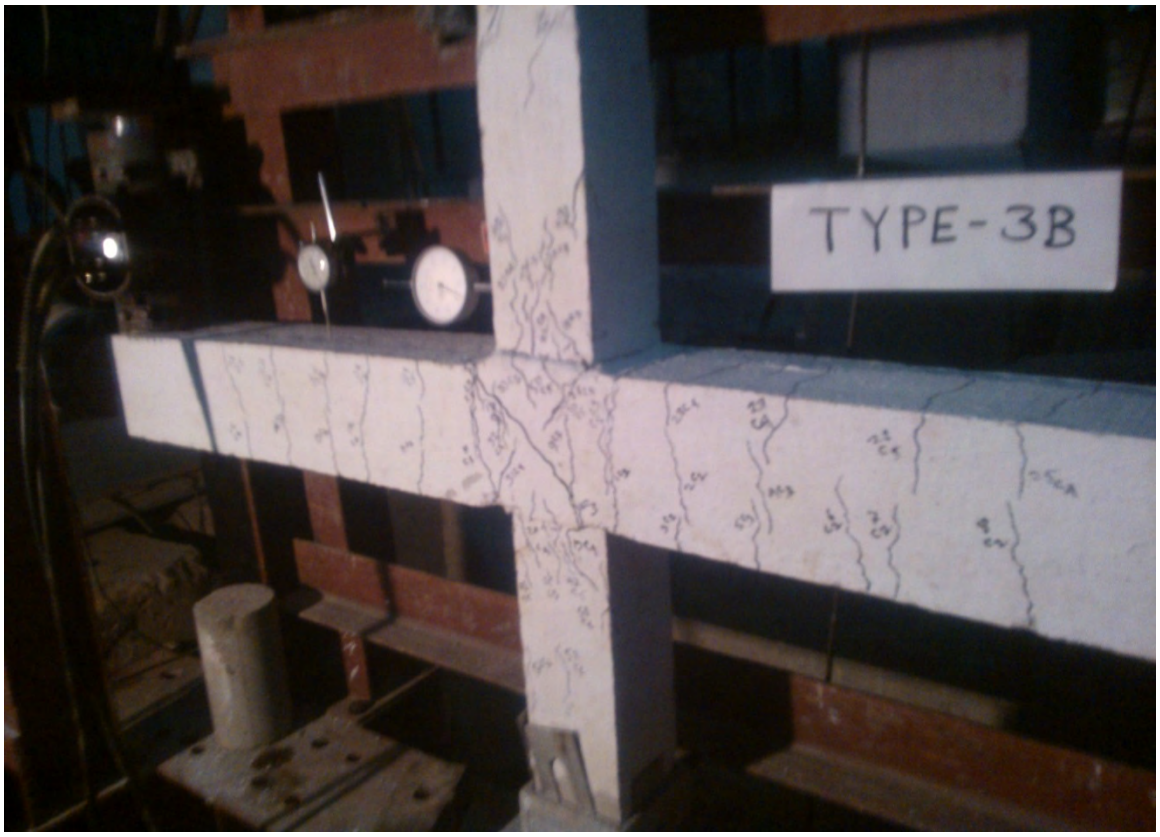

Figure 4.20: Final Crack Pattern of Type 3B Specimen

4.3.7 Cracking Characteristics and Test Results of Type 3A (Specimen 7)

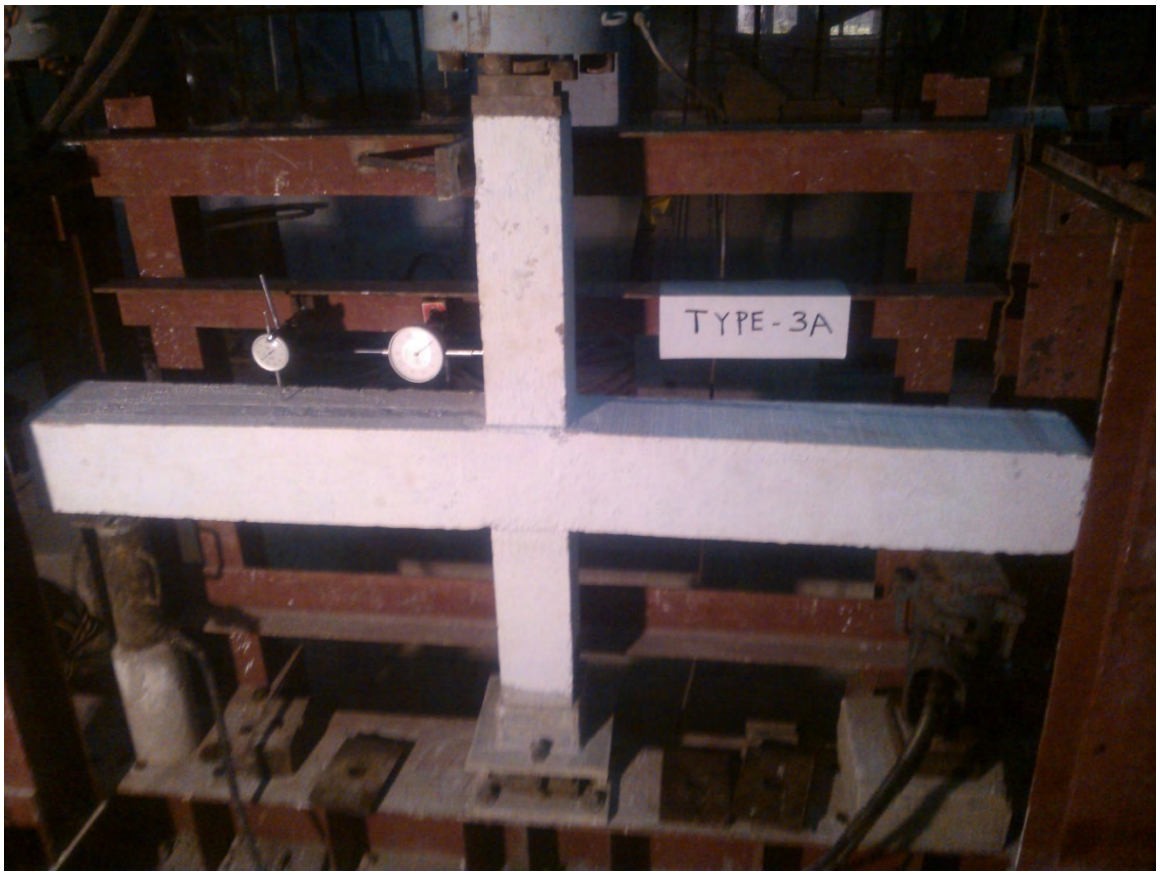

Figure 4.21: Type 3A Specimen at the Machine for Testing

The specimen Type 3A was prepared with tie at joint region. In reality after testing this specimen exhibited vertical cracking at the faces of the joint where the beams frame into the joint. The shear cracking seemed to be less widespread. The evidence of these statements can be achieved from Figure 4.22. Cyclic load application at beam by hydraulic jack was shown in Figure 4.21. First crack occurred at right side beam for forward loading when load was 41 KN with displacement of 12 mm at 3^{rd} cycle. Flexural cracks, on the column, also initiated in the same cycle. Numbers of flexural cracks appeared during 4^{th} cycle on both of the beams. At the same time a mentionable number of flexural cracks were marked on the column near the joint. With increase of cyclic loading the number and extent of vertical cracking at the face of the joint increased gradually. Maximum load for this specimen was 45 KN. After last unloading about 5 mm of displacement remained in the specimen. This type of specimen was prepared for less

wide column and much wide beam properties. Hence, it was practically observed that most of the cracking occurred at the beam where a mentionable cracking occurred at column at the same time. Figure 4.23 represents these deformation properties.

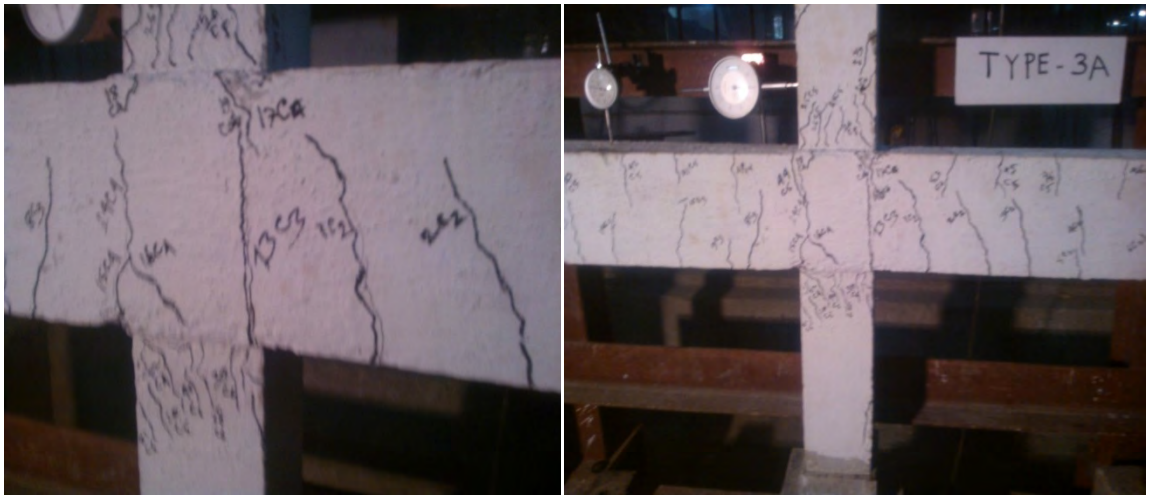

Figure 4.22: Pattern of Cracking at Joint (3A)

Figure 4.23: Final Crack Pattern of Type 3A Specimen

4.4 Load-Deformation Response

Load-deformation responses of all seven samples were monitored by dial gauges throughout each test specimen. Two dial gauges were placed to record the displacement. Load was also recorded with machine dial gauge. Load-deformation curves were drawn by giving focus on beam dial gauge readings. Category A specimens represent characteristics of joint with seismic distribution of tie at joint region and overall special tie distribution, Category B specimens represent characteristics of joint without tie at joint region and overall special tie distribution and Category C specimens represent characteristics of joint without tie at joint region and overall general tie distribution. Cyclic load was applied at a distance of 762 mm from each beam edge center point. Loading at one end was done following by unloading of that end and this process was followed to the other end. The loading and unloading process continued up to 4^{th} cycle. Static load of 100 KN (10 ton) was applied at the top of the column. In load-displacement curve displacement was placed at horizontal axis where load was placed at vertical axis. For smaller cross-section specimens displacement obtained were more compare to the specimens with larger cross-section. Also the specimens without ties at joint gave more displacement compare to the control specimens with seismic application of ties at joint. Along with the load-deformation curve of each specimen summary curve called hysteresis loop envelopes of each type were drawn with highest and lowest point of each cycle. Grand total summary curve i.e. hysteresis loop envelopes of all types were also drawn including the highest and lowest point of each cycle of all specimens. From load-deformation curves comparison of normal sample with control sample can be done. At the same time from the hysteresis loop envelopes curves at a glance the difference can be noticed.

Table 4.2: Cyclic Load-Deformation for Upper Half Cycles

Sample	Cycle	Load (KN)	Displacement (mm)
Type 1B	1st	13	10
	2nd	17	23
	3rd	11	32
	4th	09	42
Type 1A	1st	15	09
	2nd	20	21
	3rd	18	30
	4th	13	41
Type 2C	1st	19	08
	2nd	24	19
	3rd	18	28
	4th	14	40
Type 2B	1st	21	7.5
	2nd	28	16
	3rd	22	27
	4th	19	39
Type 2A	1st	23	07
	2nd	32	13
	3rd	33	24
	4th	25	38
Type 3B	1st	28	06
	2nd	39	11
	3rd	34	20
	4th	27	35
Type 3A	1st	30	05
	2nd	42	09
	3rd	45	17
	4th	40	34

Table 4.3: Cyclic Load-Deformation for Lower Half Cycles

Sample	Cycle	Load (KN)	Displacement (mm)
Type 1B	1st	14	12
	2nd	16	23
	3rd	10	33
	4th	08	44
Type 1A	1st	15	09
	2nd	20	21
	3rd	18.5	30
	4th	12	41
Type 2C	1st	18	08
	2nd	26	18
	3rd	20	29
	4th	15	40
Type 2B	1st	21	08
	2nd	28	15
	3rd	23	26
	4th	21	38
Type 2A	1st	23	07
	2nd	31	13
	3rd	32	24
	4th	27	38
Type 3B	1st	26	06
	2nd	39	12
	3rd	35	22
	4th	32	36
Type 3A	1st	29	05
	2nd	41	10
	3rd	44	19
	4th	39	34

4.4.1 Load-Deformation Response of Type 1 Specimens

Load-Deformation response Type 1B and Type 1A are shown in Figure 4.24 and 4.25. With a view to the load-deformation curve of Type 1 it can be found that Type 1B gave deviated curve where Type 1A gave smooth curve. From the figures it can be observed that within four cycles loading Type 1A specimen gave almost same highest loading for two cycles, where Type 1B specimen gave no same highest loading. This represents the more ductile quality of Type 1A. Also Type 1A specimen undergoes larger deformations without rupture before failure than Type 1B specimen. The maximum load of Type 1A sample was 20 KN, where for Type 1B sample it was 17 KN in respect of the calculated load of 15 KN for the sample. Highest load increased almost 17.65% by seismic application of ties at joint. Maximum displacement of Type 1B sample under loading was 42 mm where for Type 1A sample maximum displacement was 41 mm.

The hysteresis loop envelopes of Type 1A and Type 1B is shown in Figure 4.26. A sudden fall from the top point of Type 1B can be seen from the hysteresis loop envelopes curves. At every point of the hysteresis loop curves Type 1A specimen showed more loading value and less displacement value than Type 1B. This is obviously the sign of comparative better performance. Hence Type 1A specimen is more ductile, stiffer and stronger than Type 1B specimen.

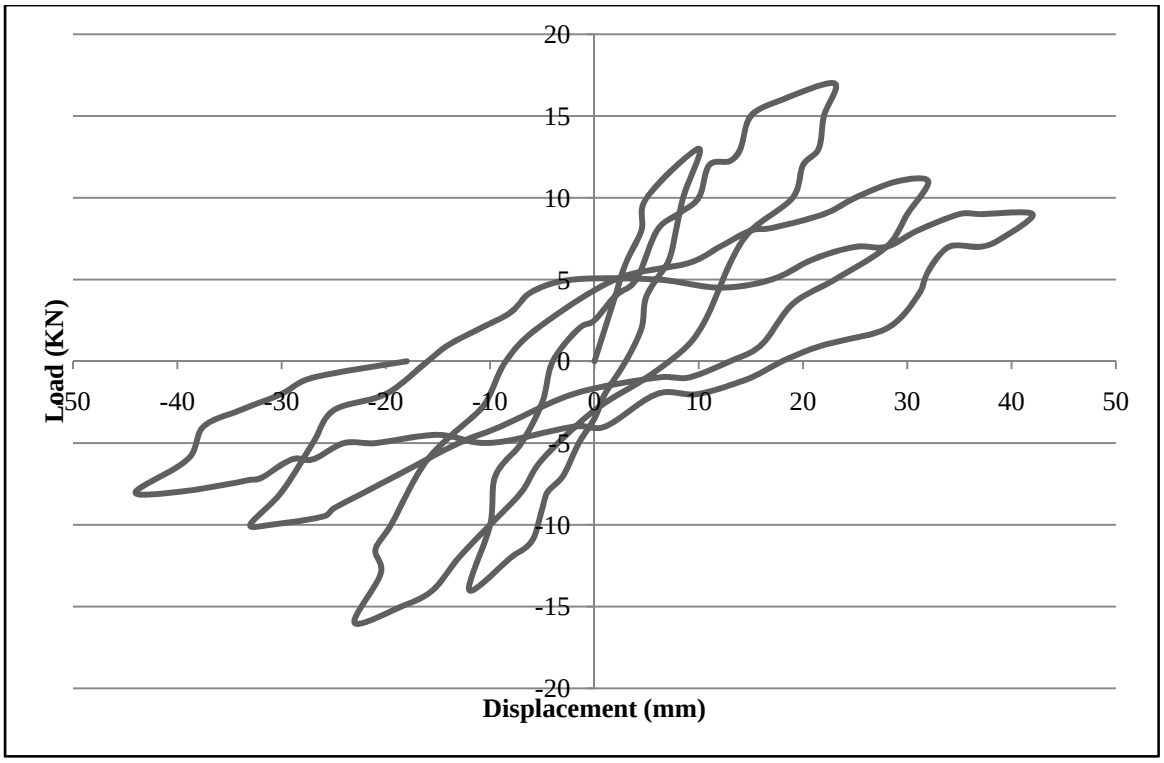

Figure 4.24: Load-Deformation Response of Type 1B Specimen (Without Tie at Joint)

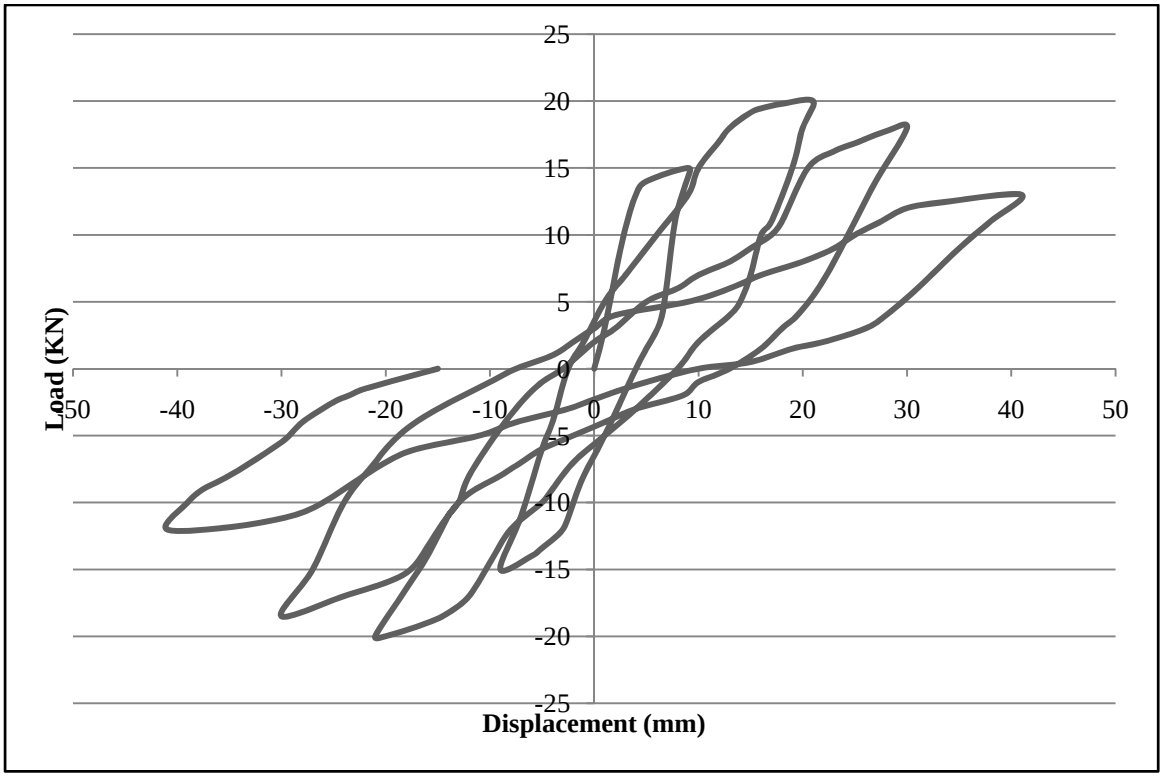

Figure 4.25: Load-Deformation Response of Type 1A Specimen (With Tie at Joint)

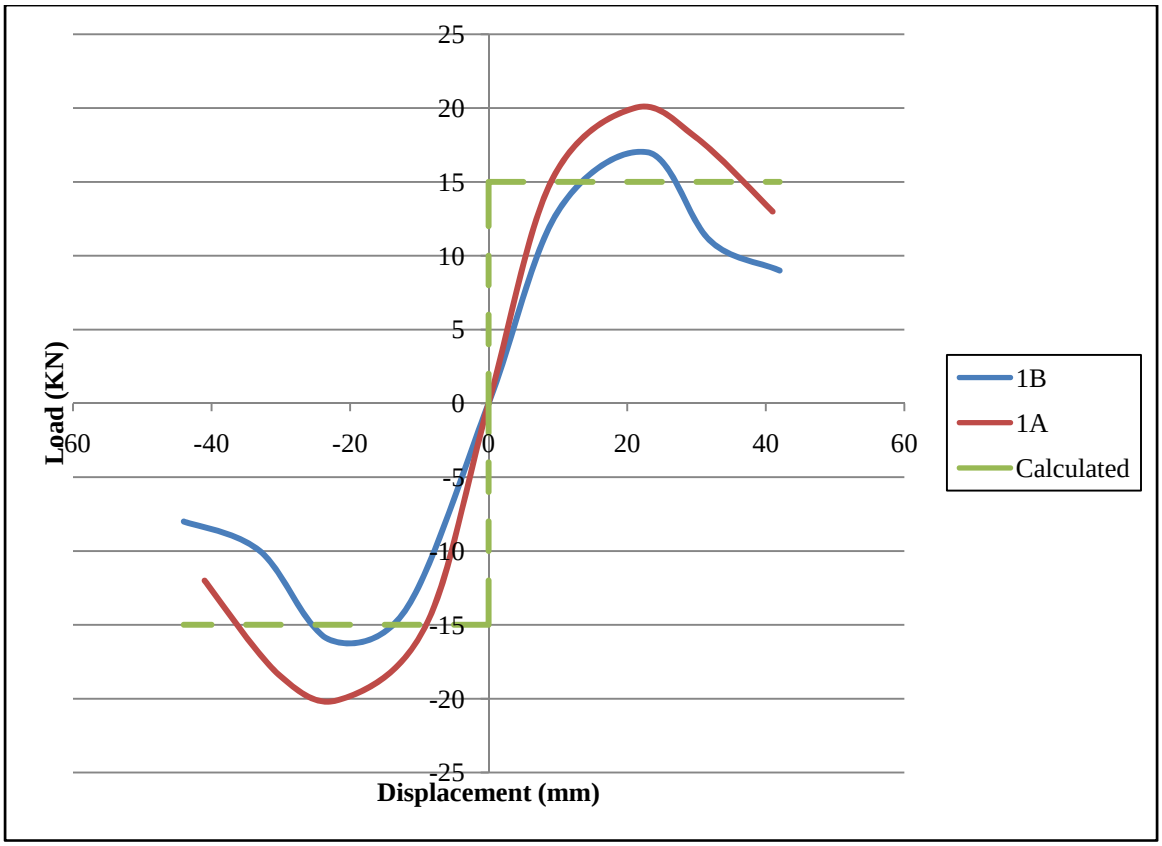

Figure 4.26: Hysteresis Loop Envelopes of Type 1A and Type 1B Specimens

4.4.2 Load-Deformation Response of Type 2 Specimens

Load-Deformation response Type 2C, Type 2B and Type 2A are shown in Figure 4.27, 4.28 and 4.29. With a view to the load-deformation curve of Type 2 it can be found that Type 2C and Type 2B gave deviated curves where Type 2A gave smooth curve. From figures it can be observed that within four cycles loading Type 2A specimen gave almost same highest loading for two cycles, where Type 2B and Type 2C specimens gave no same highest loading. This represents the more ductile quality of Type 2A. Nevertheless, Type 2A specimen undergoes larger deformations without rupture before failure than Type 2B specimen. Also Type 2B specimen undergoes larger deformations without rupture before failure than Type 2C specimen. The maximum load of Type 2A sample was 33 KN, where for Type 2B sample it was 28KN and Type 2C sample it was 24 KN in respect of the calculated load of 25 KN for the sample. Highest load increased almost 16.67% by special distribution of ties at Type 2B. Furthermore, highest load increased almost 17.86% by seismic application of ties at joint. Maximum displacement of Type 2A sample under loading was 38 mm where for Type 2C sample maximum displacement was 40 mm and for Type 2B sample maximum displacement was 39 mm.

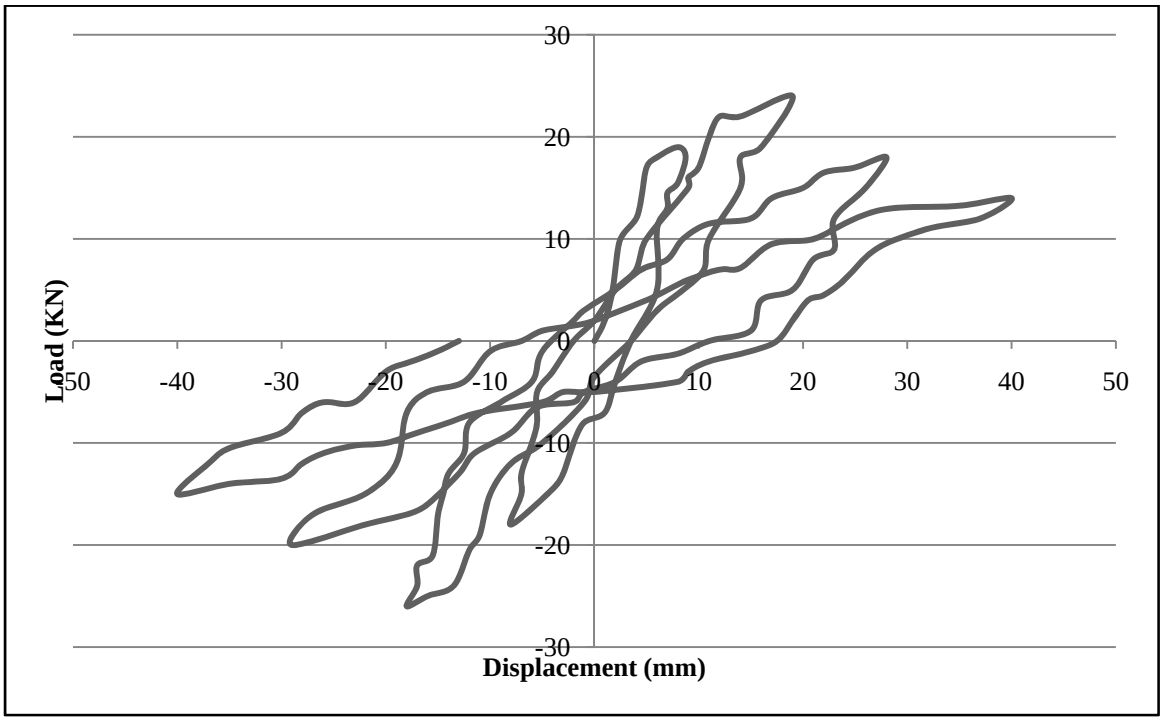

Figure 4.27: Load-Deformation Response of Type 2C Specimen (General)

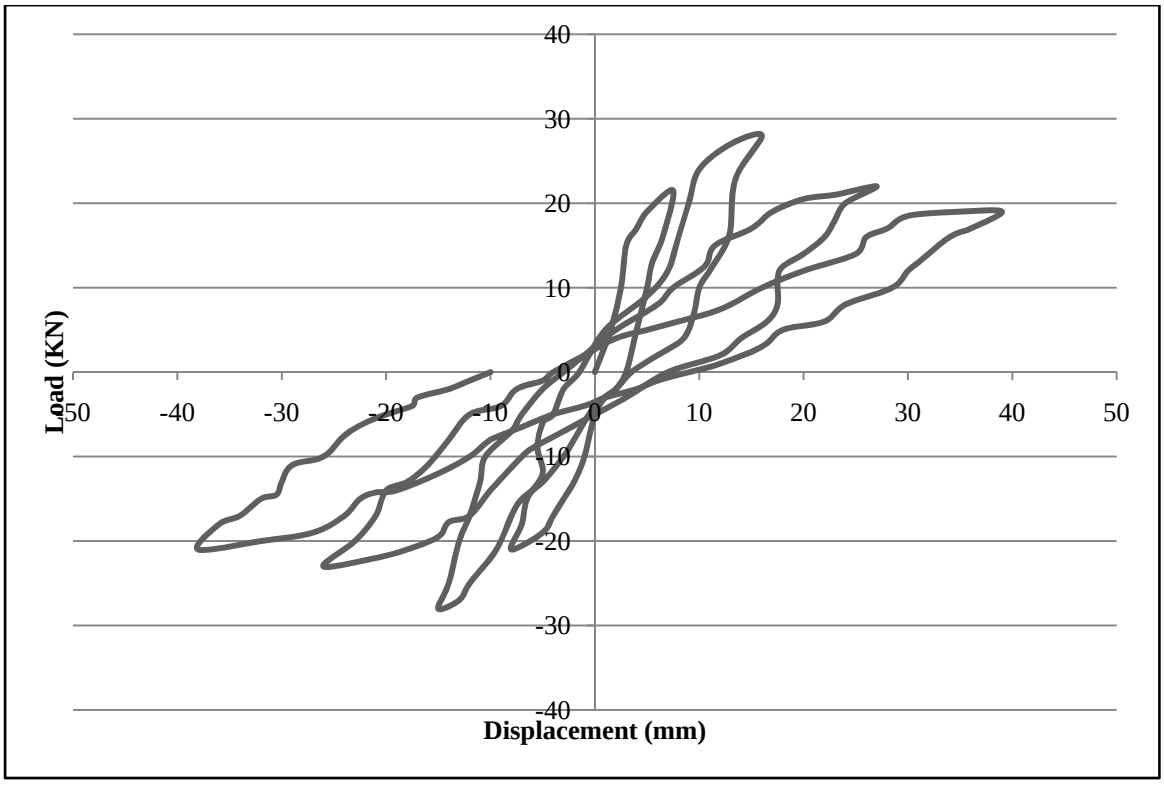

Figure 4.28: Load-Deformation Response of Type 2B Specimen (Without Tie at Joint)

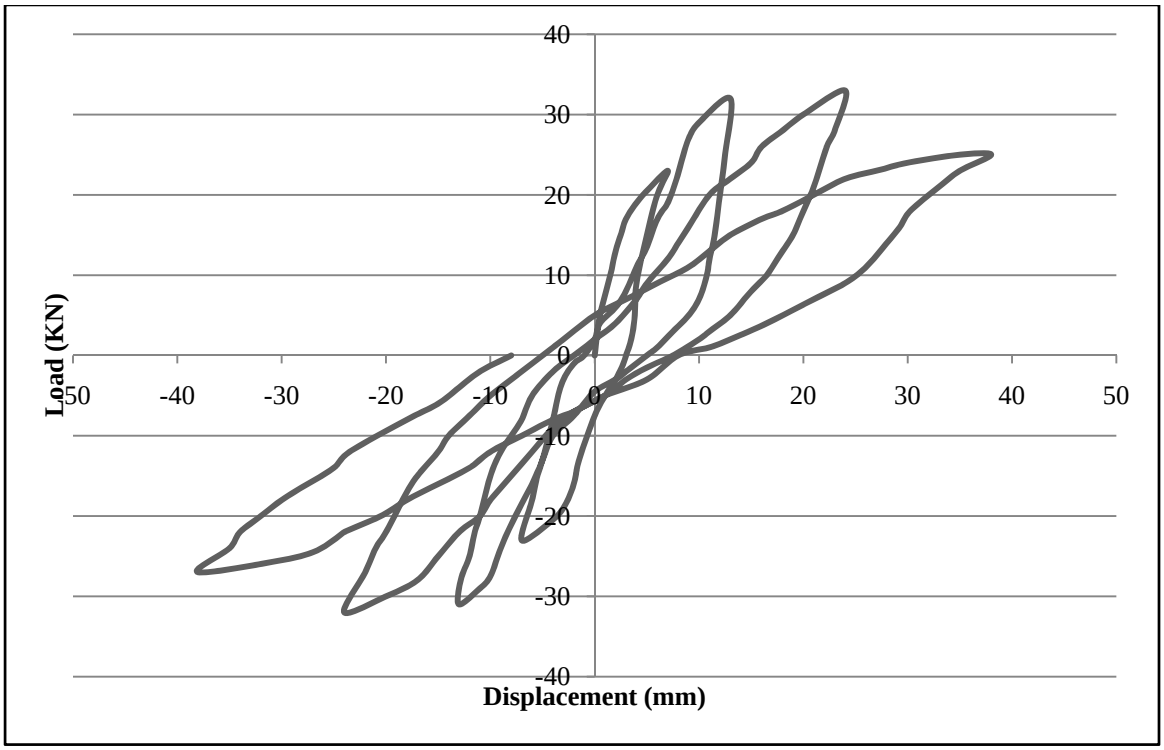

Figure 4.29: Load-Deformation Response of Type 2A Specimen (With Tie at Joint)

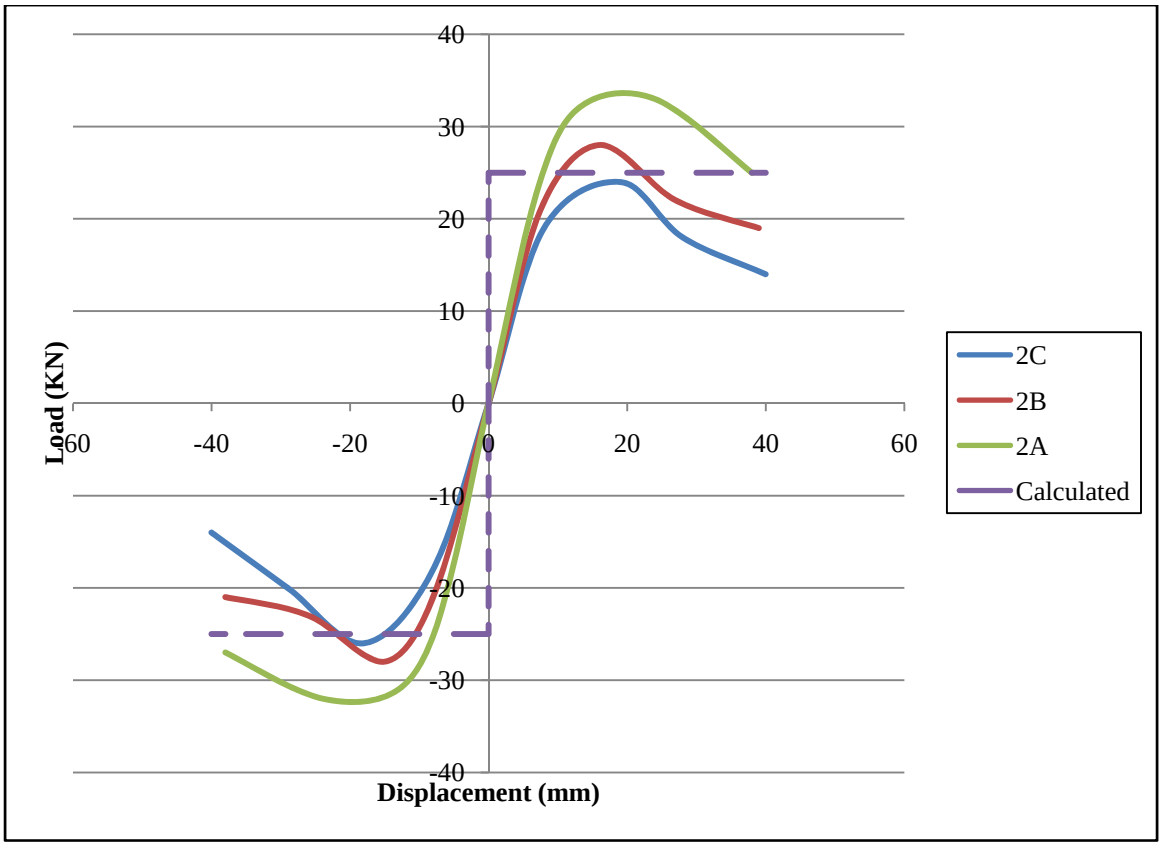

Figure 4.30: Hysteresis Loop Envelopes of Type 2A, Type 2B and Type 2C Specimens

The hysteresis loop envelopes of Type 2A, Type 2B and Type 2C is shown in Figure 4.30. A sudden fall from the top point of Type 2B and Type 2C can be seen from the hysteresis loop envelopes curves. At every point of the hysteresis loop curves Type 2A specimen showed more loading value and less displacement value than Type 2B and Type 2C. Also at every point of the hysteresis loop curves Type 2B specimen showed more loading value and less displacement value than Type 2C. This is obviously the sign of comparative better performance. Hence Type 2A specimen is more ductile, stiffer and stronger than Type 2B specimen, where Type 2B specimen is more ductile, stiffer and stronger than Type 2C specimen.

4.4.3 Load-Deformation Response of Type 3 Specimens

Load-Deformation response Type 3B and Type 3A are shown in Figure 4.31 and 4.32. With a view to the load-deformation curve of Type 3 it can be found that Type 3B gave deviated curve where Type 3A gave smooth curve. From figures it can be observed that within four cycles loading Type 3A specimen gave almost same highest loading for three cycles, where Type 3B specimen gave almost same highest loading for two cycles. This represents the more ductile quality of Type 3A. Also Type 3A specimen undergoes larger deformations without rupture before failure than Type 3B specimen. The maximum load of Type 3A sample was 45 KN, where for Type 3B sample it was 39 KN in respect of the calculated load of 37 KN for the sample. Highest load increased almost 15.38% by seismic application of ties at joint. Maximum displacement of Type 3B sample under loading was 35 mm where for Type 3A sample maximum displacement was 34 mm.

The hysteresis loop envelopes of Type 3A and Type 3B is shown in Figure 4.33. A sudden fall from the top point of Type 3B can be seen from the hysteresis loop envelopes curves. At every point of the hysteresis loop curves Type 3A specimen showed more loading value and less displacement value than Type 3B. This is obviously the sign of comparative better performance. Hence Type 3A specimen is more ductile, stiffer and stronger than Type 3B specimen.

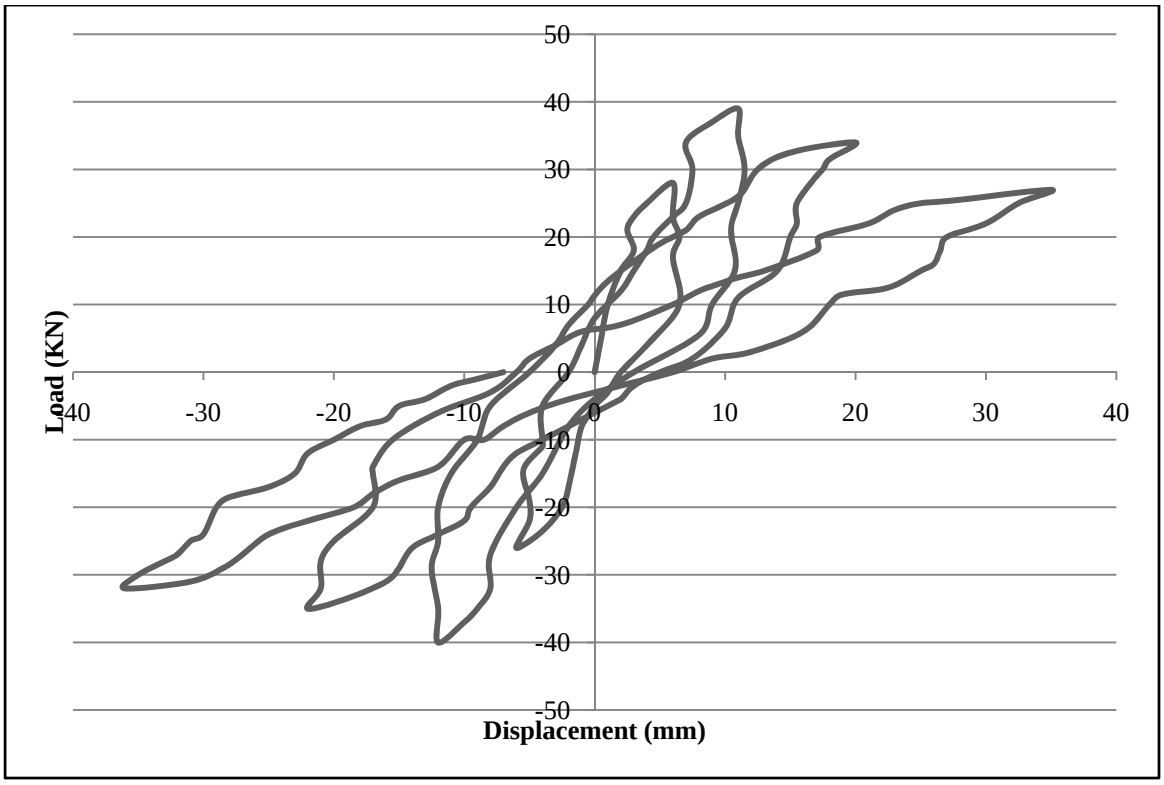

Figure 4.31: Load-Deformation Response of Type 3B Specimen (Without Tie at Joint)

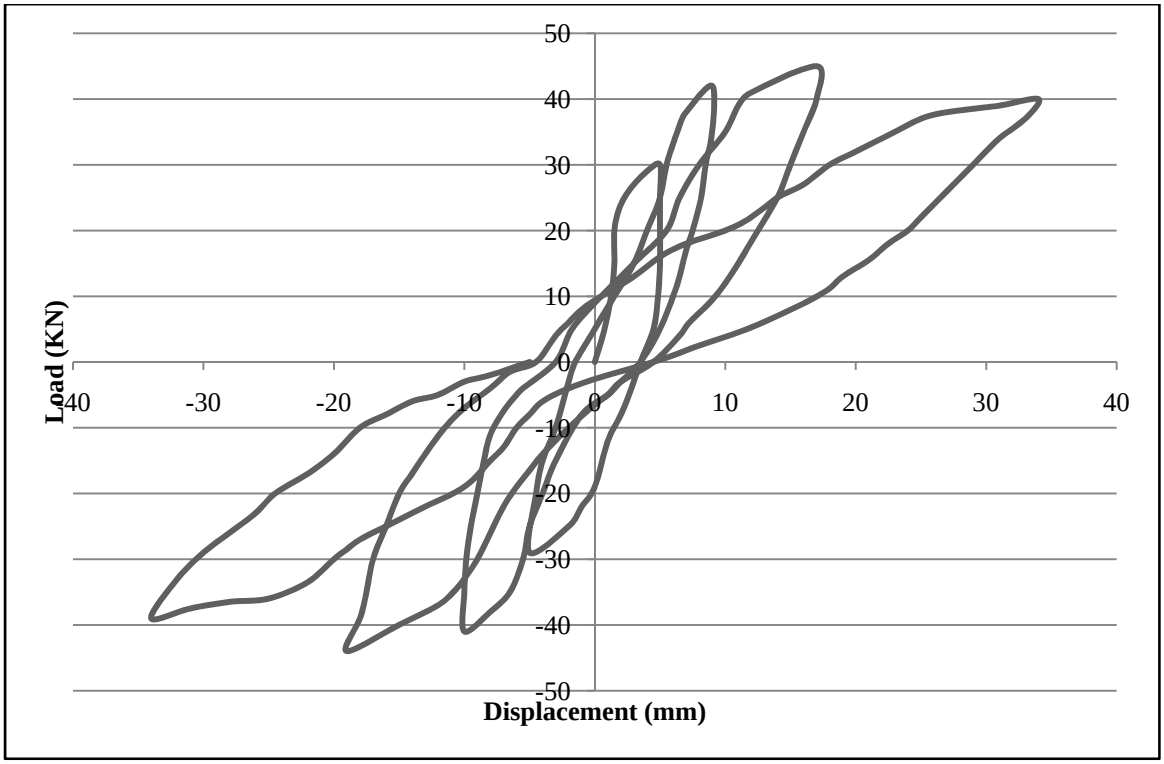

Figure 4.32: Load-Deformation Response of Type 3A Specimen (With Tie at Joint)

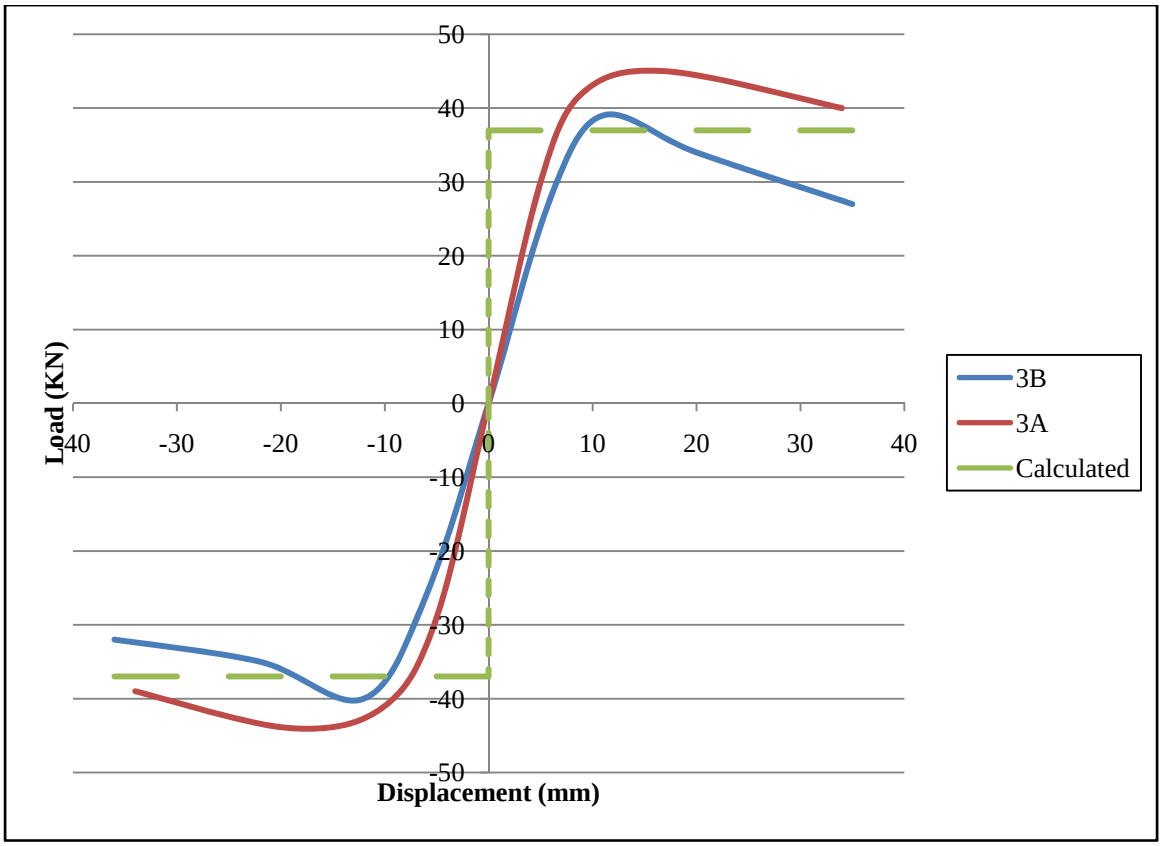

Figure 4.33: Hysteresis Loop Envelopes of Type 3A and Type 3B Specimens

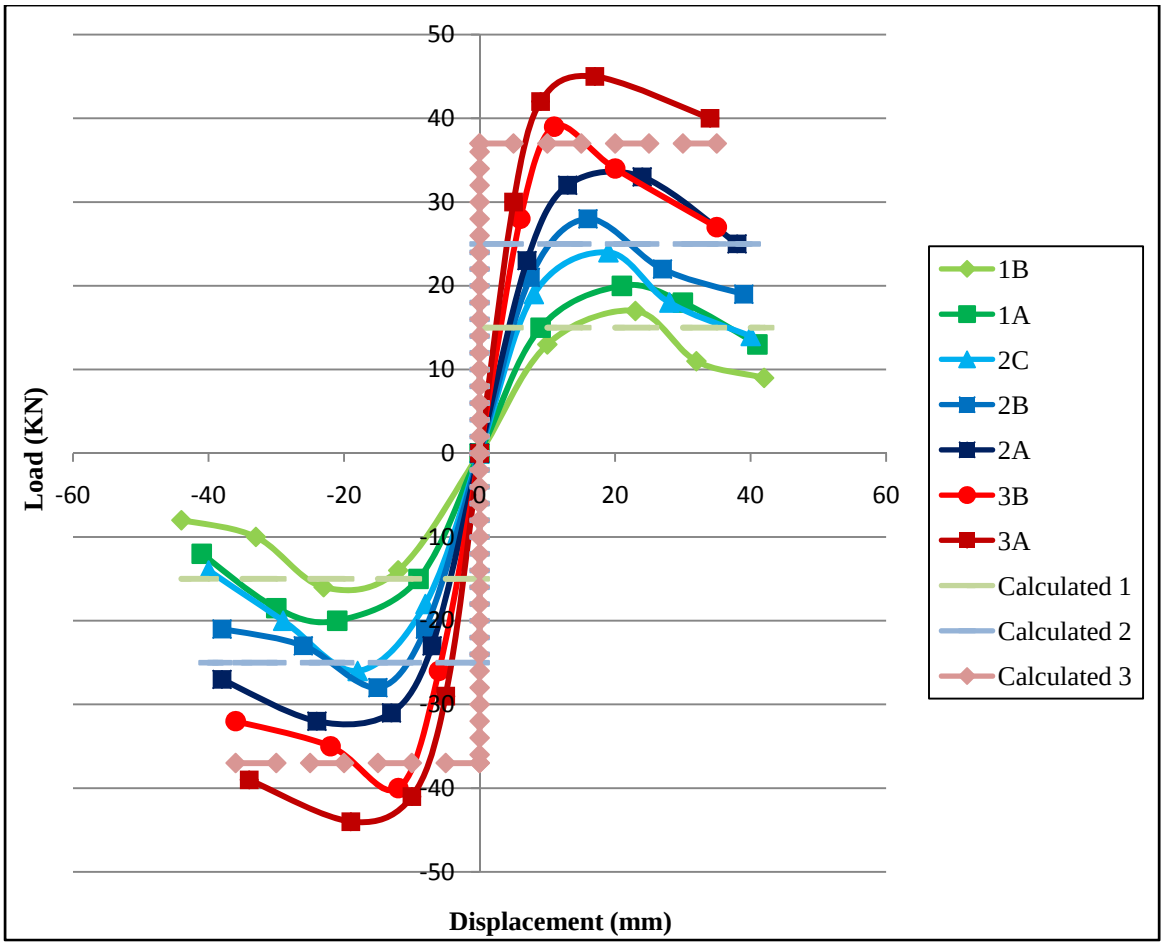

Figure 4.34: Hysteresis Loop Envelopes of Seven Specimens

4.5 Moment-Rotation Response

Load-deformation responses of all seven samples were monitored by dial gauges throughout each test specimen. Two dial gauges were placed to record the displacement. Load was also recorded with machine dial gauge. Moment-rotation curves were drawn by giving focus on beam dial gauge readings. Moment was obtained by multiplying the load with the distance from centre of joint to the point of application of cyclic load. At the same time, rotation was calculated by dividing the deformation with the distance from centre of joint to the point of application of cyclic load. Category A specimens represent characteristics of joint with seismic distribution of tie at joint region and overall special tie distribution, Category B specimens represent characteristics of joint without tie at joint region and overall special tie distribution and Category C specimens represent characteristics of joint without tie at joint region and overall general tie distribution. Cyclic load was applied at a distance of 762 mm from each beam edge center point. Loading at one end was done following by unloading of that end and this process was followed to the other end. The loading and unloading process continued up to 4^{th} cycle. Static load of 100 KN (10 ton) was applied at the top of the column. In M-ϕ curve rotation was placed at horizontal axis where moment was placed at vertical axis. For smaller cross-section specimens rotation obtained were more compare to the specimens with larger cross-section. Also the specimens without ties at joint gave more rotation compare to the control specimens with seismic application of ties at joint. Along with the moment-rotation curve of each specimen summary curve called hysteresis loop envelopes of each type were drawn with highest and lowest point of each cycle. Grand total summary curve i.e. hysteresis loop envelopes of all types were also drawn including the highest and lowest point of each cycle of all specimens. From moment-rotation curves comparison of normal sample with control sample can be done. At the same time from the hysteresis loop envelopes curves at a glance the difference can be noticed.

Table 4.4: Cyclic Moment-Rotation for Upper Half Cycles

Sample	Cycle	Moment, (KN-m)	Rotation, ϕ (Degrees)
Type 1B	1st	9.906	0.013123
	2nd	12.954	0.030184
	3rd	8.382	0.041995
	4th	6.858	0.055118
Type 1A	1st	11.43	0.011811
	2nd	15.24	0.027559
	3rd	13.716	0.03937
	4th	9.906	0.053806
Type 2C	1st	14.478	0.010499
	2nd	18.288	0.024934
	3rd	13.716	0.036745
	4th	10.668	0.052493
Type 2B	1st	16.002	0.009843
	2nd	21.336	0.020997
	3rd	16.764	0.035433
	4th	14.478	0.051181
Type 2A	1st	17.526	0.009186
	2nd	24.384	0.01706
	3rd	25.146	0.031496
	4th	19.05	0.049869
Type 3B	1st	21.336	0.007874
	2nd	29.718	0.014436
	3rd	25.908	0.026247
	4th	20.574	0.045932
Type 3A	1st	22.86	0.006562
	2nd	32.004	0.011811
	3rd	34.29	0.02231
	4th	30.48	0.044619

Table 4.5: Cyclic Moment-Rotation for Lower Half Cycles

Sample	Cycle	Moment, (KN-m)	Rotation, ϕ (Degrees)
Type 1B	1st	10.668	0.015748
	2nd	12.192	0.030184
	3rd	7.62	0.043307
	4th	6.096	0.057743
Type 1A	1st	11.43	0.011811
	2nd	15.24	0.027559
	3rd	14.097	0.03937
	4th	9.144	0.053806
Type 2C	1st	13.716	0.010499
	2nd	19.812	0.023622
	3rd	15.24	0.038058
	4th	11.43	0.052493
Type 2B	1st	16.002	0.010499
	2nd	21.336	0.019685
	3rd	17.526	0.034121
	4th	16.002	0.049869
Type 2A	1st	17.526	0.009186
	2nd	23.622	0.01706
	3rd	24.384	0.031496
	4th	20.574	0.049869
Type 3B	1st	19.812	0.007874
	2nd	29.718	0.015748
	3rd	26.67	0.028871
	4th	24.384	0.047244
Type 3A	1st	22.098	0.006562
	2nd	31.242	0.013123
	3rd	33.528	0.024934
	4th	29.718	0.044619

4.5.1 Moment-Rotation Response of Type 1 Specimens

Moment-Rotation response Type 1B and Type 1A are shown in Figure 4.35 and 4.36. With a view to the moment-rotation curve of Type 1 it can be found that Type 1B gave deviated curve where Type 1A gave smooth curve. From figures it can be observed that within four cycles loading Type 1A specimen gave almost same highest moment for two cycles, where Type 1B specimen gave no same highest moment. This represents the more ductile quality of Type 1A. Also Type 1A specimen undergoes larger rotations without rupture before failure than Type 1B specimen. The maximum moment of Type 1A sample was 15.24 KN-m, where for Type 1B sample it was 12.954 KN-m in respect of the calculated moment of 11 KN-m for the sample. Highest moment increased almost 17.65% by seismic application of ties at joint. Maximum rotation of Type 1B sample under loading was 0.055118 degrees where for Type 1A sample maximum rotation was 0.053806 degrees.

The hysteresis loop envelopes of Type 1A and Type 1B is shown in Figure 4.37. A sudden fall from the top point of Type 1B can be seen from the hysteresis loop envelopes curves. At every point of the hysteresis loop curves Type 1A specimen showed more moment value and less rotation value than Type 1B. This is obviously the sign of comparative better performance. Hence Type 1A specimen is more ductile, stiffer and stronger than Type 1B specimen.

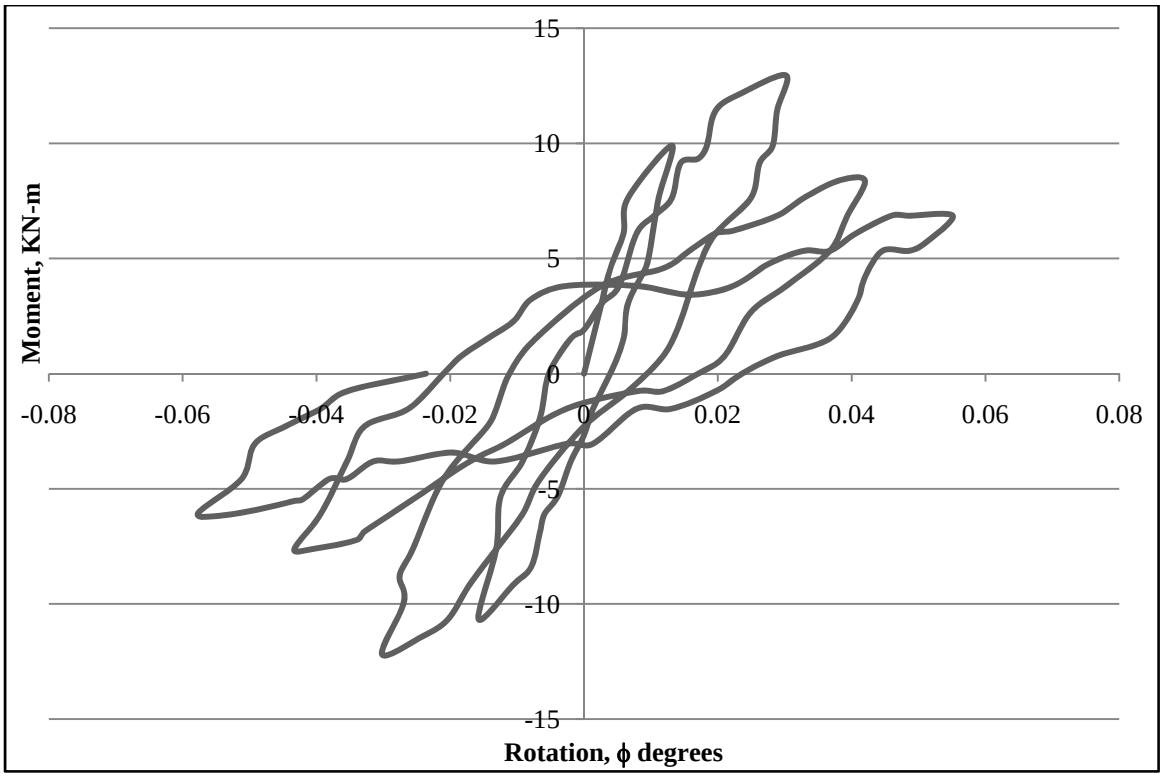

Figure 4.35: Moment-Rotation Response of Type 1B Specimen (Without Tie at Joint)

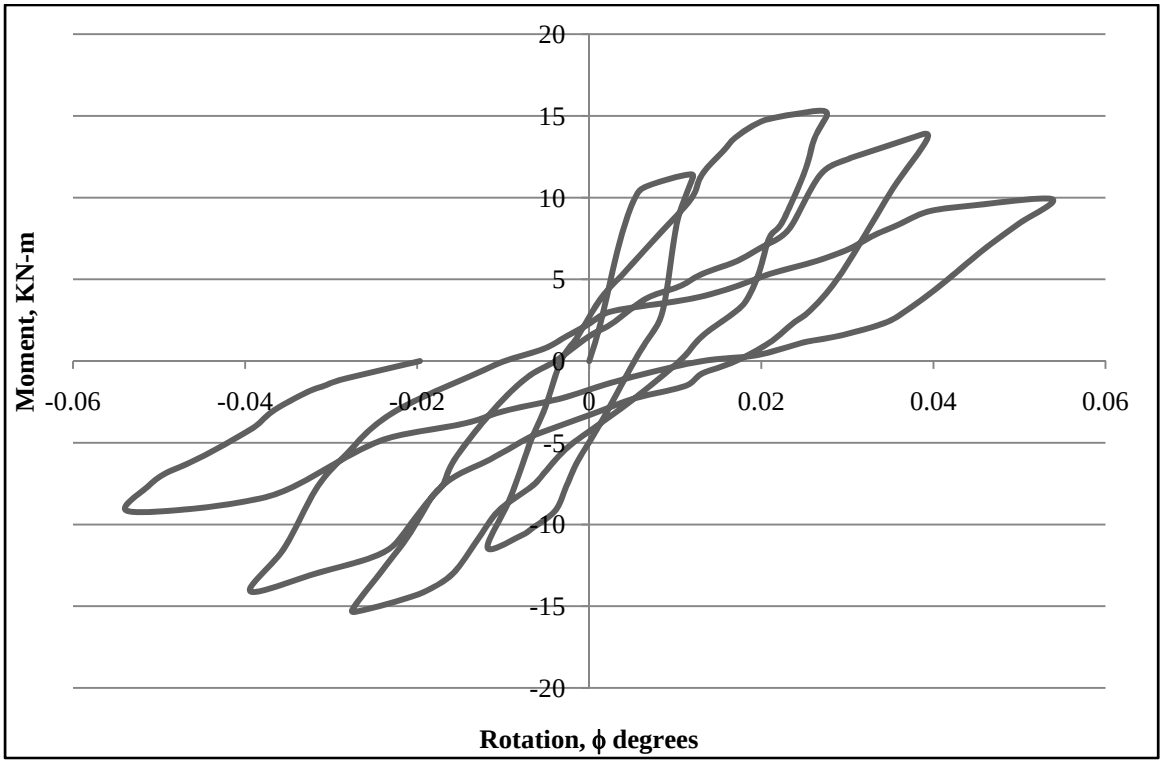

Figure 4.36: Moment-Rotation Response of Type 1A Specimen (With Tie at Joint)

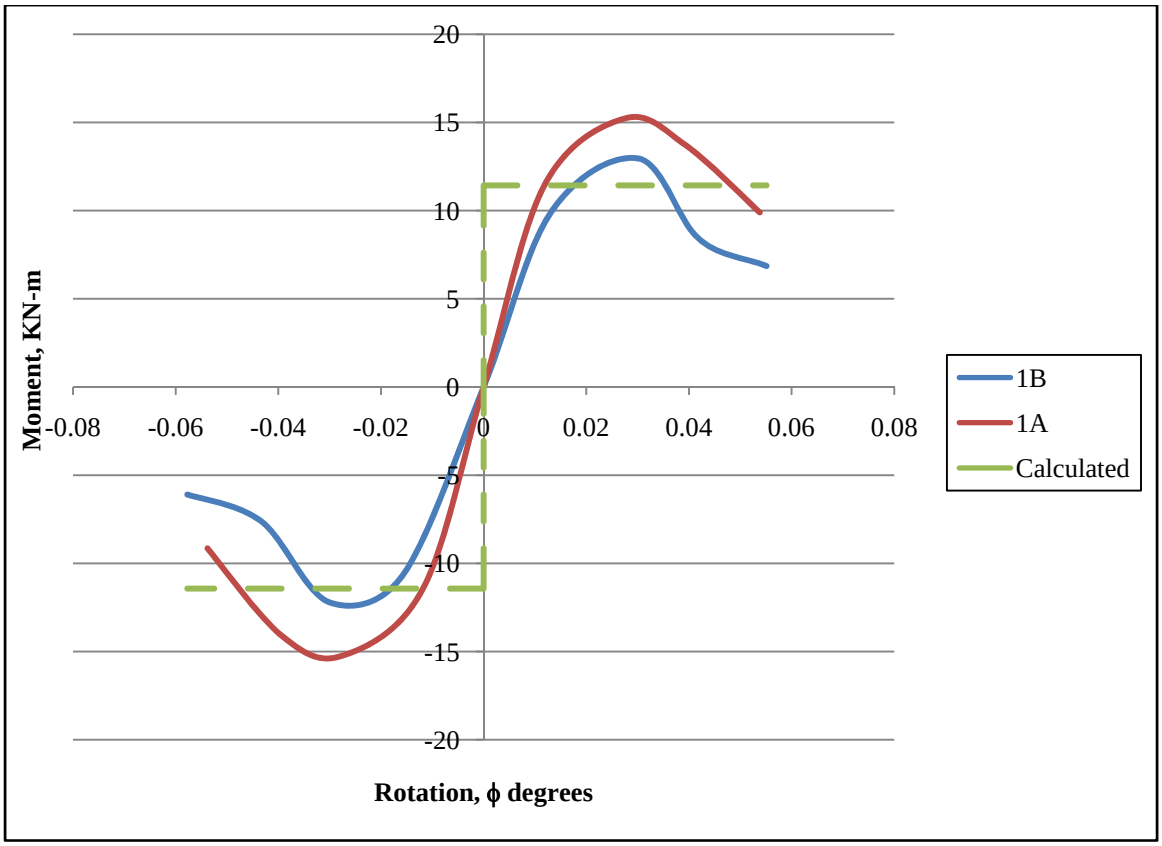

Figure 4.37: Hysteresis Loop Envelopes (M - ϕ) of Type 1A and Type 1B Specimens

4.5.2 Moment-Rotation Response of Type 2 Specimens

Moment-Rotation response Type 2C, Type 2B and Type 2A are shown in Figure 4.38, 4.39 and 4.40. With a view to the moment-rotation curve of Type 2 it can be found that Type 2C and Type 2B gave deviated curves where Type 2A gave smooth curve. From figures it can be observed that within four cycles loading Type 2A specimen gave almost same highest moment for two cycles, where Type 2B and Type 2C specimens gave no same highest moment. This represents the more ductile quality of Type 2A. Nevertheless, Type 2A specimen undergoes larger rotations without rupture before failure than Type 2B specimen. Also Type 2B specimen undergoes larger rotation without rupture before failure than Type 2C specimen. The maximum moment of Type 2A sample was 25.146 KN-m, where for Type 2B sample it was 21.336 KN-m and Type 2C sample it was 18.288 KN-m in respect of the calculated load of 19 KN-m for the sample. Highest moment increased almost 16.67% by special distribution of ties at Type 2B. Furthermore, highest moment increased almost 17.86% by seismic application of ties at joint. Maximum rotation of Type 2A sample under loading was 0.049869 degrees where for Type 2C sample maximum rotation was 0.052493 degrees and for Type 2B sample maximum rotation was 0.051181 degrees.

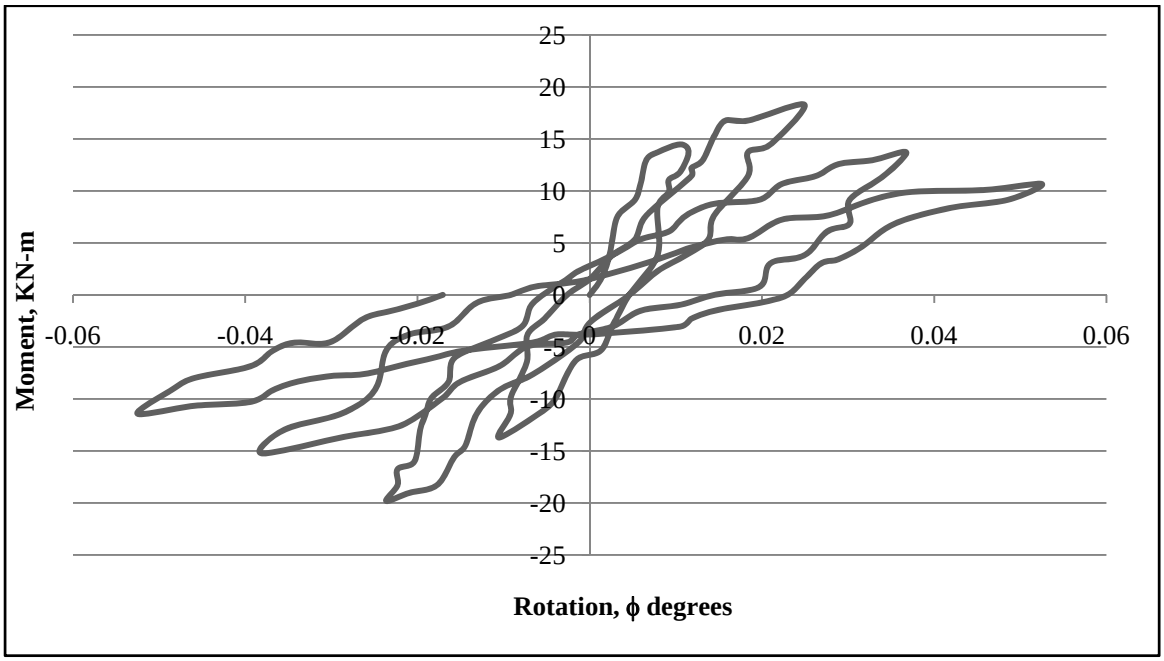

Figure 4.38: Moment-Rotation Response of Type 2C Specimen (General)

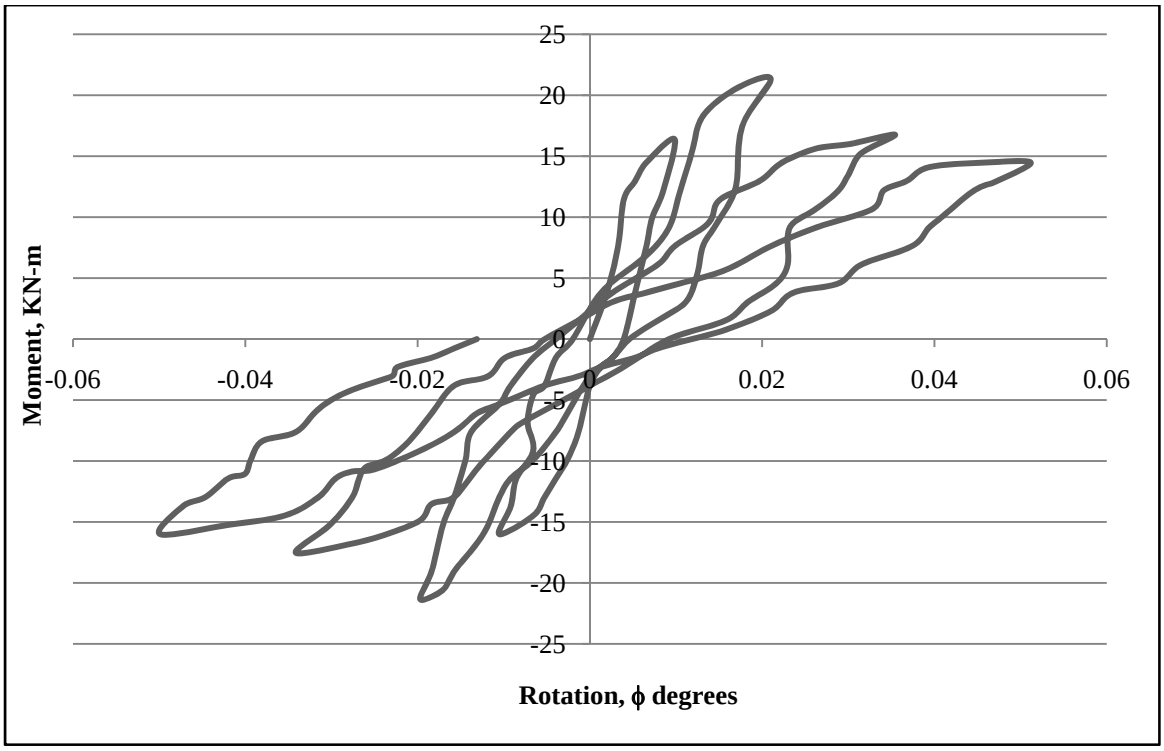

Figure 4.39: Moment-Rotation Response of Type 2B Specimen (Without Tie at Joint)

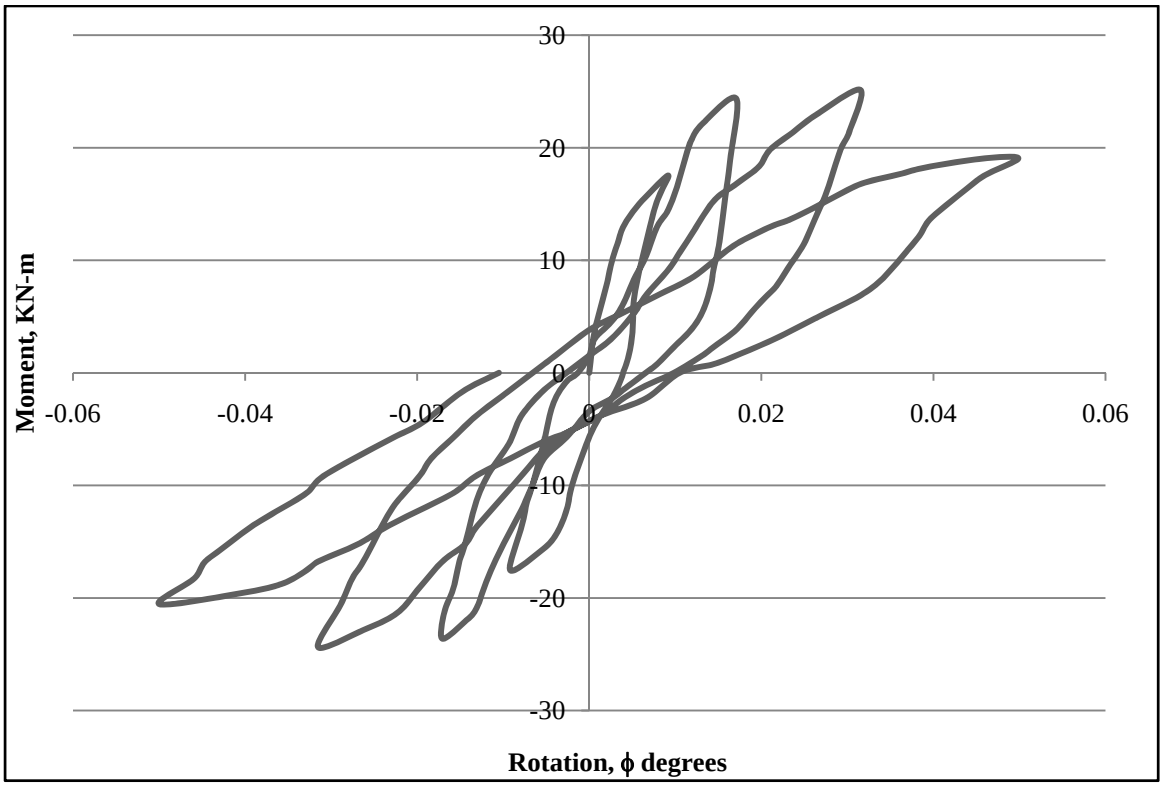

Figure 4.40: Moment-Rotation Response of Type 2A Specimen (With Tie at Joint)

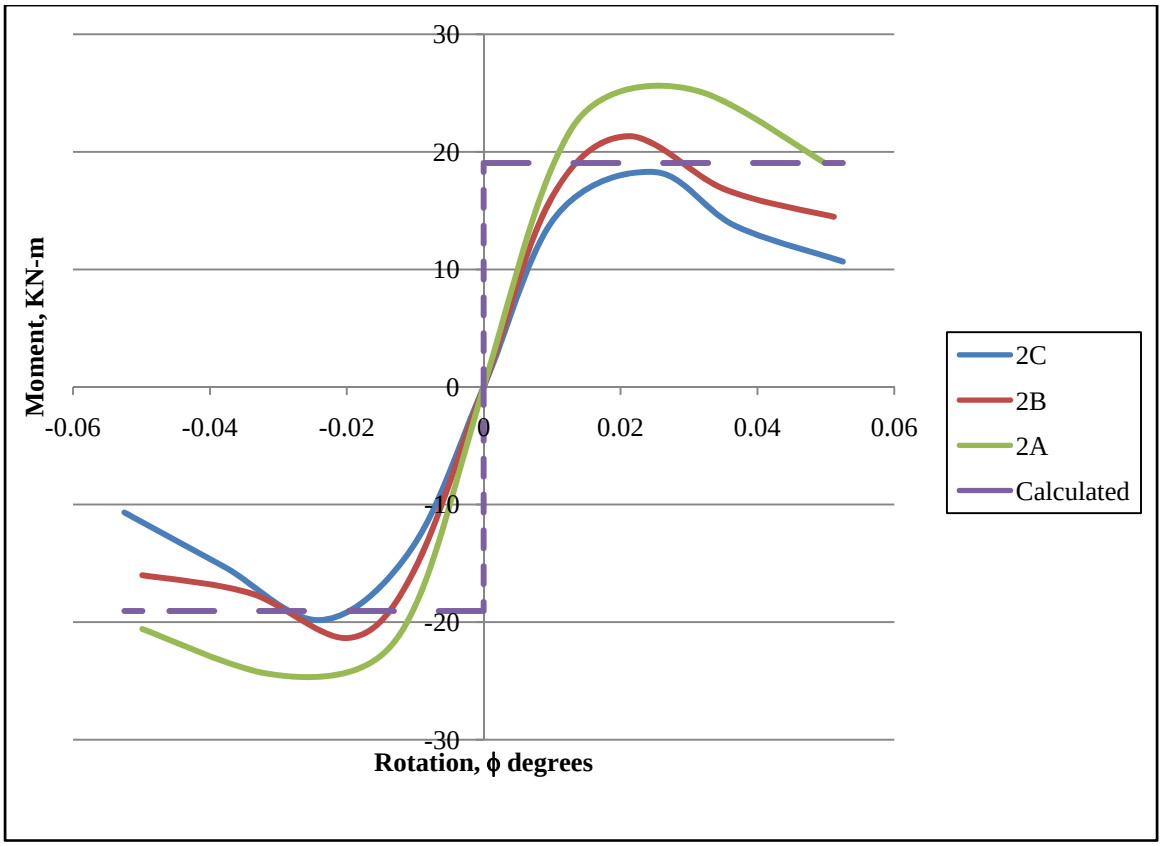

Figure 4.41: Hysteresis Loop Envelopes (M - ϕ) of Type 2A, Type 2B and Type 2C Specimens

The hysteresis loop envelopes of Type 2A, Type 2B and Type 2C is shown in Figure 4.41. A sudden fall from the top point of Type 2B and Type 2C can be seen from the hysteresis loop envelopes curves. At every point of the hysteresis loop curves Type 2A specimen showed more moment value and less rotation value than Type 2B and Type 2C. Also at every point of the hysteresis loop curves Type 2B specimen showed more moment value and less rotation value than Type 2C. This is obviously the sign of comparative better performance. Hence Type 2A specimen is more ductile, stiffer and stronger than Type 2B specimen, where Type 2B specimen is more ductile, stiffer and stronger than Type 2C specimen.

4.5.3 Moment-Rotation Response of Type 3 Specimens

Moment-Rotation response Type 3B and Type 3A are shown in Figure 4.42 and 4.43. With a view to the moment- rotation curve of Type 3 it can be found that Type 3B gave deviated curve where Type 3A gave smooth curve. From figures it can be observed that within four cycles loading Type 3A specimen gave almost same highest moment for three cycles, where Type 3B specimen gave almost same highest moment for two cycles. This represents the more ductile quality of Type 3A. Also Type 3A specimen undergoes larger rotations without rupture before failure than Type 3B specimen. The maximum moment of Type 3A sample was 34.29 KN-m, where for Type 3B sample it was 29.718 KN-m in respect of the calculated moment of 28 KN-m for the sample. Highest moment increased almost 15.38% by seismic application of ties at joint. Maximum rotation of Type 3B sample under loading was 0.045932 degrees where for Type 3A sample maximum rotation was 0.044619 degrees.

The hysteresis loop envelopes of Type 3A and Type 3B is shown in Figure 4.44. A sudden fall from the top point of Type 3B can be seen from the hysteresis loop envelopes curves. At every point of the hysteresis loop curves Type 3A specimen showed more moment value and less rotation value than Type 3B. This is obviously the sign of comparative better performance. Hence Type 3A specimen is more ductile, stiffer and stronger than Type 3B specimen.

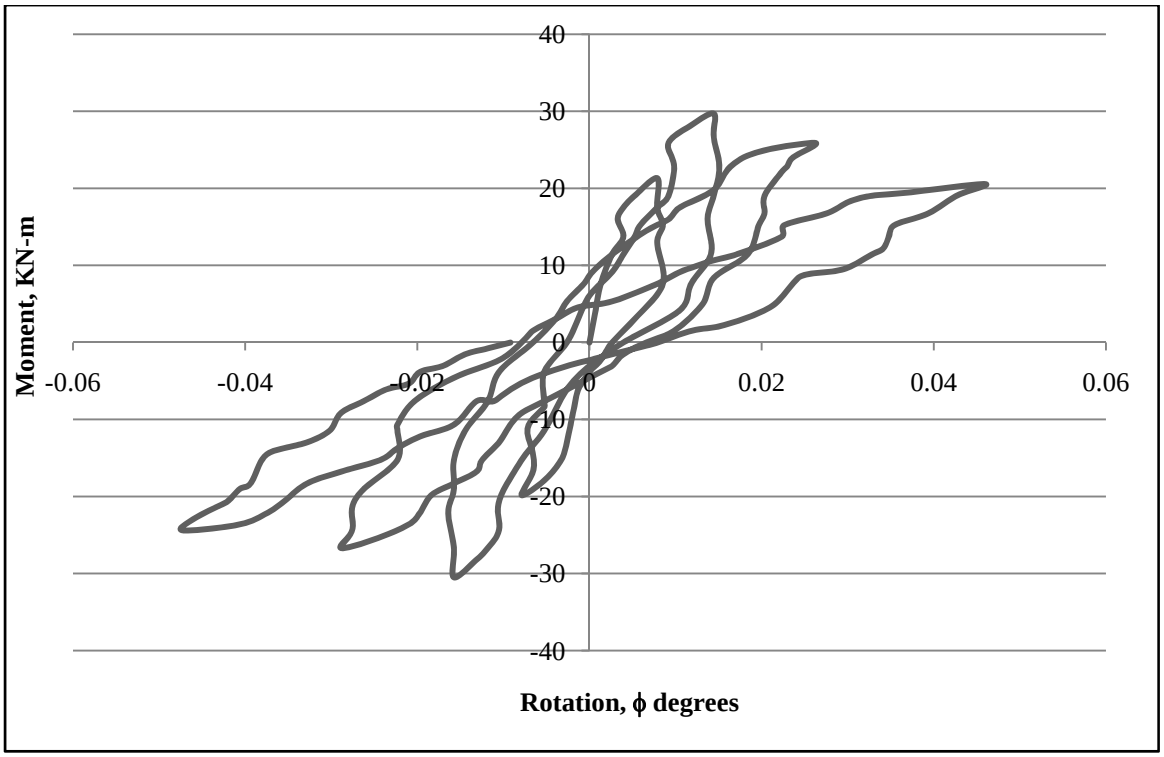

Figure 4.42: Moment-Rotation Response of Type 3B Specimen (Without Tie at Joint)

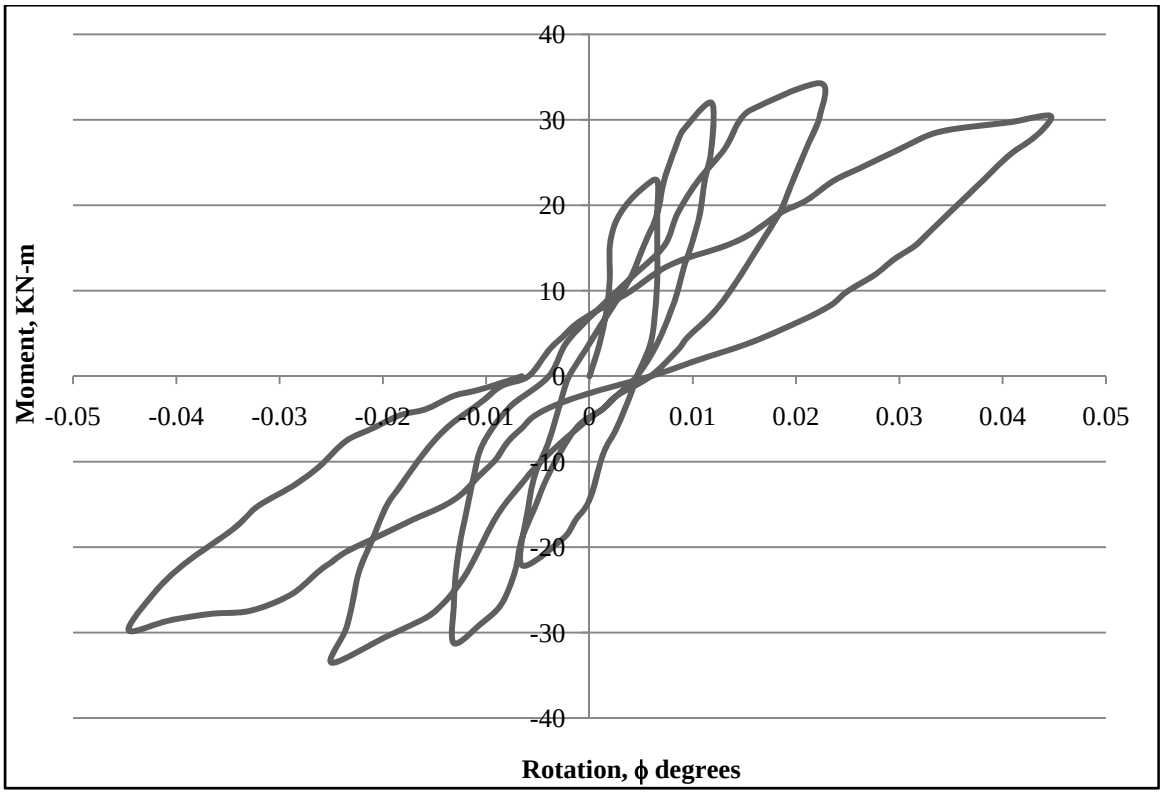

Figure 4.43: Moment-Rotation Response of Type 3A Specimen (With Tie at Joint)

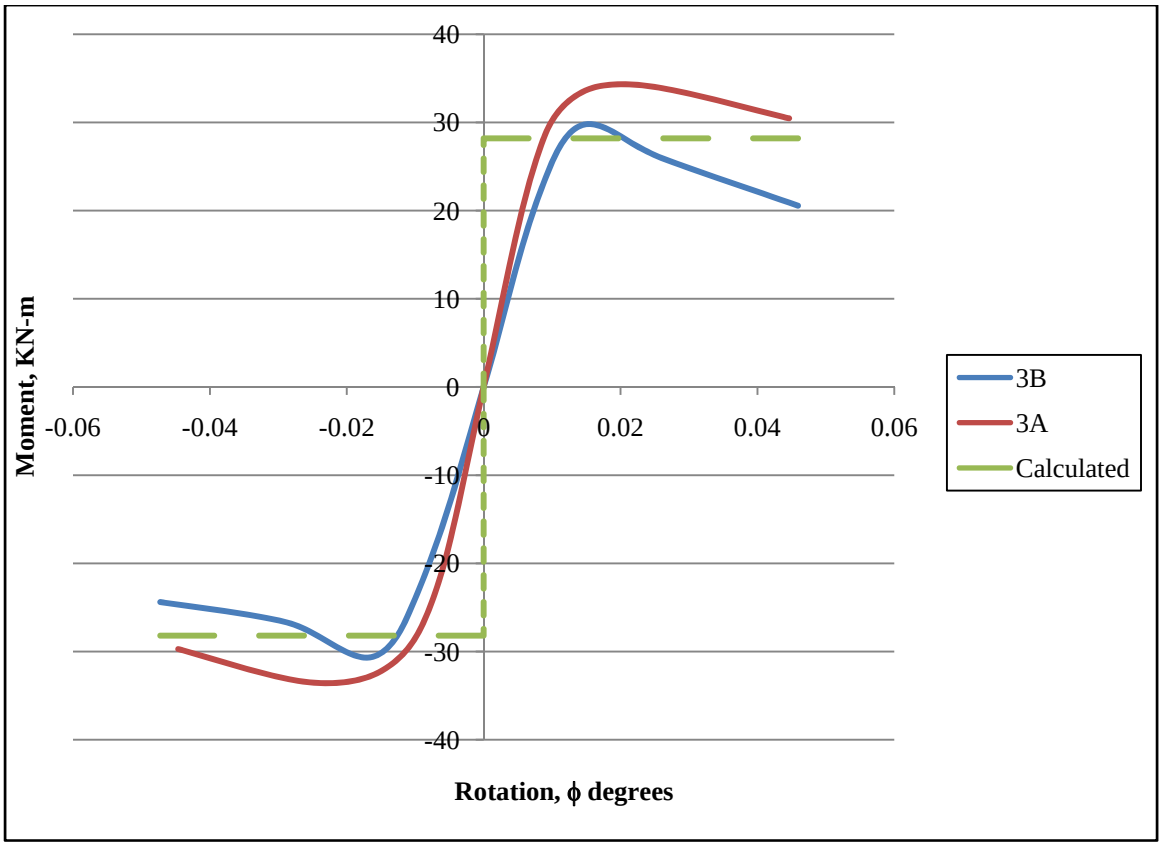

Figure 4.44: Hysteresis Loop Envelopes (M - ϕ) of Type 3A and Type 3B Specimens

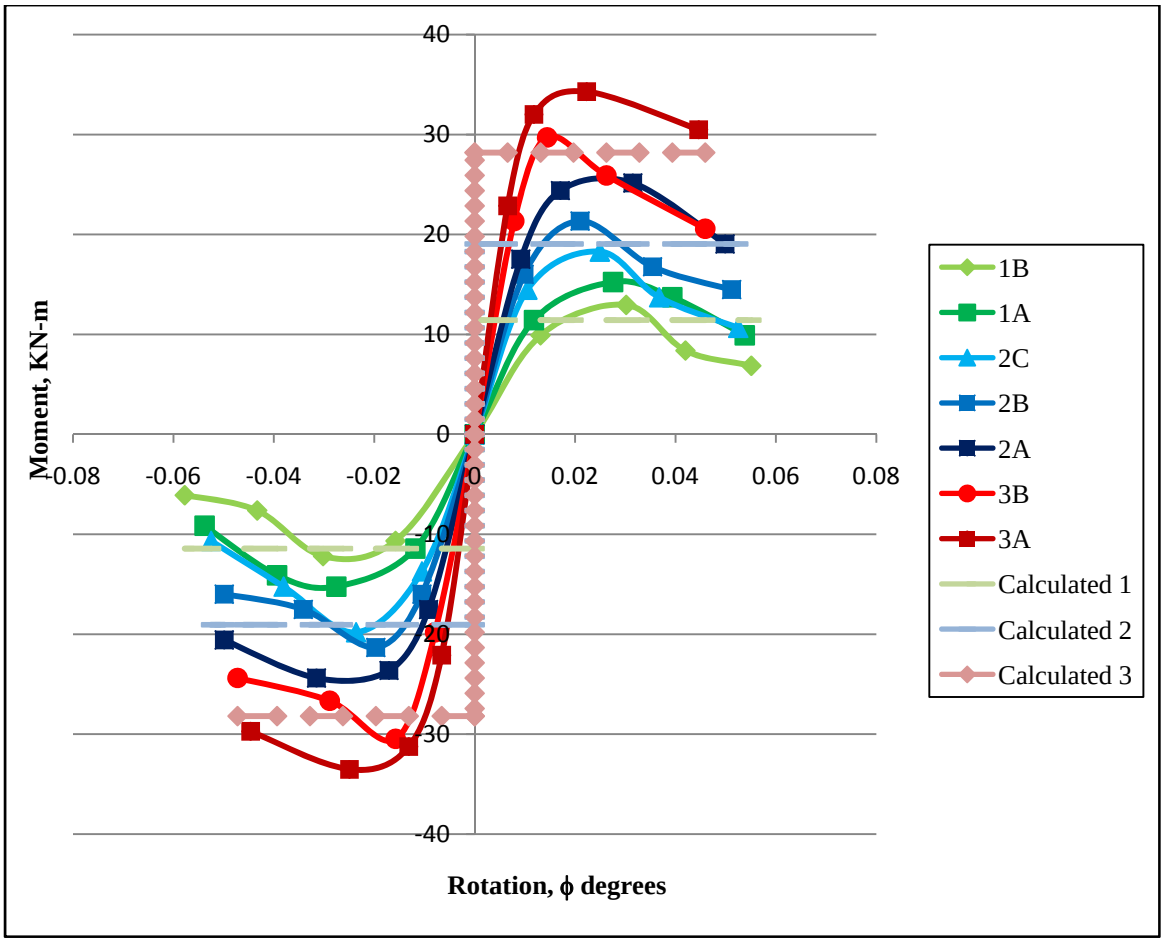

Figure 4.45: Hysteresis Loop Envelopes (M - ϕ) of Seven Specimens

4.6 Summary of Test Results of Seven Specimens

Table 4.6: Test Results of Seven Specimens

Name of the specimens	Yield Load (KN)	Yield Displacement (mm)	Calculated Load (KN)	Maximum Load (KN)	Maximum Displacement (mm)
1B	14	13	15	17	42
1A	19	12		20	41
2C	20	10	25	24	40
2B	22	09		28	39
2A	24	08		33	38
3B	31	07	37	39	35
3A	35	06		45	34

Table 4.7: Average Secant Stiffness (average of L/D) of Seven Specimens at Each Cycle

Cycle	1B	1A	2C	2B	2A	3B	3A
1st	1.24	1.67	2.32	2.72	3.29	4.50	5.90
2nd	0.72	0.95	1.41	1.81	2.42	3.40	4.39
3rd	0.32	0.61	0.67	0.85	1.36	1.65	2.49
4th	0.20	0.30	0.37	0.52	0.70	0.83	1.17

Table 4.8: Characteristics of First Crack of Seven Specimens

Type	First Crack Cycle	First Crack Side	First Crack Load (KN)	First Crack Displacement (mm)
1B	2nd	Left	16	16
1A	2nd	Left	20	15
2C	2nd	Left	22	14
2B	2nd	Left	27	13
2A	3rd	Right	31	24
3B	2nd	Left	37	09
3A	3rd	Right	41	12

4.7 Characteristics of First Crack Formation

The very first crack for all specimens appeared in joint during the loading of second cycle except Type 2A and Type 3A, for which the first crack occurred at third cycle. For specimens 1B and 1A first crack occurred at 16 KN and 20 KN when displacements were 16 mm and 15 mm respectively. For specimens 2C and 2B first crack occurred at 22 KN and 27 KN with displacements of 14mm and 13mm respectively. For specimen 2A the first crack load was 31 KN with the displacement of 24 mm at 3rd cycle. For specimens 3B and 3A first crack occurred at 37 KN and 41 KN when displacements were 09 mm and 12 mm (at 3rd cycle) respectively. Load at first crack formation of all seven samples are expressed in Figure 4.46. From the figure it can be observed that first crack load increased with the seismic application of ties at joint. It also varies according the increase in cross-section. At the same time the displacements of first crack loads were comparatively more to the samples without ties at joints.

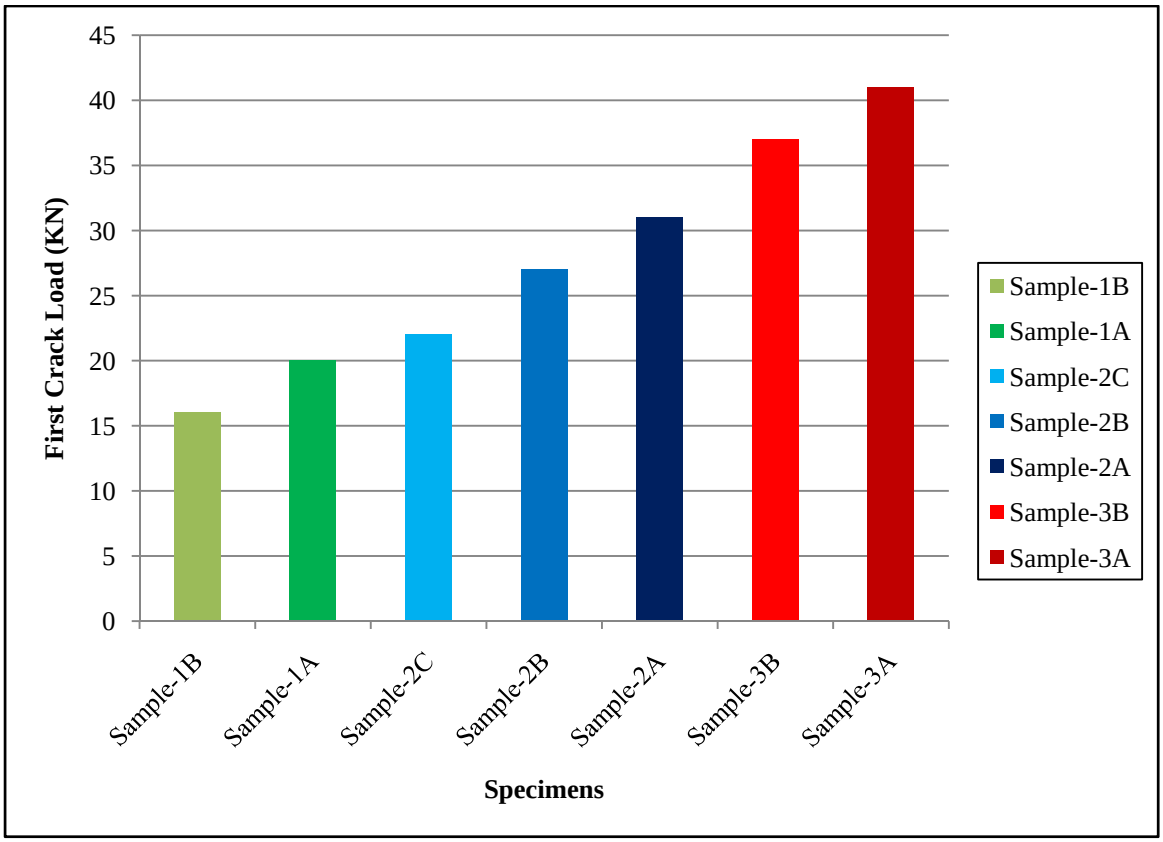

Figure 4.46: Load at First Crack Formation of Seven Specimens

4.8 Stiffness

The average stiffness obtained for the two half cycles in a hysteretic loop therefore gave the approximate stiffness for that particular cycle. In other words, the secant stiffness was formulated with standard mathematical formula,

Secant Stiffness = Shear Force/ Displacement ($k = F/\Delta$).

The values of the secant stiffness obtained for each cycle are plotted for all the specimens. The degradation of the secant stiffness is plotted, the ultimate stiffness versus corresponding cycle number for each specimen tested. Figure 4.47 shows secant stiffness of each cycle. Figure 4.48 shows degradation of stiffness of each cycle. It can be noted that as the number of cycles increases, stiffness decreases. The value of stiffness was comparatively higher in every cycle in the case of specimens with ties at joint region. However, as the number of cycles increases, the rate of degradation of stiffness decreases in the case of specimens with ties at joint region. Stiffness after first cycle and fourth cycle are shown in Figure 4.49 and 4.51. The increase in stiffness between different categories at first cycle and fourth cycle are shown in Figure 4.50 and 4.52. For Type 1A stiffness varies from 1.67 to 0.31 where for Type 1B it varies from 1.30 to 0.21. Again, for Type 2A stiffness varies from 3.29 to 0.68 where for Type 2B it varies from 2.80 to 0.49 and for Type 2C it varies from 2.38 to 0.35. Lastly, for Type 3A stiffness varies from 6.00 to 1.18 where for Type 3B it varies from 4.67 to 0.77.

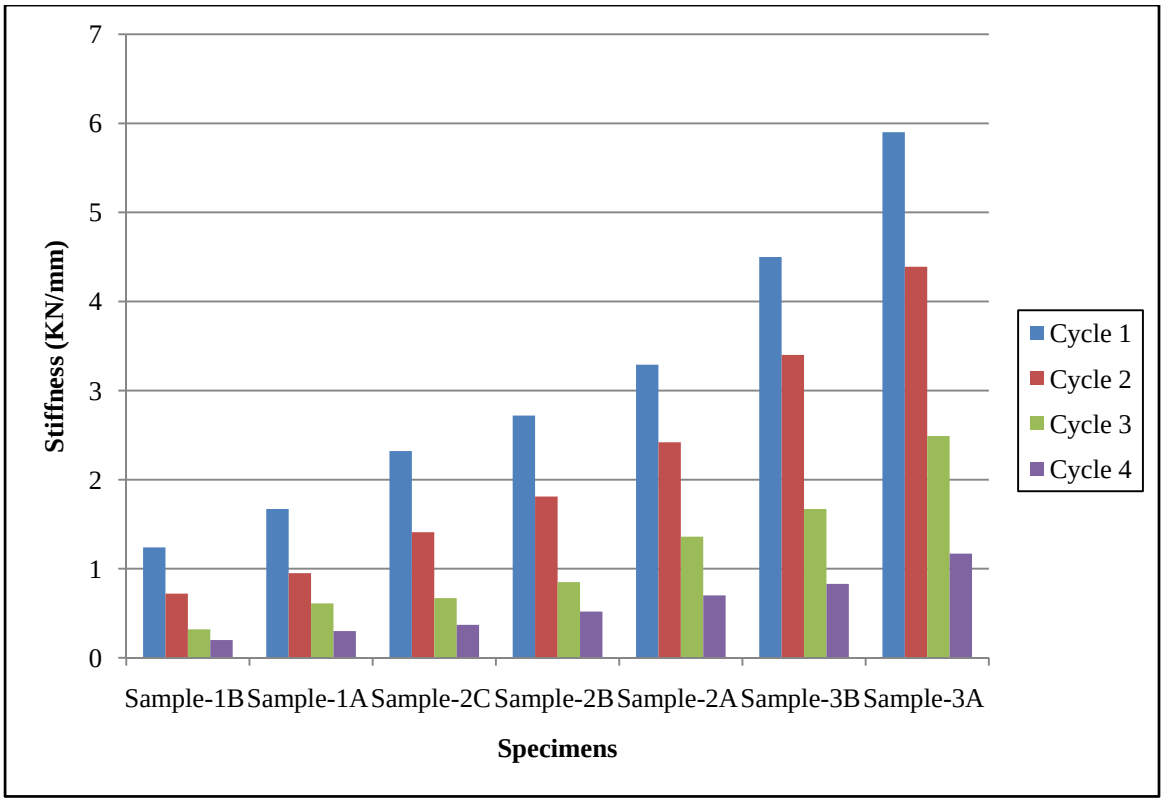

Figure 4.47: Average Secant Stiffness of Each Cycle for Seven Samples

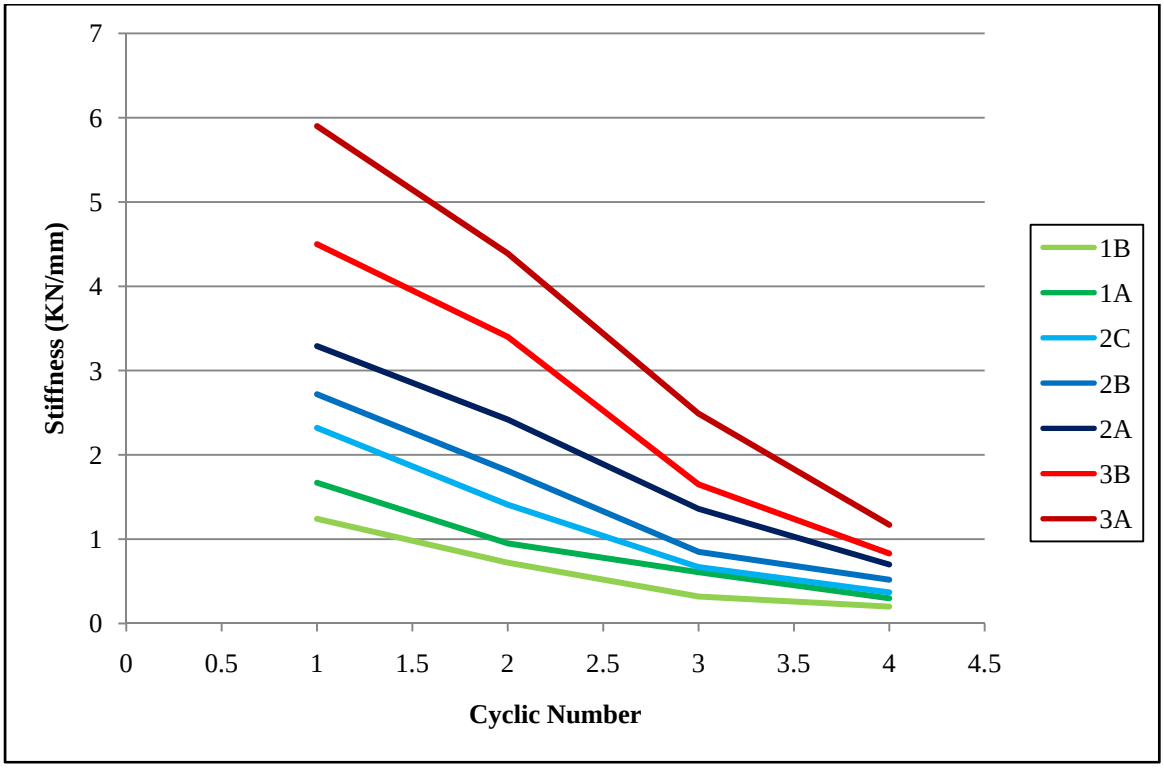

Figure 4.48: Degradation of Stiffness of Each Cycle for Seven Specimens

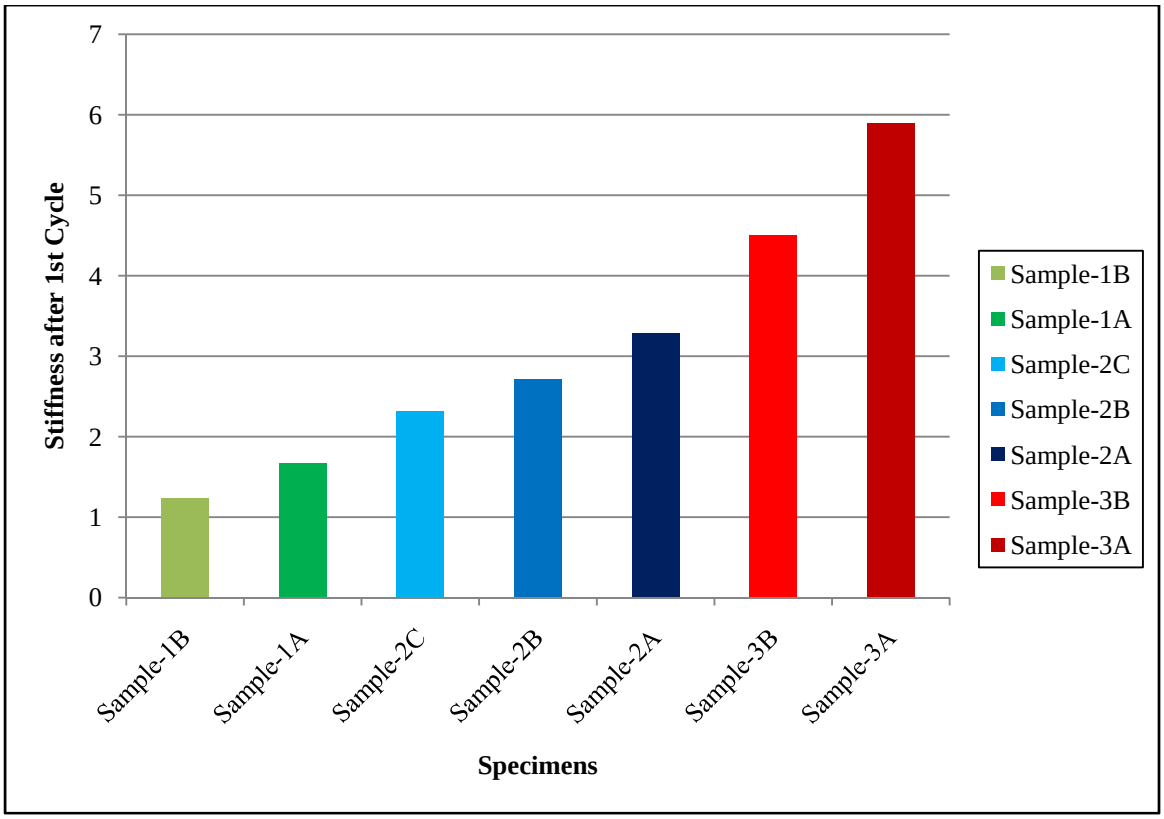

Figure 4.49: Stiffness after 1st Cycle of Seven Samples

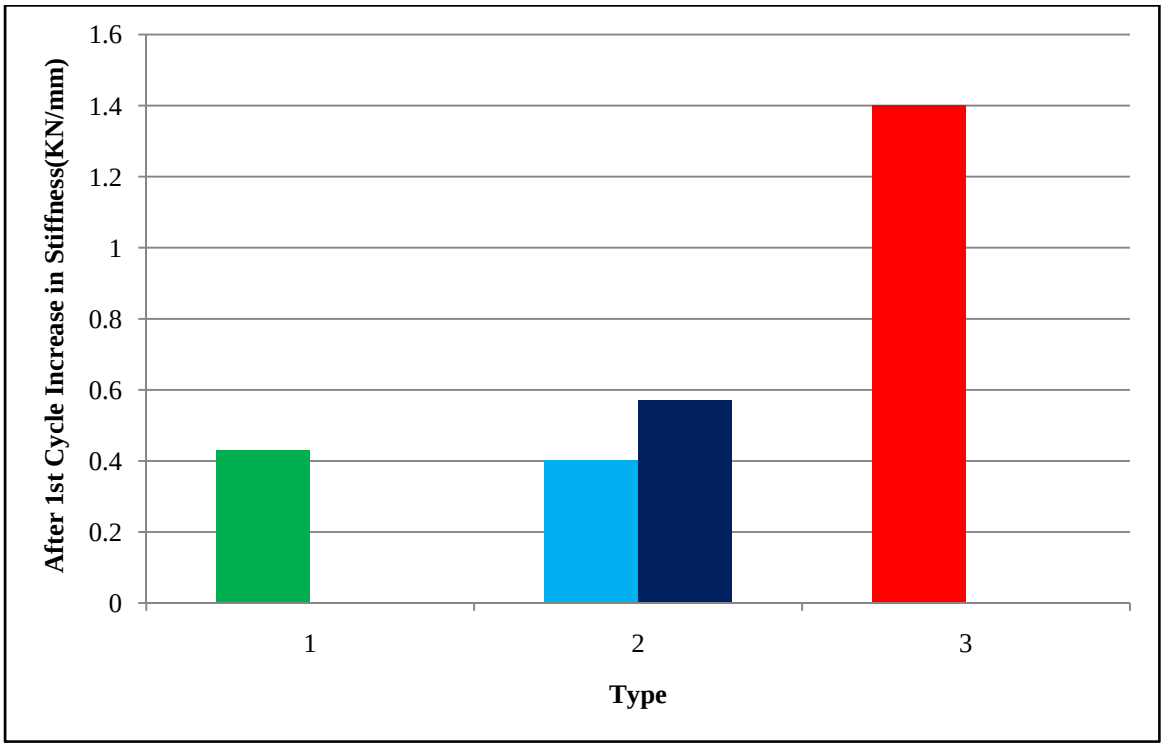

Figure 4.50: Increase in Stiffness between Different Categories at 1st Cycle

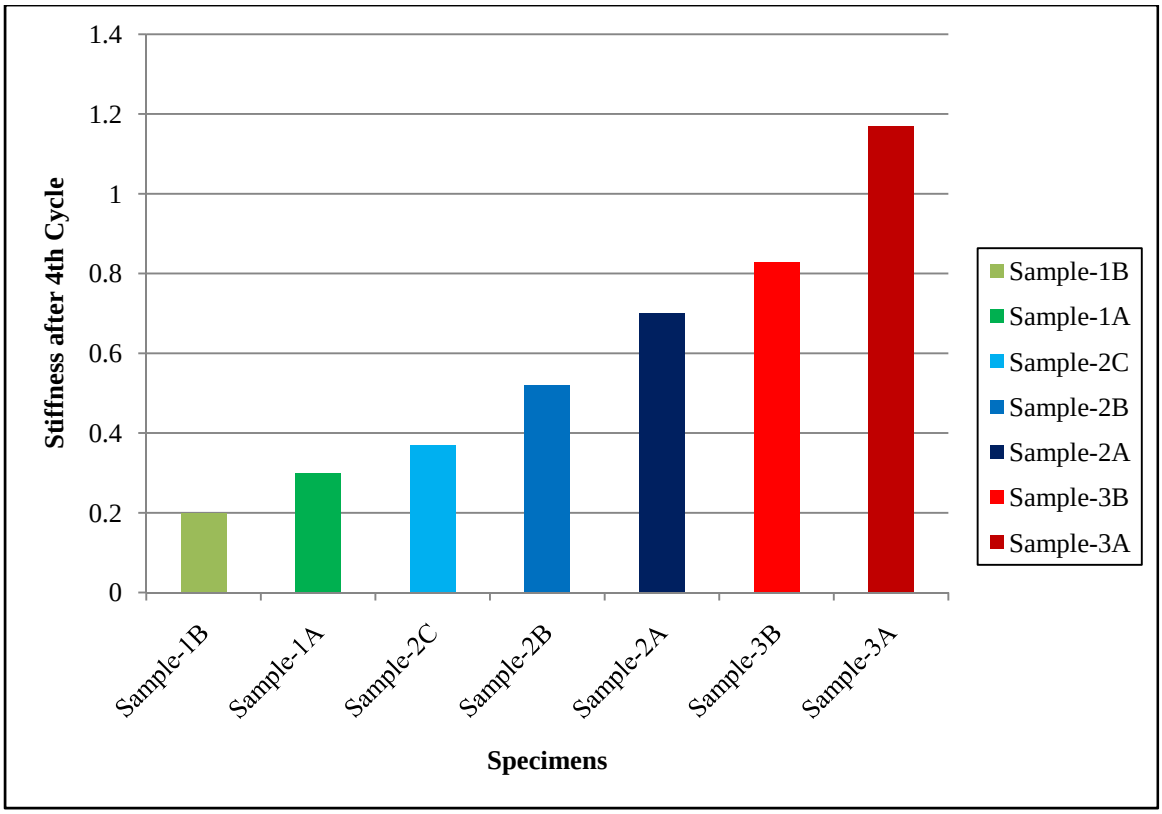

Figure 4.51: Stiffness after 4th Cycle of Seven Samples

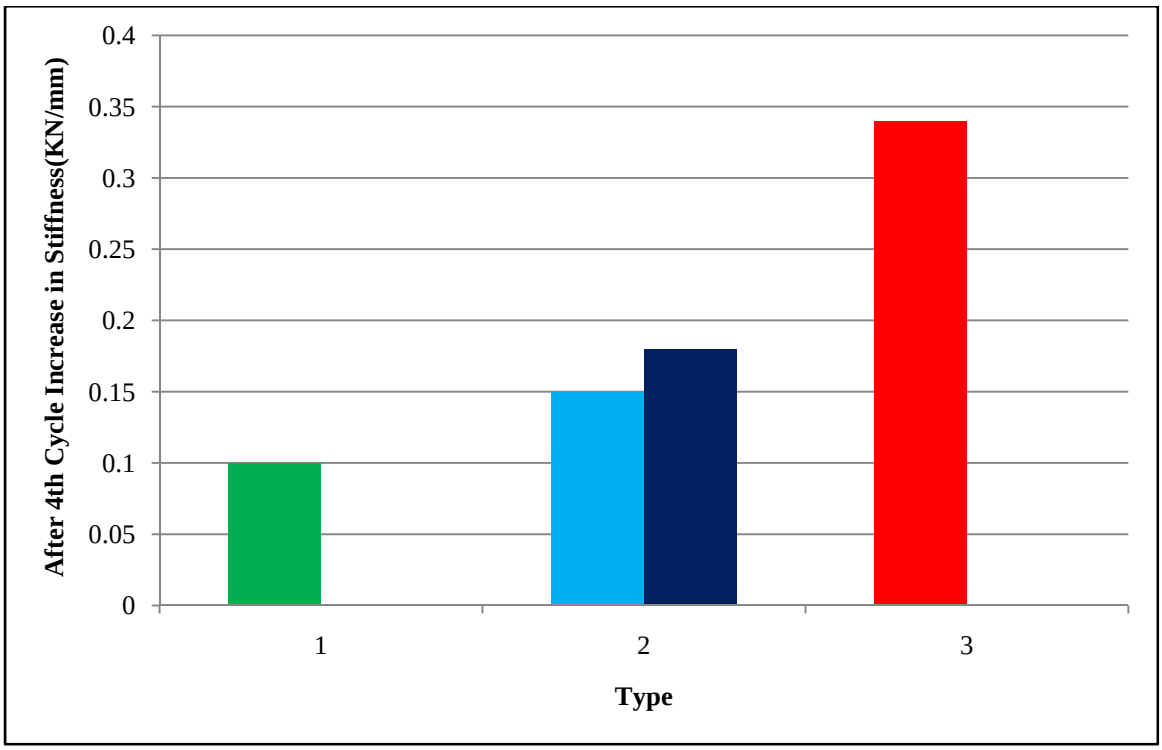

Figure 4.52: Increase in Stiffness between Different Categories at 4th Cycle

4.9 Load Characteristics

Beam-column joints with seismic application of ties at joint region exhibited more strength than joints without ties. Hence specimens with ties at joint region sustained at comparatively higher load than specimens without ties. Figure 4.53 represents the load of the specimens at every cycle of forward loading and Figure 4.54 represents the load of the specimens at every cycle of reverse loading. The maximum loads of joints with ties were also more than joints without ties. Figure 4.55 express the maximum load of all seven specimens. With the increase of cross-section of joints maximum load increased and the seismic effect of ties at joint to increase strength also increased. This can be observed from Figure 4.56. Maximum load increased from 17 KN to 20 KN for Type 1B to Type 1A. In case of Type 2C, 2B and 2A it increased from 24 KN, 28KN to 33KN. For Type 3B to Type 3A maximum load increased from 39 KN to 45 KN.

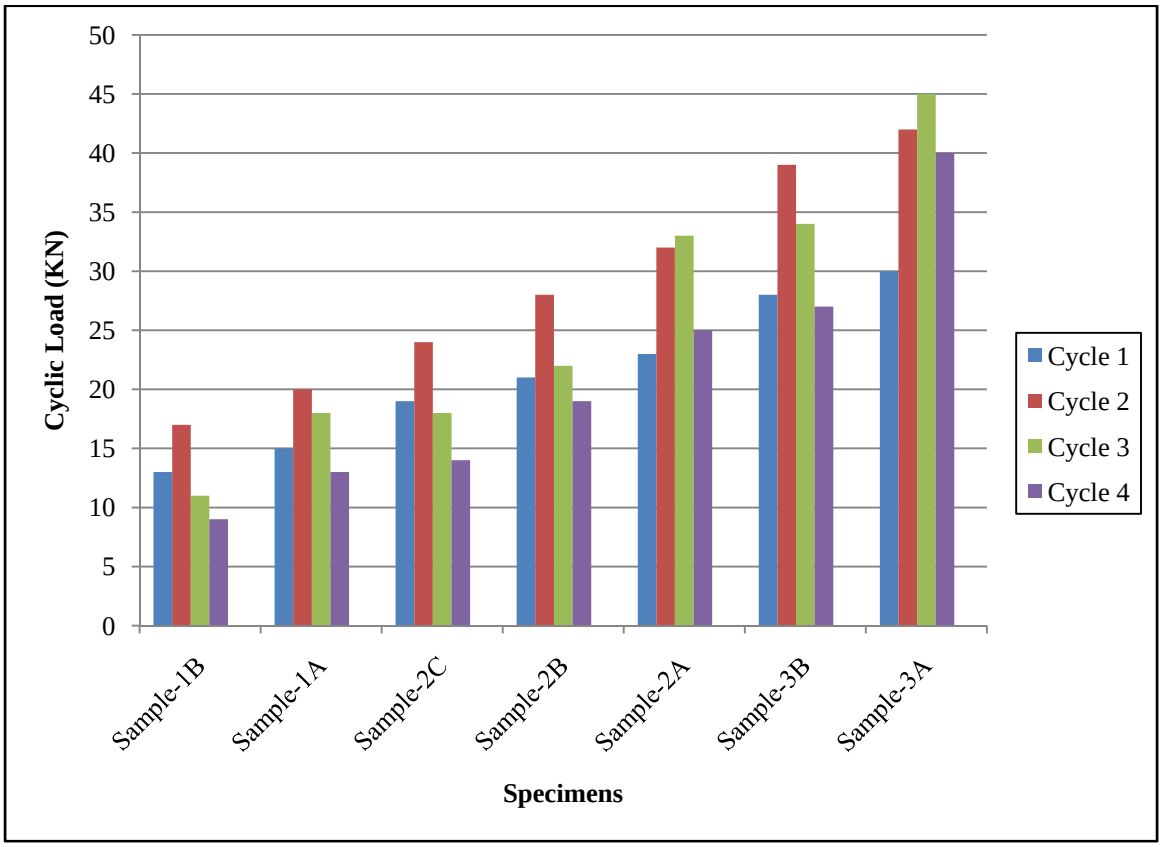

Figure 4.53: The Load of the Specimens at Every Cycle for Upper Half Cycles

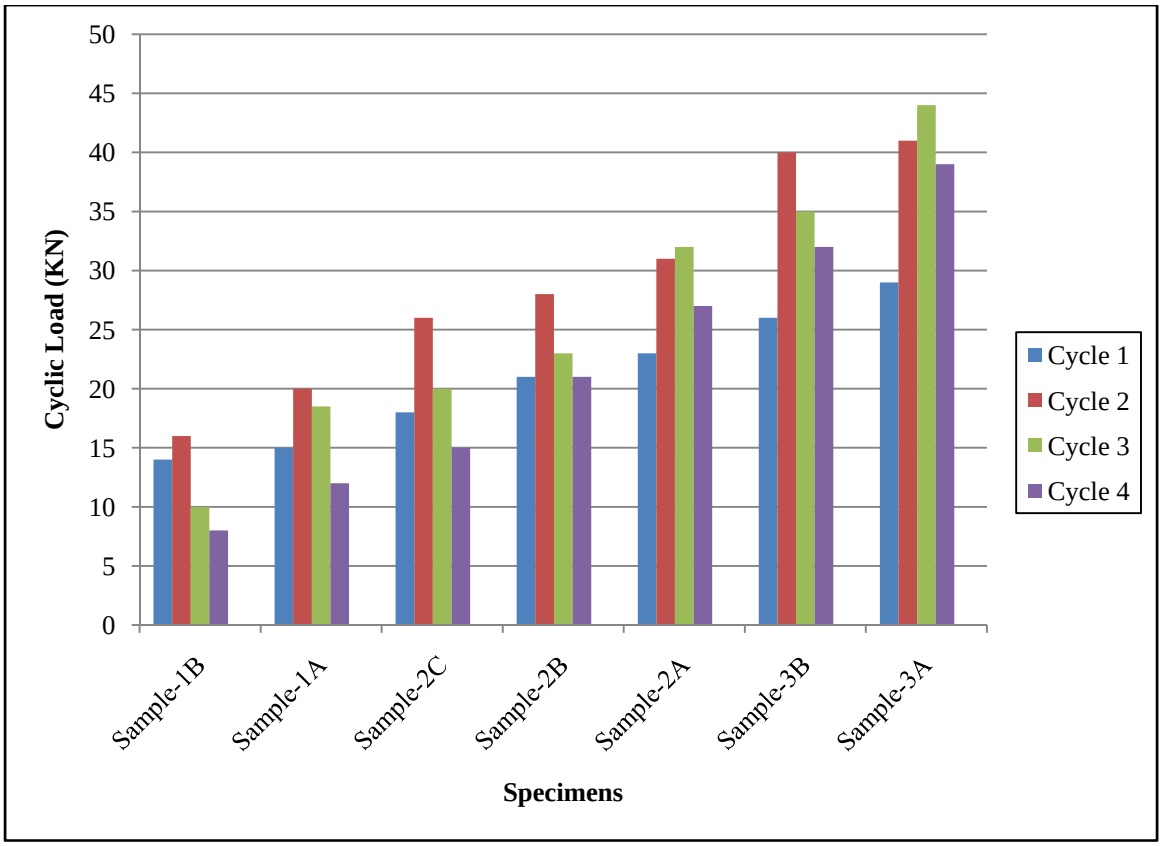

Figure 4.54: The Load of the Specimens at Every Cycle for Lower Half Cycles

From Figure 4.53 and Figure 4.54 it can be observed that within four cycles loading, control specimens gave almost similar loading for adjacent several cycles, which represent its more ductile quality. But general specimens did not show this property.

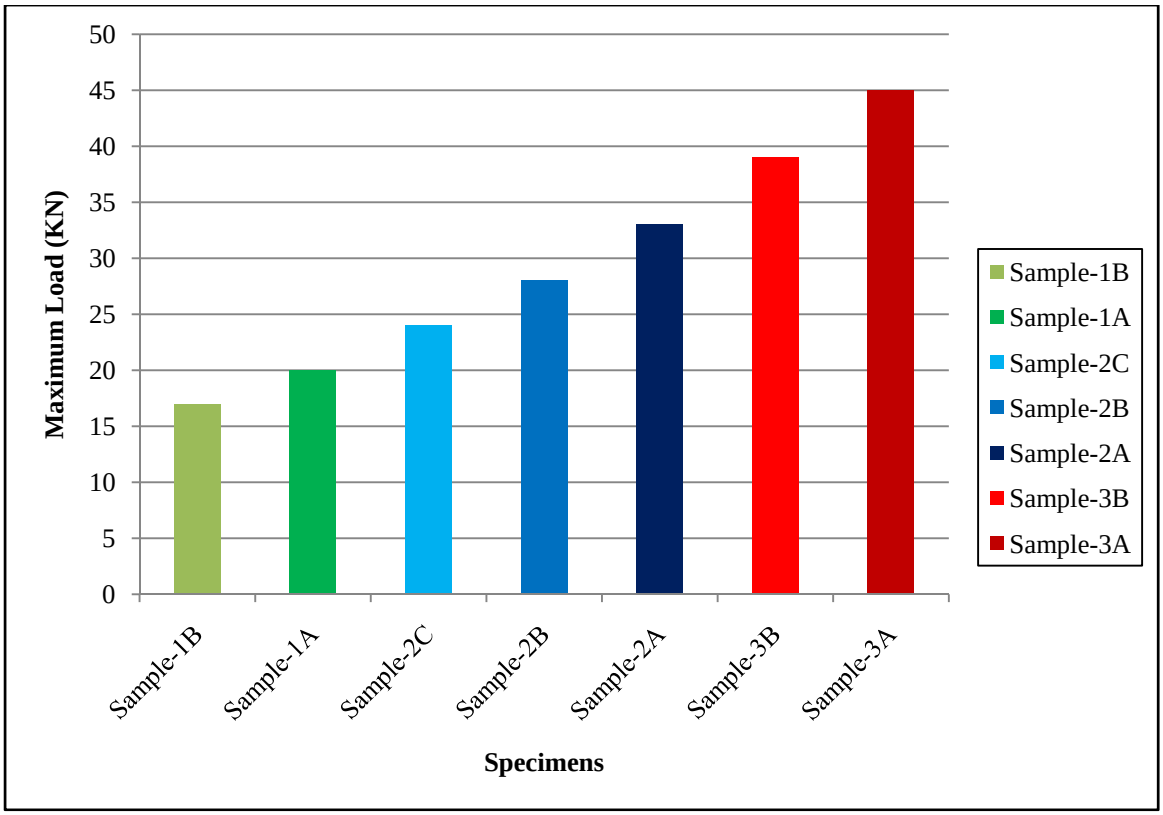

Figure 4.55: Maximum Load of All Seven Specimens

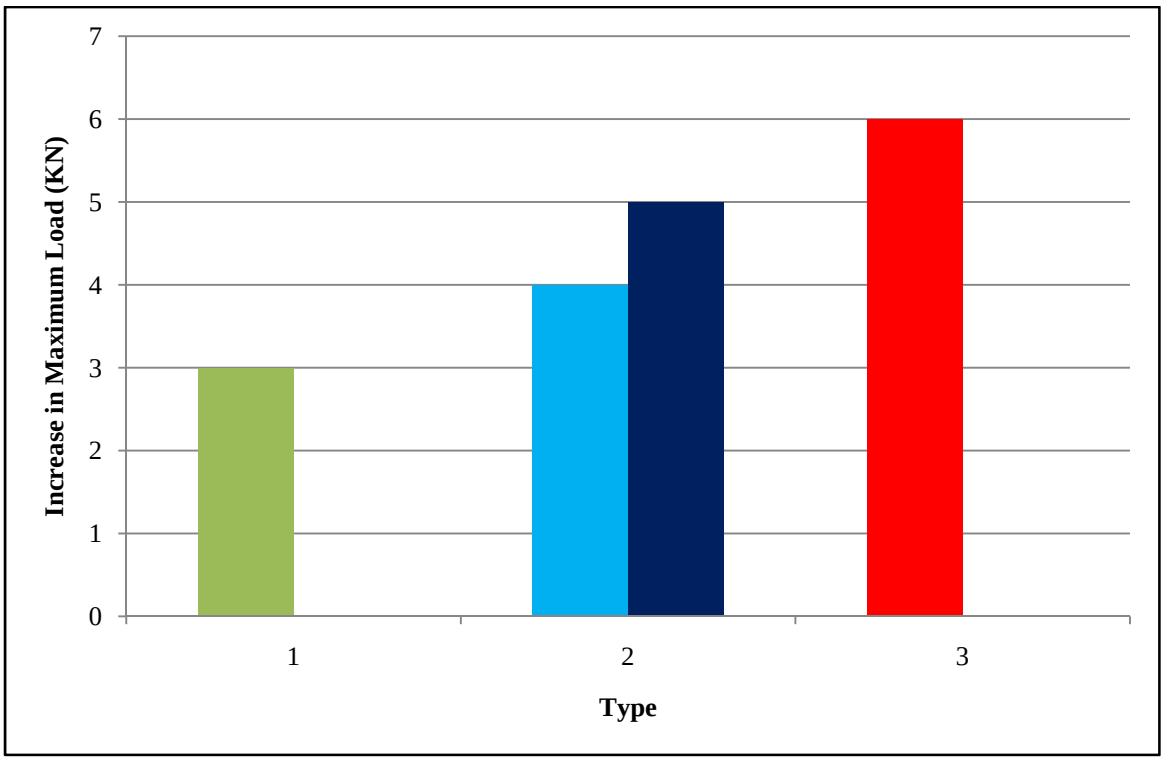

Figure 4.56: Increase in Maximum Load between Different Categories

4.10 Maximum Displacement

Table 4.9: Maximum Displacement of Each Specimen during Test

Specimen	Maximum Displacement
Type 1B	42
Type 1A	41
Type 2C	40
Type 2B	39
Type 2A	38
Type 3B	35
Type 3A	34

Table 4.9 summarized the maximum displacements of every specimens of different type during loading and unloading of four cycles. It was found that the maximum displacements were decreasing with the increasing size of cross-section and seismic application of ties at joint region. Figure 4.57 represents the maximum displacement of all seven specimens.

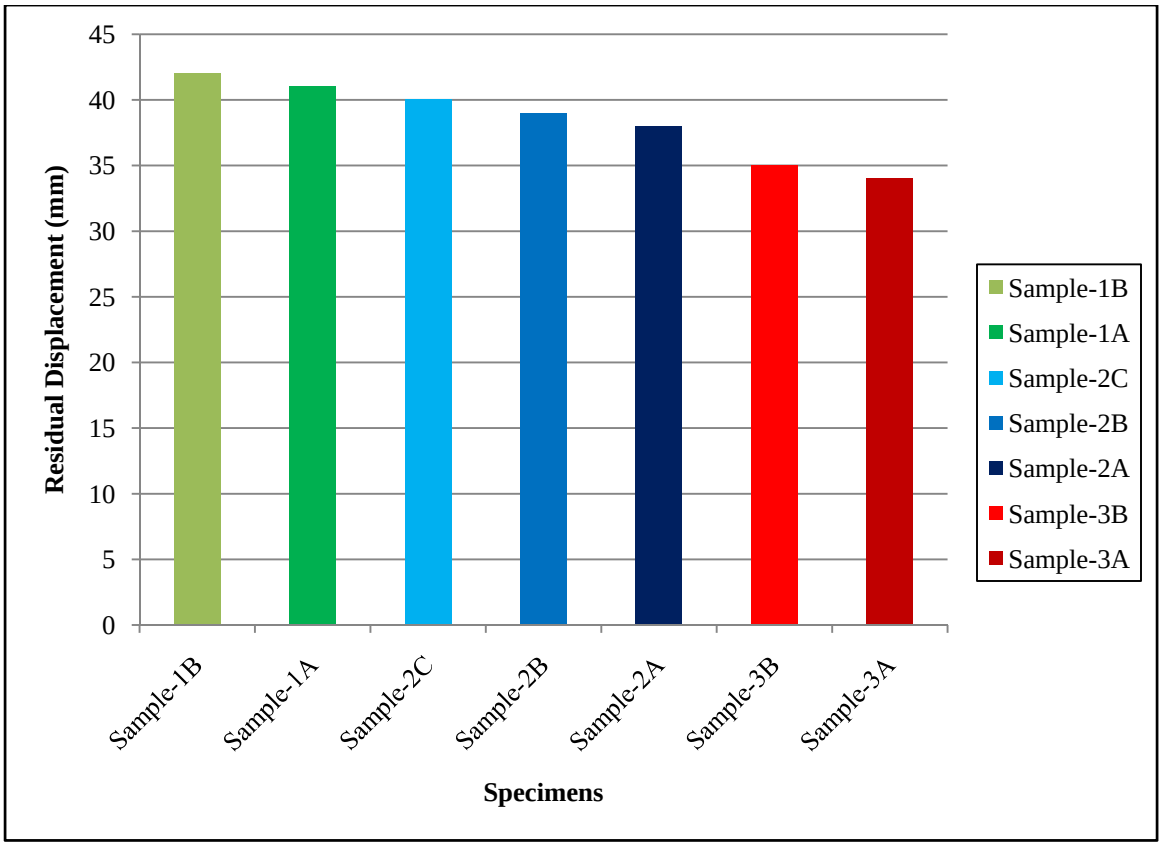

Figure 4.57: Maximum Displacement of Seven Specimens

4.11 Residual Displacement

Table 4.10: Residual Displacement of Each Specimen after Test

Specimen	Residual Displacement
Type 1B	18
Type 1A	15
Type 2C	13
Type 2B	10
Type 2A	08
Type 3B	07
Type 3A	05

Table 4.10 summarized the residual displacements of every specimens of different type after total removal of both cyclic and vertical loading. It was found that the residual displacements were decreasing with the increasing size of cross-section and seismic application of ties at joint region. Figure 4.58 represents the residual displacement of all seven specimens.

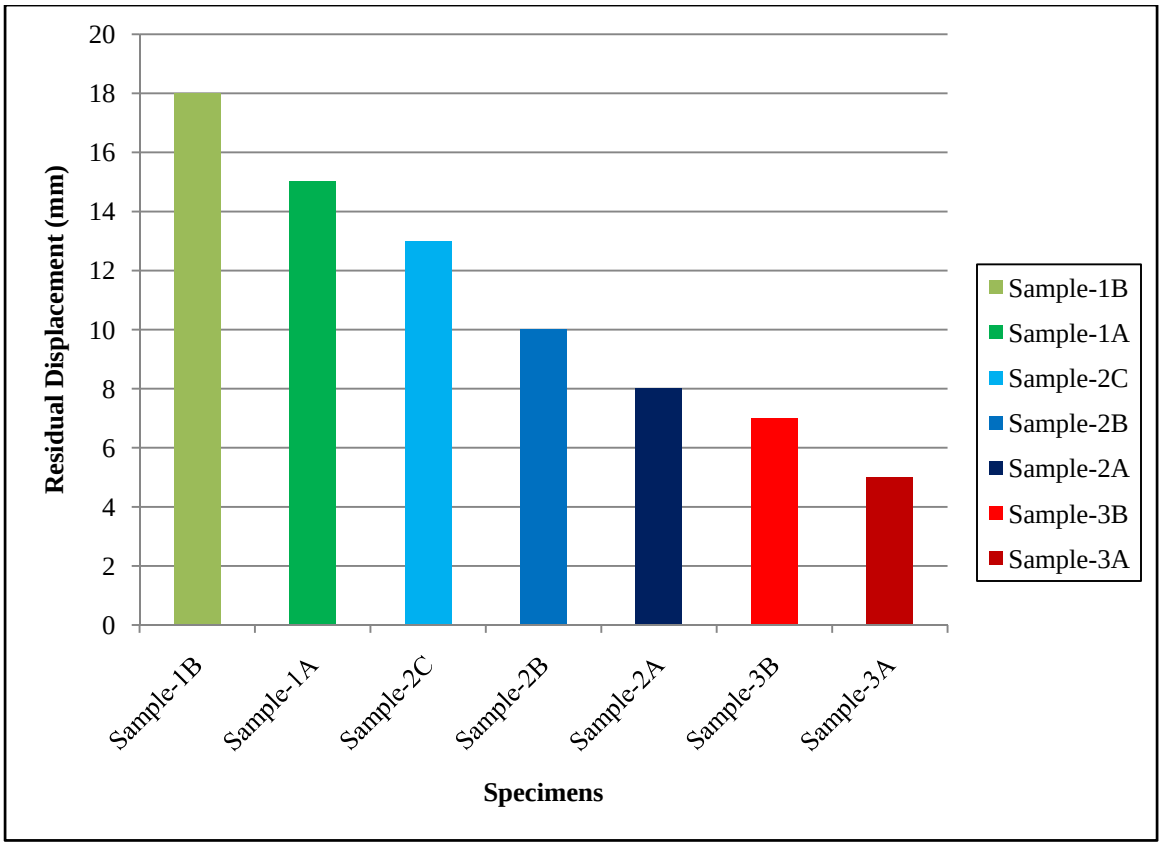

Figure 4.58: Residual Displacement of Seven Specimens after Removal of Load

CHAPTER 5

CONCLUSIONS AND RECOMMENDATIONS

5.1 Summary

Beam-column joints are identified as potentially one of the critical components of reinforced concrete moment resisting frames because of transferring beam end loads to the column due to gravity as well as all kinds of lateral loadings. Severe damage within a joint panel may trigger deterioration of the overall performance of reinforced concrete beam-column connections and thus the frame too.

A comprehensive experimental program was carried out to investigate the static cyclic loading behavior of beam-column joints with and without additional ties at the joint region. Seven half-scale specimens of reinforced concrete beam-column joints were constructed considering three categories of joints. These test categories were a) joint region with and without seismic ties, b) application of conventional and seismic stirrups in the joint region and c) different column to beam cross-section ratios which were considered to observe their effects on the performance of beam to column joint.

The specimens subjected to cyclic incremental vertical loading at the ends of the beams with sustained gravity load. Different crack patterns were observed for different categories of specimens. Specimens without ties at joint region showed diagonal cracking at joint where control specimens with ties displayed vertical cracking at the faces of the joint where the beams frame into the joint. The experimental data obtained in four deflection controlled cycles were used to study overall performance. Load-displacement as well as moment-rotation characteristics were obtained. At the same time maximum loads, load at first crack formation, maximum as well as residual deflections and secant stiffness were measured or observed. Finally, the test results of beam-column joints with and without seismic ties at joint region of different types of cross-section were compared.

The specimen with general distribution of overall stirrups and without ties at joint region performed poorly. The reinforced concrete beam-column joints with seismic ties at the joint region showed improved performance in respect of load deformation characteristics, moment rotation behavior, relative (secant) stiffness, initiating first crack, maximum displacement at the end of loading cycles and residual displacement at the end of fourth cycle. Moreover, providing additional ties at joint region is the most effective way of strengthening the beam-column joints.

Analyzing comparison, it was observed that the performance of beam-column joints with seismic ties at joint region were shown relatively better cyclic loading performance than joints with general distribution of overall stirrups in beams and ties in columns and with no seismic ties in joint region.

5.2 Conclusions

The beam-column joint specimens experimented in the study represented their behaviour under cyclic loading. Based on the results obtained from the experiments of the specimens, the following conclusions can be drawn:

a) Beam-column joints with seismic ties exhibited better seismic performance than the joints without ties. The specimens with ties at joints showed adequate sustainability throughout loading cycles.
b) Maximum load resisted after last cycle of beam-column joints were increased about 15% - 20% simply by applying adequate ties at joint region.
c) Beam-column joints without ties showed diagonal cracking at maximum load of fourth cycle where joints with ties expressed vertical cracking at the faces of the joint where the beams frame into the joint.
d) Beam-column joints without ties in the experiment were almost 15% - 20% less strong than beam-column joints with ties.

e) Concrete at joints with ties were not brittle and hence resisted the maximum load of the fourth cycle with minimum number of cracking. But concrete at joints without ties were brittle and resisted the maximum load of the fourth cycle with maximum number of cracking.

f) The loads at first crack formation were comparatively higher at specimens with ties at joints than the specimens without ties at joints.

g) The maximum loads after forth cycle of beam-column joints with ties were 3 kN – 6 kN much higher than the beam-column joints without ties.

h) Increase in Stiffness of beam-column joints with ties were 0.40 – 1.40 than those of without ties.

i) The stiffness degradation rates at different cycles were less to samples with ties at joints than the samples without ties at joints.

j) The beam end displacements at the end of different cycles of beam-column joints with ties were comparatively less than those of the joints without ties at joint region.

k) Non-seismic distribution of stirrups in beam and ties in column shows the worst joint performance. By applying seismic distribution of stirrups and ties in beam and column, the maximum load after forth cycle increased by almost 16%.

5.3 Recommendations for Further Study

This research suggests following recommendations for further investigation.

a) This research considered only interior joints; exterior joints and knee joints can be considered for the same study.

b) A comparative study can be made between experimental measurements and finite element analysis results.

c) Further research can be done by implying dynamic cyclic loading instead of static cyclic loading.

d) Research can be done by application of FRP (Fiber Reinforced Polymer) at joints to improve beam-column joint behavior.

e) Full scale model of beam-column joint specimen may be investigated to get more accurate results.

REFERENCES

ACI Committee 352 (2002), 352R-02: “Recommendation for design of beam-column joints in monolithic reinforced concrete structures,” American Concrete Institute, Farmington Hills, MI.

ACI 318M-08 (2008). “Building Code Requirements for Reinforced Concrete,” American Concrete Institute, Detroit, Michigan.

Attaalla, S.A. (2004), “General analytical model for normal shear stress of type 2 normal and high strength concrete beam-column joints,” ACI Struct. J., 101(1), 65-75.

Bindhu, K.R., Jaya, K.P. and Manicka Selvam, V.K. (2008). “Seismic resistance of exterior beam-column joints with non-conventional confinement reinforcement detailing,” Struct. Eng. Mech., 30(6), 733-761.

Chalioris, C.E., Favvata, M.J. and Karayannis, C.G. (2008), “Reinforced concrete beam-column joints with crossed inclined bars under cyclic deformations,” Earthq. Eng. Struct. D., 37(6), 881-897.

Cheung, P.C., Paulay, T. and Park, R. (1993), “Behavior of beam column joints in seismically-loaded RC frames,” Struct. Eng., 71(8), 129-138.

Dhakal, R.P., Pan, T.C. and Tsai, K.C., (2003). “Enhancement of Beam-Column Joint by RC Jacketing,” online citation http://hdl.handle.net/10092/4198.

Eligehausen, R., Popov, E.P., and Bertero, V.V. (1983) “Local Bond Stress-slip Relationships of Deformed Bars under Generalised Excitations.” Report UCB/EERC-83/19, Earthquake Engineering Research Center, University of California, Berkeley, 178p.

Eurocode 8 (2003), EN 1998-1:2003, “Design provision for earthquake resistant structures.” General rules specification rules for various materials and elements, European Committee for Standardization, Brussels.

GB 50010-2002, “Code for design of concrete structures,” Construction Ministry of China.

Genesio, G, Eligehausen, R., Pampanin (2010-1). “Seismic assessment of pre-1970s RC beam-column joints.” 14th European Conference on Earthquake Engineering, Ohrid, Macedonia.

Ghobarah, A., and El-Amoury, T. (2005). “Seismic rehabilitation of deficient exterior concrete frame joints.” J. Compos. Constr., 9(5), 408–416.

Goto, Y. and Joh, O., (2004), “Shear resistance of RC interior eccentric beam-column joints,” 13th World Conference on Earthquake Engineering, Vancouver, Canada, 649.

Hakuto, S., Park, R., and Tanaka, H. (2000). “Seismic Load Tests on Interior and Exterior Beam-Column Joints with Substandard Reinforcing Details.” Structural journal, ACI, 97(1), pp11-25.

Hwang, S. and Lee, H. (2000), “Analytical model for predicting shear strengths of interior reinforced concrete beam-column joints for seismic resistance,” ACI Struct. J., 97(1), 35-44.

Ichinose, T. (1991). “Interaction between Bond at Beam Bars and Shear Reinforcement in RC Interior Joints, Design of Beam-Column Joints for Seismic Resistance.” SP-123, American Concrete Institute, Farmington Hills, Mich., pp. 379-400.

Joh, O., Goto, Y, and Shibata, T., (1989), “Influence of joint reinforcement to shear resistance characteristic in RC exterior beam column connection (in Japanese),” Proceedings of the Japan Concrete Institute, 11(2), 537-542.

Joh., Osamu., Goto Yasuaki. (2000). “Beam Column Joint Behavior after Beam Yielding in R/C Ductile Frames.” paper presented on 12 WCEE Conference, Auckland, New Zealand., 30January-04 February.

Karayannis, C.G., Chalioris, C.E. and Sirkelis, G.M. (2008), “Local retrofit of exterior RC beam-column joints using thin RC jackets : an experimental study,” Earthq. Eng. Struct. D., 37(5), 727-746.

Kim, J., LaFave, J.M. and Song, J. (2007). “A new statistical approach for joint shear strength determination of RC beam-column connections subjected to lateral earthquake loading,” Struct. Eng. Mech., 27(4), 439-456.

Leon, R.T. (1990), “Shear strength and hysteretic behavior of interior beam-column joints,” ACI Struct. J., 87(1),3-11.

Liu, C., (2006). “Seismic Behaviour of Beam-Column Joint Subassemblies Reinforced With Steel Fibers,” Master of Engineering Thesis, University of Canterbury, Christchurch, New Zealand.

MacGregor, J.G. (1988), “Reinforced concrete mechanics and design,” Prentice-Hall, Englewood Cliffs, NJ.

MayField, B., Kong, K.F. and Bennison, A. (1971), “Corner joint details in structural light weight concrete,” ACI J. Proc., 68(5), 366-372.

Murty, C.V.R., Rai, D., Bajpai, K.K., Jain, S.K., (2003). “Effectiveness of reinforcement details in exterior reinforced concrete beam-column joints for earthquake resistance,” ACI Structural journal 100(2), 149-156.

Nilson, A.H., Darwin, D. and Dolan, C.W. (2004), “Design of concrete structure,” thirteenth edition, McGraw-Hill, New York.

Pampanin, S., Calvi, G M., and Moratti, M., (2002), “Seismic Behaviour of R.C. Beam-Column Joints Designed for Gravity Loads.” paper presented on 12th European Conference on Earthquake Engineering., 9-13 September , London.

P.C. Varghese (2010), “Advanced Reinforced Concrete Design,” second edition, New Delhi – 110001.

Popov, E.P. (1984), “Bond and anchorage of reinforcing bars under cyclic loading,” ACI J. Proc., 81(4), 340-349.

Paulay, T. and Priestley, M.J.N. (1992). “Seismic Design of Reinforced Concrete and Masonry Buildings.” John Wiley Publications, New York.

Ray W. Clough and Joseph Penzien (1993). “Dynamics of Structures,” Second Edition, McGraw – Hill, Inc, New York.

Saatcioglu, M., And Razvi, S. R., “Displacement based design of reinforced concrete columns for confinement,” ACI Structural Journal, V. 99, No.1, January- February 2002, pp. 3 - 11.

Shiohara, Hitoshi., and Kusiara, Fumio. (2010). “An Overlooked Failure Mechanism of Reinforced Concrete Beam-Column Joints,” proceedings of the 9th U.S. National and 10th Canadian Conference on Earthquake Engineering, July 25-29, Toronto, Ontario, Canada.

Uma, S.R., and Prasad, A.Meher., (2005). “Seismic Behavior of Beam Column Joints in Reinforced Concrete Moment Resisting Frames.” document no IITK- GSDMA-EQ-31-V1-0, IITK-GSDMA Project on Building Code.

Xilin Lu, Tonny H. Urukap, Sen Li and Fangshu Lin (2011). “Seismic behavior of interior RC beam-column joints with additional bars under cyclic loading.” College of Civil Engineering, Tongji University, Shanghai, China.

APPENDIX

A.1 Plastic Yield Moment of Beams and Columns

Ultimate plastic moment strength of the beams and columns are calculated based on the rectangular compressive stress block which is approximated by 0.85f_c'. When the reinforcing steel begins to yield large deformation commence. This is taken as the ultimate capacity of steel. At this point, tension force in the steel,

=

From theory of flexural members,

$Tult = Cult$

And $k'd = \frac{C\ ult}{0.85fc'b}$ (Where $k'd$ is the distance from the compression face to the cracked elastic neutral axis)

Or, a = $\frac{Asfy}{0.85fc'b}$ ……...…….(A.1)

$Mp = Tult(d - \frac{k'd}{2})$

Or, Mp = $Asfy(d - \frac{a}{2})$ .....(A.2)

Calculated plastics moment capacity of the beams and columns of all the samples before strengthening the joints are shown through Table A.1.1 and A.1.2.

A.1.1 Calculated Plastics Moment Capacity of the Beams

f_c'= 32 Mpa = 32 x 145 psi = 4640 psi = 4.64 ksi, (1 Mpa = 145 psi)

f_y = 550 Mpa = 79750 psi = 79.75 ksi

Cross-sectional area of 10 mm Φ = 3 No. bar = 0.11 in^2

Beam length = 2000/2 = 1000 mm = 39 in

Applied load at length, L = 39 – 9 = 30 in = 762 mm = 0.762m

Type 1:

b = 125 mm = 4.92 in

d = (125 – 20) mm = 105 mm = 3.74 in

As = 4 x 0.11 = 0.44 in^2

a = $\frac{\text{Asfy}}{0.85\text{fc}'\text{b}} = \frac{0.44\text{x}79.75}{0.85\text{x}4.64\text{x}4.92} = 1.808$

a/2 = 0.904

$Mp = \text{Asfy}(\text{d} - \frac{a}{2})$

= 0.44 x 79.75 (3.74 - 0.904) = 99.51 Kin

Load = $\frac{\text{Mp}}{L} = \frac{99.51}{30} = 3.32$ Kip = 3.32 x 4.545 = 15 KN, (1 Kip = 4.545 KN).

$Mp =$ 15 x 0.762 = 11 KN-m.

Type 2:

b = 150 mm = 5.90 in

d = (150 – 20) mm = 130 mm = 4.72 in

As = 5 x 0.11 = 0.55 in^2

a = $\frac{\text{Asfy}}{0.85\text{fc}'\text{b}} = \frac{0.55\text{x}79.75}{0.85\text{x}4.64\text{x}5.90} = 1.88$

a/2 = 0.94

$Mp = \text{Asfy}(\text{d} - \frac{a}{2})$

= 0.55 x 79.75 (4.72 - 0.94) = 165.80 Kin

Load = $\frac{\text{Mp}}{L} = \frac{165.80}{30} = 5.53$ Kip = 5.53 x 4.545 = 25 KN

$Mp =$ 25 x 0.762 = 19 KN-m.

Type 3:

b = 175 mm = 6.89 in

d = (175 – 20) mm = 155 mm = 5.70 in

As = 6 x 0.11 = 0.66 in^2

a = $\frac{\text{Asfy}}{0.85\text{fc}'\text{b}} = \frac{0.66\text{x}79.75}{0.85\text{x}4.64\text{x}6.89} = 1.94$

a/2 = 0.97

Mp = Asfy$(\text{d} - \frac{a}{2})$

= 0.66 x 79.75 (5.70 - 0.97) = 248.96 Kin

Load = $\frac{\text{Mp}}{L} = \frac{248.96}{30}$ = 8.30 Kip = 8.30 x 4.545 = 37 KN

$Mp =$ 37 x 0.762 = 28 KN-m.

Table A.1.1: Plastic Moment Strength of Beams

Model Type	As (in^2)	$k'd$ Or, a	Applied Load at length (mm)	Mp (kip-in)	Mp (KN-m)	P_{ult} (kip)	P_{ult} (ton)	P_{ult} (kN)
Type 1	0.44	1.808	762	99.51	11	3.32	1.50	15
Type 2	0.55	1.88	762	165.80	19	5.53	2.50	25
Type 3	0.66	1.94	762	248.96	28	8.30	3.70	37

A.1.2 Calculated Plastics Moment Capacity of the Columns

Applied load at Column length, L = 1500/2 = 750 mm = 29.5 in

b = 150 mm = 5.90 in

d = (150 – 20) mm = 130 mm = 4.72 in

As = 6 x 0.11 = 0.66 in^2

a = $\frac{\text{Asfy}}{0.85\text{fc}'\text{b}} = \frac{0.66\text{x}79.75}{0.85\text{x}4.64\text{x}5.90} = 2.26$

a/2 = 1.13

Mp = Asfy$(\text{d} - \frac{a}{2})$

= 0.66 x 79.75 (4.72 – 1.13) = 188.96 Kin

Load = $\frac{\text{Mp}}{L} = \frac{188.96}{29.5}$ = 6.41 Kip = 6.41 x 4.545 = 29 KN

$Mp =$ 29 x 0.762 = 22 KN-m.

Table A.1.2: Plastic Moment Strength of Columns

Model Type	As (in^2)	$k'd$ Or, a	Applied Load at length (mm)	Mp (kip-in)	Mp (KN-m)	Pult (kip)	Pult (ton)	Pult (kN)
Type 1,2 & 3	0.66	2.26	750	188.96	22	6.41	2.90	29

A.2 Design Details of Different Beam-column Joints

Following P.C. Varghese (2010), "Advanced Reinforced Concrete Design," second edition, New Delhi – 110001.

A.2.1 Joint Type 1 Design

1. Check the strength of column :

For # 10 mm ϕ, As = 78.54 mm^2

Percentage of steel, $\rho = \frac{As}{bd} = \frac{6\times 78.54\times 100}{150\times 150} = 2.09\%$

This is more than 0.8% and less than 6%. (OK)

Bending capacity of each column,

$\frac{\rho}{fck} = \frac{2.09}{32} = 0.0653$

$M_u = 0.0653\ f_{ck}\ bD^2$

$= 0.653\times 32\times 150\times 150^2 = 7.05\times 10^6$

Column above and below have twice capacity,

$M_{uc} = 2\times 7.05\times 10^6 = 14.10\times 10^6 = 14.10$ KNm

$2\ M_{uc} = 2\times 14.10\times 10^6 = 28.20\times 10^6 = 28.20$ KNm

2. Check the stability condition of the column with capacity of beams :

M_u of beam with 2 # 10 mm ϕ at top and 2 # 10 mm ϕ at bottom,

$\rho = \frac{A_s}{bd} = \frac{2\times 78.54}{125\times 125} = 0.01005$

$R_u = \phi\rho f_y(1- \frac{\rho f_y}{1.7 f_{ck}})$

$= 0.9\times 0.01005\times 550\times(1- \frac{0.01005\times 550}{1.7\times 32}) = 4.47$

$M_u = R_u bd^2$

$M_{u1} = M_{u2} = 4.47 \times 125 \times 125^2 = 8.73 \times 10^6$ Nmm = 8.73 KNm

$\frac{\sum M_{col}}{\sum M_{beam}} = \frac{2 \times 14.10 \times 10^6}{(8.73+8.73) \times 10^6} = 1.62 > 1.2$

Hence the column failure will not take place. (OK)

3. Check the anchorage of bars :

Extend the longitudinal beam bars through the column,

The empirical requirement is, $\frac{depth\ of\ column}{beam\ bar\ diameter} \geq 20$

$= \frac{150}{10} = 15$

4. Confinement by transverse steel :

Assume 8 mm ϕ stirrup,

Dimension of core = b – (2×cover) + (2×diameter of the hoop)

= 150 – (2×20) + (2×8) = 126 mm < 300 mm

So cross ties is not required.

H = The larger dimension of the confining hoop = 126 mm

S = $\frac{dimension}{4}$ or, 100 but not less than 75

$= \frac{150}{4} = 37.5$ or, 100 but not less than 75

Adopt, S = 75 mm.

Special confining reinforcement shall be provided over a length from each joint face, towards mid-span, and on either side of any section, where flexural yielding may occur under the effect of earthquake forces. The length shall not be less than

Larger lateral dimension of the member at the section where yielding may occurs

1/6 of the clear span of the member

450mm.

For more strength, $\frac{2}{3}$ of the clear span of the member provided.

Provide $\frac{2}{3}$ length from middle S @ 75 mm and rest $\frac{1}{3}$ length S @ 150 mm c/c.

$A_{sh} = 0.18SH(\frac{A_g}{A_k} - 1)\frac{f_{ck}}{f_y}$

$= 0.18\times75\times126\times(\frac{150^2}{126^2} - 1)\times\frac{32}{550} = 41.29$ mm^2

Adopt 8 mm ϕ (50.27 mm^2) bars for ties.

5. Check shear in column :

Story height, h = 1500 mm

$V_{col} = \frac{1.2(M_u^L+M_u^R)}{h}$

$= \frac{1.2(8.73+8.73)\times10^6}{1500} = 13968$ N

$\nu = \frac{V_{col}}{bd} = \frac{13968}{150\times150} = 0.621$

IS 456 Values,

Assume A_{st} = 0.5%,

$\tau_c = 0.49$

P_w = Column factor load in N

Factor = $1 + \frac{3P_w}{bdf_{ck}}$

$= 1 + \frac{3\times100\times10^3}{150\times150\times32} = 1.42 < 1.5$

$\tau'_c = 0.49\times1.42 = 0.70$ N/mm^2

Hence it is safe.

ACI values,

$\tau'_c = 0.13\sqrt{f_{ck}}(1 + 0.07\frac{P_w}{A_g})$

$= 0.13\times\sqrt{32}\times (1 + \frac{0.07\times100\times10^3}{150\times150}) = 0.96$ N/mm^2

6. Find the shear in joint :

(Both beam moments are clockwise)

V_{s1} = top steel area of beam = 2×78.54 = 157.08 mm^2

V_{s2} = bottom steel area of beam = 2×78.54 = 157.08 mm^2

$T = V_{s1}\times f_y = 157.08\times550 = 86.39\times10^3$ N = 86.39 KN

$C = V_{s2}\times f_y = 157.08\times550 = 86.39\times10^3$ N = 86.39 KN

$V_{col} = \frac{(M_u^L+M_u^R)}{h}$

$= \frac{(8.73+8.73)\times10^6}{1500} = 11.64\times10^3$ N = 11.64 KN

$V_u = T + C - V_{col}$

= 86.39 + 86.39 - 11.64 = 161. 14 KN

7. Check by joint committee recommendation :

γ for internal joint = 20,

h_{col} = depth of column = 150 mm

$b_j = \frac{b_{b+b_c}}{2} = \frac{125+150}{2} = 137.5$ mm

Strength of joint,

$V_n = 0.083\gamma\, b_j h_{col} \sqrt{f_{ck}}$

$= 0.083 \times 20 \times 137.5 \times 150 \times \sqrt{32}$

$= 193.68 \times 10^3$ N

$= 193.68$ KN > 161.14 KN

Hence the joint is safe in shear. (OK)

A.2.2 Joint Type 2 Design

1. Check the strength of column :

For # 10 mm ϕ, As = 78.54 mm^2

Percentage of steel, $\rho = \frac{As}{bd} = \frac{6 \times 78.54 \times 100}{150 \times 150} = 2.09\%$

This is more than 0.8% and less than 6%. (OK)

Bending capacity of each column,

$\frac{\rho}{fck} = \frac{2.09}{32} = 0.0653$

$M_u = 0.0653\, f_{ck}\, bD^2$

$= 0.653 \times 32 \times 150 \times 150^2 = 7.05 \times 10^6$

Column above and below have twice capacity,

$M_{uc} = 2 \times 7.05 \times 10^6 = 14.10 \times 10^6 = 14.10$ KNm

$2\, M_{uc} = 2 \times 14.10 \times 10^6 = 28.20 \times 10^6 = 28.20$ KNm

2. Check the stability condition of the column with capacity of beams :

M_u of beam with 3 # 10 mm ϕ at top and 2 # 10 mm ϕ at bottom,

$\rho_1 = \frac{A_{s1}}{bd} = \frac{3 \times 78.54}{150 \times 150} = 0.0105$

$R_{u1} = \phi\rho f_y(1- \frac{\rho_1 f_y}{1.7 f_{ck}})$

$= 0.9\times0.0105\times550\times(1- \frac{0.0105\times 550}{1.7\times 32}) = 4.65$

$\rho_2 = \frac{A_{s2}}{bd} = \frac{2\times 78.54}{150\times 150} = 0.007$

$R_{u2} = \phi\rho f_y(1- \frac{\rho_2 f_y}{1.7 f_{ck}})$

$= 0.9\times0.007\times550\times(1- \frac{0.007\times 550}{1.7\times 32}) = 3.22$

$M_{u1} = R_{u1}bd^2$

$M_{u1} = 4.65\times150\times150^2 = 15.69\times10^6$ Nmm = 15.69 KNm

$M_{u2} = R_{u2}bd^2$

$M_{u2} = 3.22\times150\times150^2 = 10.87\times10^6$ Nmm = 10.87 KNm

$\frac{\sum M_{col}}{\sum M_{beam}} = \frac{2\times 14.10\times10^6}{(15.69+10.87)\times10^6} = 1.1 < 1.2$

Hence the column failure will take place. (Not OK)

3. Check the anchorage of bars :

Extend the longitudinal beam bars through the column,

The empirical requirement is, $\frac{depth\ of\ column}{beam\ bar\ diameter} \geq 20$

$= \frac{150}{10} = 15$

4. Confinement by transverse steel :

Assume 8 mm ϕ stirrup,

Dimension of core = b – (2×cover) + (2×diameter of the hoop)

= 150 – (2×20) + (2×8) = 126 mm < 300 mm

So cross ties is not required.

H = The larger dimension of the confining hoop = 126 mm

S = $\frac{dimension}{4}$ or, 100 but not less than 75

= $\frac{150}{4}$ = 37.5 or, 100 but not less than 75

Adopt, S = 75 mm.

Special confining reinforcement shall be provided over a length from each joint face, towards mid-span, and on either side of any section, where flexural yielding may occur under the effect of earthquake forces. The length shall not be less than

Larger lateral dimension of the member at the section where yielding may occurs

1/6 of the clear span of the member

450mm.

For more strength, $\frac{2}{3}$ of the clear span of the member provided.

Provide $\frac{2}{3}$ length from middle S @ 75 mm and rest $\frac{1}{3}$ length S @ 150 mm c/c.

(For type C joint provide S @ 150 mm c/c for full length.)

$A_{sh} = 0.18SH(\frac{A_g}{A_k} - 1)\frac{f_{ck}}{f_y}$

$= 0.18\times75\times126\times(\frac{150^2}{126^2} - 1)\times\frac{32}{550} = 41.29$ mm^2

Adopt 8 mm ϕ (50.27 mm^2) bars for ties.

5. Check shear in column :

Story height, h = 1500 mm

$V_{col} = \frac{1.2(M_u^L+M_u^R)}{h}$

$= \frac{1.2(15.69+10.87)\times10^6}{1500} = 21248$ N

$\nu = \frac{V_{col}}{bd} = \frac{21248}{150\times150} = 0.944$

IS 456 Values,

Assume A_{st} = 0.5%,

$\tau_c = 0.49$

P_w = Column factor load in N

Factor = $1 + \frac{3P_w}{bdf_{ck}}$

$= 1 + \frac{3\times100\times10^3}{150\times150\times32} = 1.42 < 1.5$

$\tau'_c = 0.49\times1.42 = 0.70$ N/mm^2

Hence it is safe.

ACI values,

$\tau'_c = 0.13\sqrt{f_{ck}}(1 + 0.07\frac{P_w}{A_g})$

$= 0.13\times\sqrt{32}\times (1 + \frac{0.07\times100\times10^3}{150\times150}) = 0.96$ N/mm^2

6. Find the shear in joint :

(Both beam moments are clockwise)

V_{s1} = top steel area of beam = 3×78.54 = 235.62 mm^2

V_{s2} = bottom steel area of beam = 2×78.54 = 157.08 mm^2

$T = V_{s1}\times f_y = 235.62\times550 = 129.59\times10^3$ N = 129.59 KN

$C = V_{s2}\times f_y = 157.08\times550 = 86.39\times10^3$ N = 86.39 KN

$V_{col} = \frac{(M_u^L+M_u^R)}{h}$

$= \frac{(15.69+10.87)\times10^6}{1500} = 17.71\times10^3$ N = 17.71 KN

$V_u = T + C - V_{col}$

$= 129.59 + 86.39 - 17.71 = 198.27$ KN

7. Check by joint committee recommendation :

γ for internal joint = 20,

h_{col} = depth of column = 150 mm

$b_j = \frac{b_{b+b_c}}{2} = \frac{150+150}{2} = 150$ mm

Strength of joint,

$V_n = 0.083\gamma\, b_j h_{col}\sqrt{f_{ck}}$

$= 0.083\times20\times150\times150\times\sqrt{32}$

$= 211.28\times10^3$ N

= 211.28 KN > 198.27 KN

Hence the joint is safe in shear. (OK)

A.2.3 Joint Type 3 Design

1. Check the strength of column :

For # 10 mm ϕ, As = 78.54 mm^2

Percentage of steel, $\rho = \frac{As}{bd} = \frac{6\times 78.54\times 100}{150\times 150} = 2.09\%$

This is more than 0.8% and less than 6%. (OK)

Bending capacity of each column,

$\frac{\rho}{fck} = \frac{2.09}{32} = 0.0653$

$M_u = 0.0653\ f_{ck}\ bD^2$

$= 0.653 \times 32 \times 150 \times 150^2 = 7.05 \times 10^6$

Column above and below have twice capacity,

$M_{uc} = 2 \times 7.05 \times 10^6 = 14.10 \times 10^6 = 14.10$ KNm

$2\ M_{uc} = 2 \times 14.10 \times 10^6 = 28.20 \times 10^6 = 28.20$ KNm

2. Check the stability condition of the column with capacity of beams :

   M_u of beam with 3 # 10 mm ϕ at top and 3 # 10 mm ϕ at bottom,

$\rho = \frac{A_s}{bd} = \frac{3 \times 78.54}{175 \times 175} = 0.0077$

$R_u = \phi \rho f_y (1 - \frac{\rho f_y}{1.7 f_{ck}})$

$= 0.9 \times 0.0077 \times 550 \times (1 - \frac{0.0077 \times 550}{1.7 \times 32}) = 3.51$

$M_u = R_u bd^2$

$M_{u1} = M_{u2} = 3.51 \times 175 \times 175^2 = 18.81 \times 10^6$ Nmm $= 18.81$ KNm

$\frac{\sum M_{col}}{\sum M_{beam}} = \frac{2 \times 14.10 \times 10^6}{(18.81 + 18.81) \times 10^6} = 0.75 < 1.2$

Hence the column failure will take place. (Not OK)

3. Check the anchorage of bars :

Extend the longitudinal beam bars through the column,

The empirical requirement is, $\frac{depth\ of\ column}{beam\ bar\ diameter} \geq 20$

$= \frac{150}{10} = 15$

4. Confinement by transverse steel :

Assume 8 mm ϕ stirrup,

Dimension of core = b – (2×cover) + (2×diameter of the hoop)

= 150 – (2×20) + (2×8) = 126 mm < 300 mm

So cross ties is not required.

H = The larger dimension of the confining hoop = 126 mm

S = $\frac{dimension}{4}$ or, 100 but not less than 75

= $\frac{150}{4}$ = 37.5 or, 100 but not less than 75

Adopt, S = 75 mm.

Special confining reinforcement shall be provided over a length from each joint face, towards mid-span, and on either side of any section, where flexural yielding may occur under the effect of earthquake forces. The length shall not be less than

Larger lateral dimension of the member at the section where yielding may occurs

1/6 of the clear span of the member

450mm.

For more strength, $\frac{2}{3}$ of the clear span of the member provided.

Provide $\frac{2}{3}$ length from middle S @ 75 mm and rest $\frac{1}{3}$ length S @ 150 mm c/c.

A_{sh} = 0.18SH($\frac{A_g}{A_k}$ - 1)$\frac{f_{ck}}{f_y}$

= 0.18×75×126×($\frac{150^2}{126^2}$ - 1)×$\frac{32}{550}$ = 41.29 mm^2

Adopt 8 mm ϕ (50.27 mm^2) bars for ties.

5. Check shear in column :

Story height, h = 1500 mm

V_{col} = $\frac{1.2(M_u^L+M_u^R)}{h}$

$= \frac{1.2(18.81+18.81)\times10^6}{1500}$ = 30096 N

$\nu = \frac{V_{col}}{bd} = \frac{30096}{150\times150}$ = 1.34

IS 456 Values,

Assume A_{st} = 0.5%,

τ_c = 0.49

P_w = Column factor load in N

Factor = $1 + \frac{3P_w}{bdf_{ck}}$

$= 1 + \frac{3\times100\times10^3}{150\times150\times32}$ = 1.42 < 1.5

τ'_c = 0.49×1.42 = 0.70 N/mm^2

Hence it is safe.

ACI values,

$\tau'_c = 0.13\sqrt{f_{ck}}(1 + 0.07\frac{P_w}{A_g})$

$= 0.13\times\sqrt{32}\times (1 + \frac{0.07\times100\times10^3}{150\times150})$ = 0.96 N/mm^2

6. Find the shear in joint :

(Both beam moments are clockwise)

V_{s1} = top steel area of beam = 3×78.54 = 235.62 mm^2

V_{s2} = bottom steel area of beam = 3×78.54 = 235.62 mm^2

$T = V_{s1}\times f_y = 235.62\times550 = 129.59\times10^3$ N = 129.59 KN

$C = V_{s2}\times f_y = 235.62\times550 = 129.59\times10^3$ N = 129.59 KN

$V_{col} = \frac{(M_u^L + M_u^R)}{h}$

$= \frac{(18.81+18.81)\times 10^6}{1500} = 25.08\times 10^3$ N = 25.08 KN

$V_u = T + C - V_{col}$

= 129.59 + 129.59 – 25.08 = 234.10 KN

7. Check by joint committee recommendation :

γ for internal joint = 20,

h_{col} = depth of column = 150 mm

$b_j = \frac{b_{b+b_c}}{2} = \frac{175+150}{2}$ = 162.50 mm

Strength of joint,

$V_n = 0.083\gamma\, b_j h_{col}\sqrt{f_{ck}}$

$= 0.083\times 20\times 162.50\times 150\times\sqrt{32}$

$= 228.89\times 10^3$ N

= 228.89 KN < 234.10 KN

Hence the joint is not safe in shear. (Not OK).